Thermal Neutrons Position Sensitive Gas Detectors

Bruno Guérard

ILL

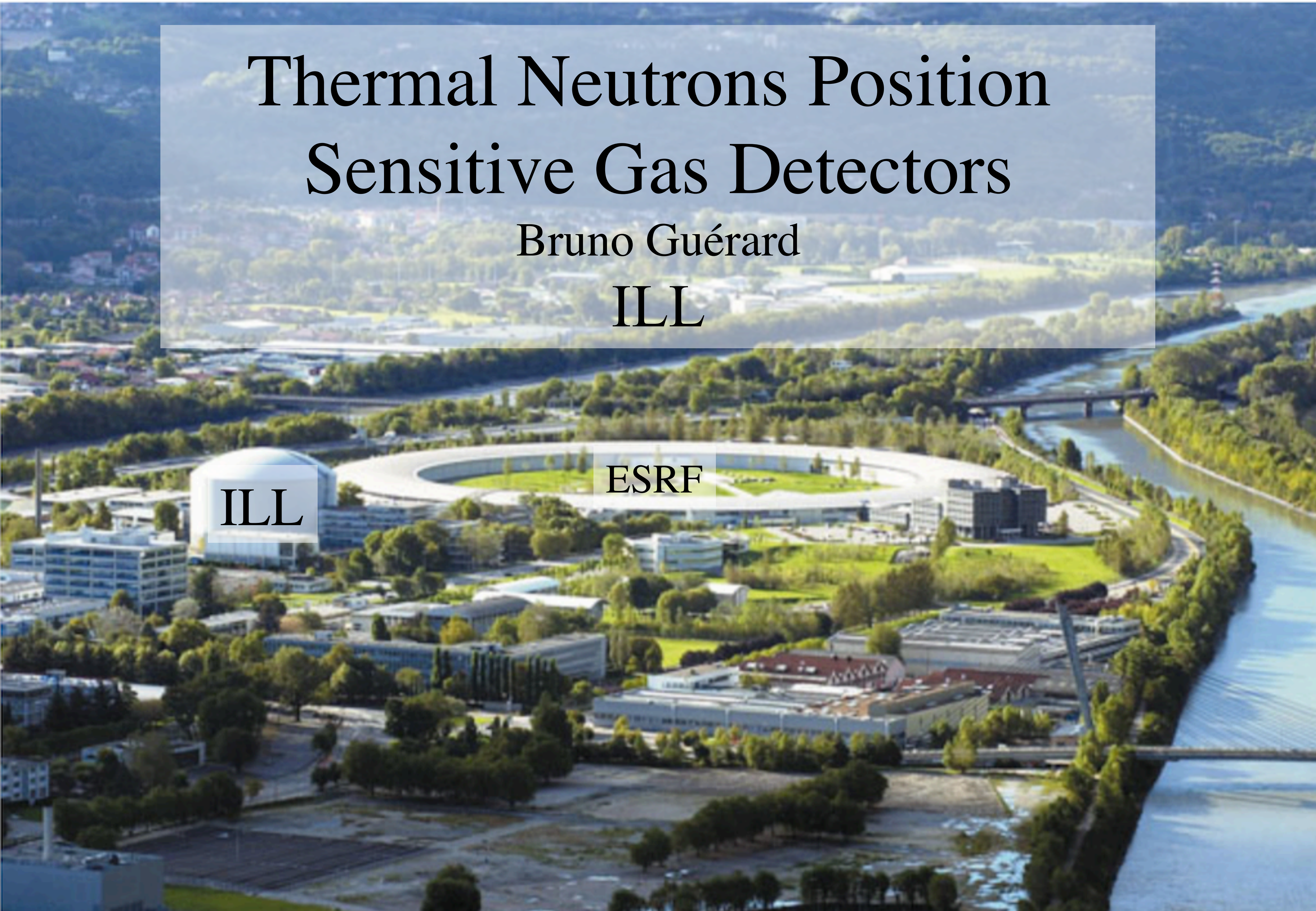

NEUTRONS FOR SCIENCE

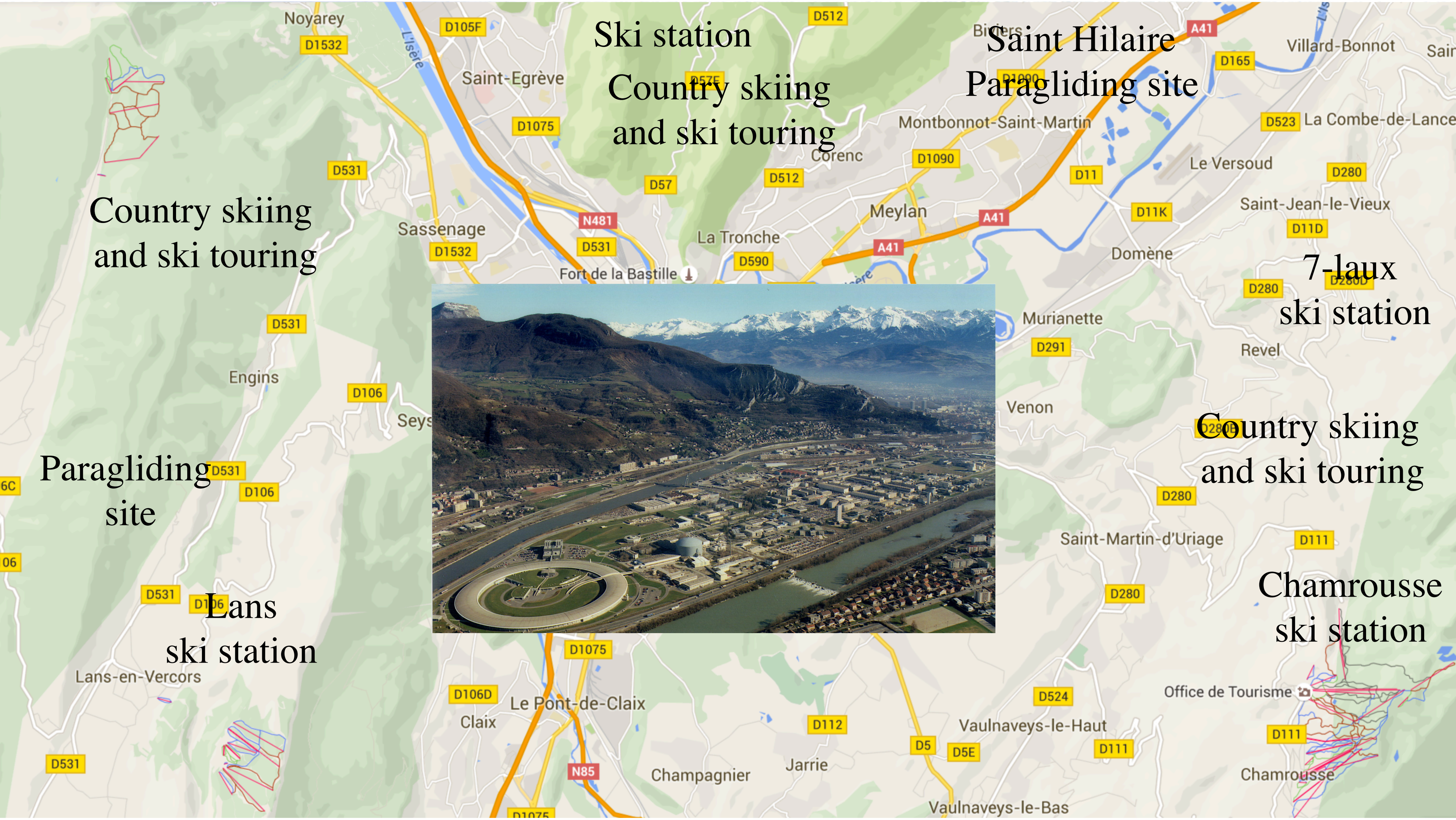

One difficulty in Grenoble is to decide where to go, and what to do in the week end

<u>Objective of the presentation</u>:
to give some flavor about the challenges, constraints, and specificities of detector development in the field of neutron scattering science.

2 types of neutron sources for neutron scattering science

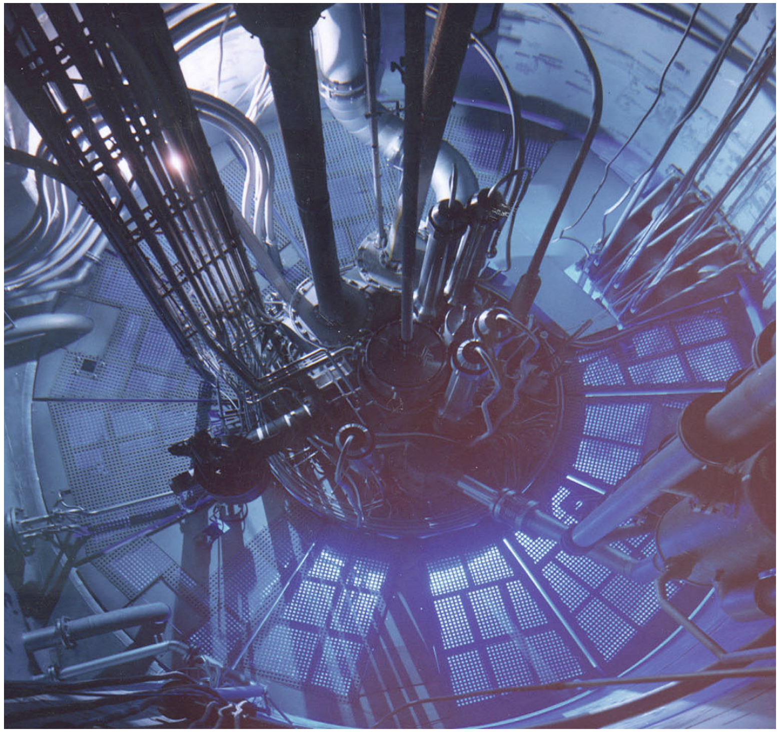

Reactor of the ILL (France)
In operation since 1972
93% ^{235}U enriched fuel element
Flux = 1.2 x 10^{15} n/cm^2.s

ISIS (UK) spallation source
proton beam power : 0.16 MW
Pulse frequency : 50 Hz
Peak Flux = 2.3 x 10^{15} n/cm^2.s
Average Flux = 2 x 10^{12} n/cm^2.s

… But the same detectors

General specifications for detectors

Neutrons are less interacting with matter than X-Rays

Material samples must have a sufficient volume (several mm^3) to produce enough measurement statistics in a reasonable time

→ Spatial resolution is generally not an issue (>=sample size)
In the range of mm to cm

→ Background noise is critical (fast neutrons, electronics, gammas)
Counting mode > integrating mode

→ High detection efficiency is required
>= 80% for thermal neutrons (1.8 Å)

Neutron instruments cover a broad range of applications

The parameters of the detector must be optimized for each instrument:

- Counting rate (from Hz to MHz) local and global
- Spatial resolution (from mm to cm)
- Sensitive area (from 10 cm^2 to 30 m^2)
- 1D or 2D
- Operation in vacuum or in air

Additional requirements :

- Low gamma sensitivity
- Uniformity of response
- High detection efficiency
- Stability over long period (10 years)
- Maintainability
- Acceptable cost
- Accessible technique for the lab

- On a **Single Crystal Diffractometer** (SXD), one needs to correctly …

  1/separate Bragg peaks,

  2/measure the center of gravity, and

  3/minimize the background under the peak.

detectors of 0.5 m2 with a resolution 1-2 mm FWHM are needed.

- 1 mm resolution in one direction is needed for **reflectometers**

- 5-8 mm in 2D for **SANS** (Small Angle Scattering) over 1 m^2

- 20-30 mm in 2D for **Energy spectrometers** over tens of m^2

Global Context

We shall focus on Position Sensitive thermal Neutron Gas Detectors operated in counting mode (called "GPSD" in the following)

GPSD are broadly used at the ILL and in other neutron institutes since the beginning of these facilities. I will mainly speak about development at the ILL.

Since the beginning, only 2 isotopes have been used for the capture of neutrons:
^{10}B (in the form of the $^{10}BF_3$ gas), and
^{3}He which gradually replaced $^{10}BF_3$ since the end of the 80s.

$^{10}BF_3$ being very toxic and less efficient than ^{3}He, there was no reason to continue with $^{10}BF_3$ detectors; they were simply banished at the ILL and elsewhere at the end of the 90s

The ^{3}He shortage crisis

The New York Times

New York Times November 23, 2009
Shortage Slows a Program to Detect Nucle
Bombs

By MATTHEW L. WALD
WASHINGTON — The Department of Homeland Security has spent $230 million to devel better technology for detecting smuggled nuclear bombs but has had to stop deploy the new machines because the United State has run out of a crucial raw material, experts say.

The ingredient is helium 3, an unusual forn of the element that is formed when tritium, an ingredient of hydrogen bombs, decays. Bu the government mostly stopped making tritiu in 1989.

"I have not heard any explanation of why th was not entirely foreseeable," said Representative Brad Miller, Democrat of Nor Carolina, who is the chairman of a House subcommittee that is investigating the problem.

October 2009 Physics Today 21

issues & events

US government agencies work to minimize damage due to helium-3 shortfall

Stiff new competition from security applications for a limited supply of helium-3 threatens research in low-temperature physics, neutron scattering, and medicine, for example.

Helium-3 is becoming scarcer and pricier because of a huge jump in demand paired with a dwindling supply. A US government multiagency panel is prioritizing allocation of ^{3}He and seeking alternative technologies to reduce demand for the gas.

much bigger users of ^{3}He, and medical research, defense manufacturing, and well-logging are among the other uses for the gas.

According to Kimberly Koeppel of the DNDO, the "releasable numbers ... are that the anticipated supply-

spread medical use. That is, for techniques potentially available in every hospital worldwide."

But the current crisis came as a surprise to most. Typically, scientists find out about the shortage when they try to order ^{3}He or instruments that use it.

www.sciencemag.org SCIENCE VOL 326 6 NOVEMBER 2009

Helium-3 Shortage Could Put Freeze On Low-Temperature Research

The weird effects of quantum mechanics often emerge at extremely low temperatures. So 3 years ago, Moty Heiblum, a physicist at the Weizmann Institute of Science in Rehovot, Israel, ordered a large "dilution refrigerator," which uses frigid liquid helium as a coolant and can chill tiny electronic devices to within a thousandth of a ... illikelvin. But ... n Cryogenics

large neutron-scattering facilities used to probe materials, such as the one at the new Japan Proton Accelerator Research Complex (J-PARC) in Tokai. The projected need for that application alone exceeds 100,000 liters over the next 6 years. J-PARC researchers need 16,000 liters of helium-3 to complete detectors for 15 of 23 beamlines, says J-PARC's Masatoshi Arai: "If we cannot get helium-3 and detectors, ... [then] we can-

- Usage has exceeded supply for several years
- Stockpiles are dwindling
- US production was about 40% of the demand prior to 2008
- Governments are being forced to prioritize uses
- Alternatives are needed for large area neutron detectors

In 2008 started the so-called "^{3}He shortage crisis" which resulted in very fast increase of price (80 €/liter →3000 €/liter in 4 years) together with a strong reduction of its availability (see Ralf's talk yesterday)

Directors of neutron science facilities met in 2010 to decide priorities for the development of ^{3}He alternative with 3 technical solutions:

- Scintillators (broadly used technique)
- $^{10}B_4C$ films in proportional gas counters (new technique)
- $^{10}BF_3$ (abandoned technique)

Some people announced the end of ^{3}He detectors.

They predicted that scintillators would be the main alternative.

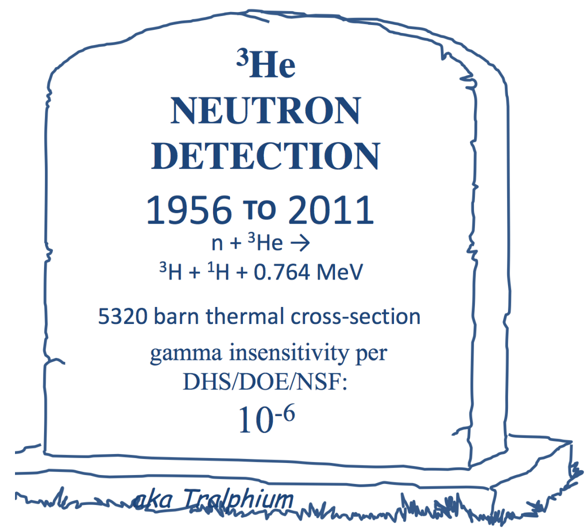

The death of ^{3}He did not happen: ^{3}He availability is now stable and its high cost is acceptable at least for small and medium size GPSDs.

Web page of GE/Reuter Stokes :

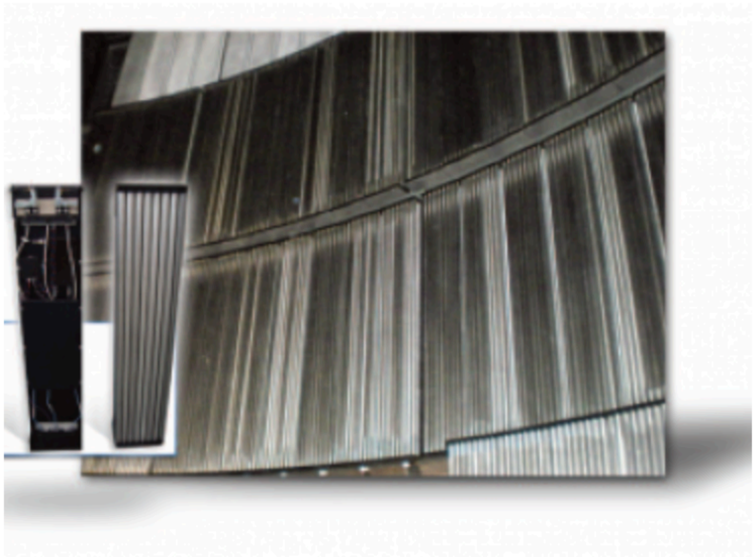

Helium-3 Position Sensitive Detector

GE offers the Reuter Stokes helium-3 filled position sensitive detectors and standard helium-3 detectors for the neutron scattering industry. The Reuter Stokes position sensitive detectors are used in neutron scattering facilities throughout the world and have become the benchmark detectors for the industry. These detectors provide a scalable solution for everything from SANS instruments to large Time of Flight instruments.

Since the helium-3 supply situation has stabilized we have been able to get a reliable supply of gas to enable us to continue to supply detectors for both small and large area coverage.

Features and Benefits

- High resistive anode material to enable accurate position resolution through charge division.
- Adjustable helium-3 pressures up to 30 bar to optimize detector efficiency from short to long neutron wavelengths.
- Diameters of 8 mm up to >50 mm and active lengths up to 3 meters.
- Thin wall construction to minimize neutron absorption in the detector walls.
- All brazed and welded construction to provide a long operational life.
- Customized construction to enable a variety of connections and vacuum penetrations when required.

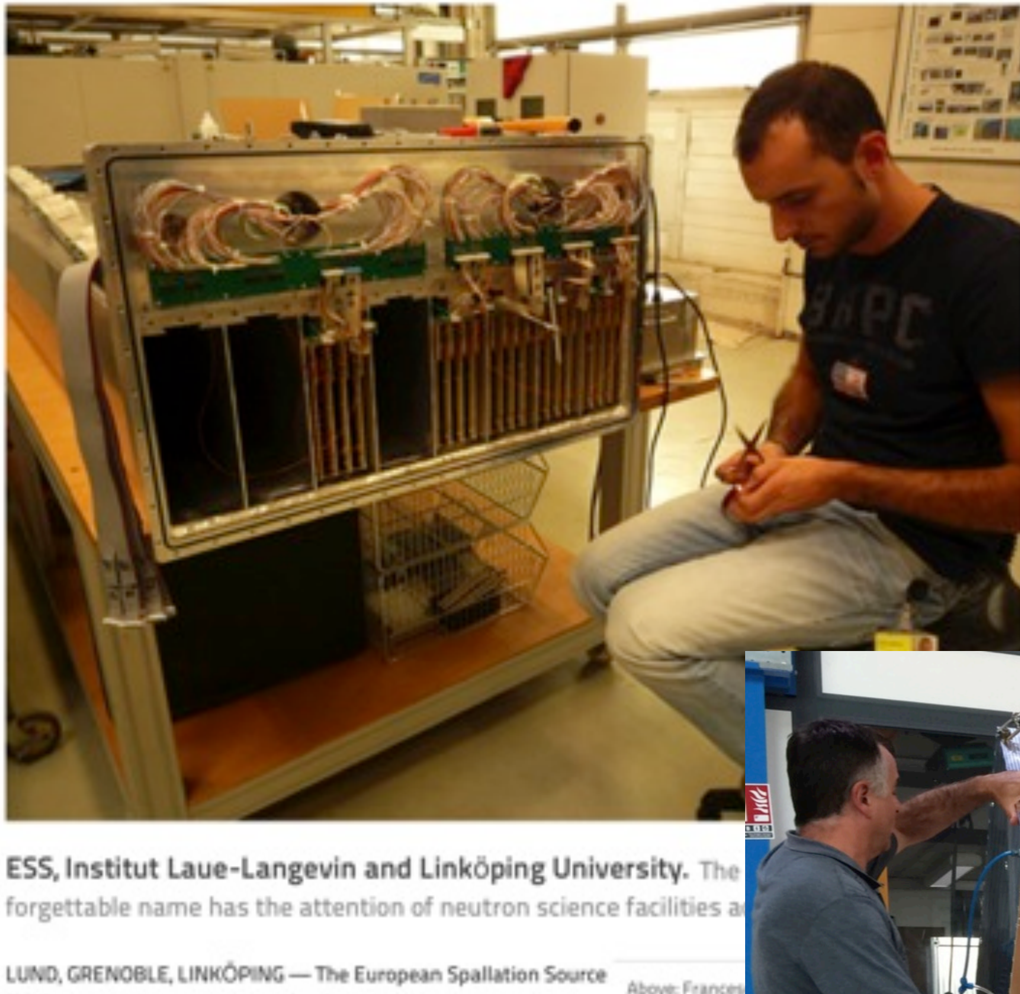

Competition between different techniques creates a stimulating research environment

Besides ^{3}He detector development, a new technique, called MultiGrid, based on ^{10}B thin films neutron convertors, is developed for large area detectors by ILL, ESS, and Linkoping University since 2010.

Recent development of GPSDs with both ^{3}He and ^{10}B neutron convertors is very active and successful nowadays. Some examples will be shown.

Important figures (see previous talks)

1/ Neutron reactions

The kinetic energy of slow neutrons (relevant to materials science) is of the order of a few meV (not MeV !) → the (n,p) elastic scattering reaction is not applicable.

Fission reaction is ok, but fissile elements are not accessible in large quantities, or in the gas state.

The best option to detect thermal neutrons is to detect charged particles emitted in the gas after a capture reaction.

2/ Neutron convertors

- n + ^{3}He → ^{3}H + ^{1}H + 0.764 MeV (σ_c = 5330 barns @1.8 Å)
- n + ^{6}Li → ^{4}He + ^{3}H + 4.79 MeV (937 barns)
- n + ^{10}B → ^{7}Li* + ^{4}He →^{7}Li + ^{4}He + 2.31 MeV + γ (0.48 MeV) (93%)
  (3840 barns) → ^{7}Li + ^{4}He + 2.79 MeV (7%)
- n + ^{14}N → ^{14}C + ^{1}H + 0.626 MeV (1.8 barns)
- n + ^{157}Gd → Gd* → gamma-ray spectrum + conversion electron spectrum (~70 keV)
- n + ^{235}U → xn + fission fragments + ~160 MeV (<x> ~ 2.5) (698 barns)

For thermal neutrons, σ_c increases linearly with λ

Natural isotopical fraction

^{10}B: 19.8% ^{6}Li: 7.6% ^{157}Gd: 15,7%

NEUTRONS FOR SCIENCE

3/ Particle selection

Due to low background noise requirement, it is necessary to exploit the difference of signature between n and γ interactions in order to maximise the neutron detection efficiency and to keep the gamma sensitivity at an acceptable level.

→ This is usually done by applying a pulse height discrimination in the electronics readout.

Integrating (non counting) devices like CCD camera are used at the ILL only to orient crystals before doing the real experiment.

General considerations on technical development in the ILL detector lab

Large area, low resolution, limited count rate, simple design

The 30 m^2 detector of the IN5 TOF Energy spectrometer at the ILL

Small area, high resolution, high count rate, complex technique

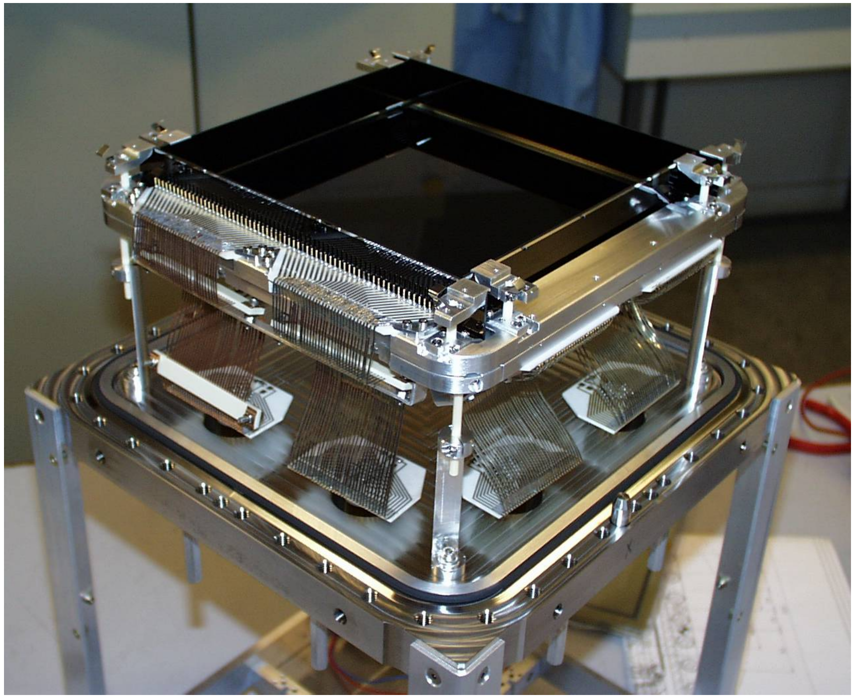

The MSGC developed for the D19 Single Crystal Diffractometer

General considerations on technical development in the ILL detector lab

- Almost all detectors used at the ILL are GSPDs
- Apart one exception (the D22 SANS instrument), all of them have been developed and fabricated at the ILL
- The diversity of requirements, together with a continuous process of improvement of the instruments in neutron scattering science results in a complex market for neutron detector fabricants
- The number of companies involved in this market is very small, and they can provide only detectors which are relatively simple to produce

General considerations on technical development in the ILL detector lab

Technical development can be very fun …

- You have good ideas, enough resources and enough time to go deeply in the understanding of technical problems, and your collaborators are very motivated

- There is good communication and mutual trust between your team and the instrument responsible (future user of the detector), as well as with the directors, resulting in a well defined detector specification, and a solid project organization.

- The effort of your team results in an operational detector delivered on time on the instrument, making the scientist very happy.

General considerations on technical development in the ILL detector lab

In reality …

- After the project has been approved (a new detector for a new instrument, or for an instrument upgrade), discussion on detector specifications start, and you will be kindly invited to announce a delivery date, and a price with +-10% contingency, sometimes without knowing exactly what the technical solution is going to be.
- There is no tolerance for unsuccessful development

→ It is important to anticipate this situation by pushing the development wherever the detector performance is a bottleneck.

→ Development is a step by step process, with each step showing an exploitable benefit.

There is only a limited internal budget for technical development, but several ways to find it outside, in particular through European projects, or bilateral collaborations.

Charge of the ILL detector lab

- The ILL detector laboratory provides high quality neutron detectors to the ILL instruments and must guaranty their operation with high reliability.
- We must be able to repair a detector in an acceptable delay to minimise the instrument unavailability.
- We are making decisive breakthroughs in concepts, and we develop them up to concrete operational detectors.
- Our 3 patents (MSGC, Multi-Tube, Multi-Grid) are oriented towards optimal performance and reliability of the instruments.
- We help our associates by giving access to our technology

V. Buridon
BrightnESS
post-doc

D. Roulier
SINE2020
Post-doc

JC Buffet
(mech engineer)

S. Cuccaro
(mech technician)

J. Pentenero
(mech technician)

J. Marchal
(physicist)

B. Guérard
(physicist)

JF Clergeau
(physicist)

Competences and equipment

- Ultra-high vacuum, gas handling systems, high purity vessels, high voltage, mechanical mounting, metrology
- High precision machining of mechanical pieces (metal, ceramics)
- Physics of detectors: based on the physical process of neutron interaction in gas, signal development, and data treatment, the SDN specifies, studies, fabricates, tests and maintains gas detectors that best sweet the ILL instruments.

- Well equipped laboratory for detector mounting and maintenance (ILL3) with high quality vacuum and gas systems, crane, outgasing chambers, clean room...
- 2 small detectosr labs
- 2 neutron beam lines (CT1 and CT2)
- Tooling machines (wire spark erosion, 3-axis tooling center, ..)-->many of the mechanical pieces of detectors are built in house

Origin of GPSD development at the ILL

ILL first neutrons in 1971: single proportional gas counters and photographic films
→ long time for acquiring or treating data.

In the late 60's: simultaneous development of Gas Position Sensitive Detectors (GPSD) at CEA/LETI and ILL and at CERN

- *R. Allemand, J. Jacobe and E. Roudaut French patent n° 148.589 (18 April **1968**), Dispositif détecteur de neutrons*
- *G. Charpak, R. Bouclier, T. Bressani, J. Favier and C. Zupancic, Nuclear Instrum. And Methods 62 (**1968**), 235*

A large area PSD working with BF3 in charge collection mode installed at the ILL.

The MWPC invented by Charpak started to show its great potential for particle identification in High Energy Physics (HEP).

These innovations are at the origin of a fruitful development of neutron MWPCs at BNL, ILL, and ORL.
By providing a better use of scattered neutrons, progresses with these detectors drastically changed the conditions of neutron instrumentation in neutron scattering science.

The beginning of GPSDs: MWPC (1968, G. Charpak)

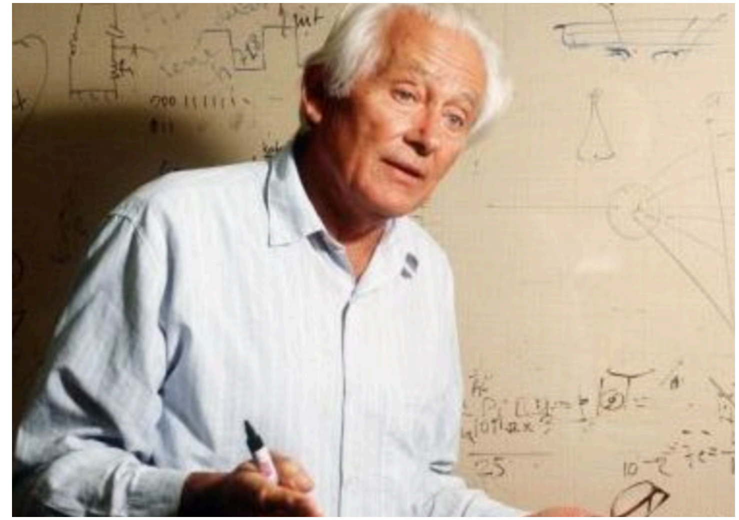

Idea: make a proportional counter with a lot of anodes placed between 2 cathode planes

By looking at which wires were fired → can determine the position of the particle

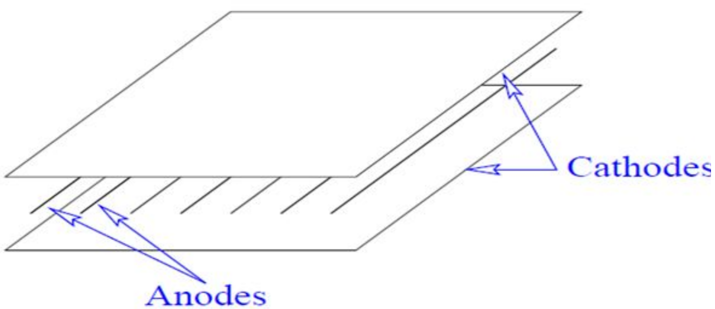

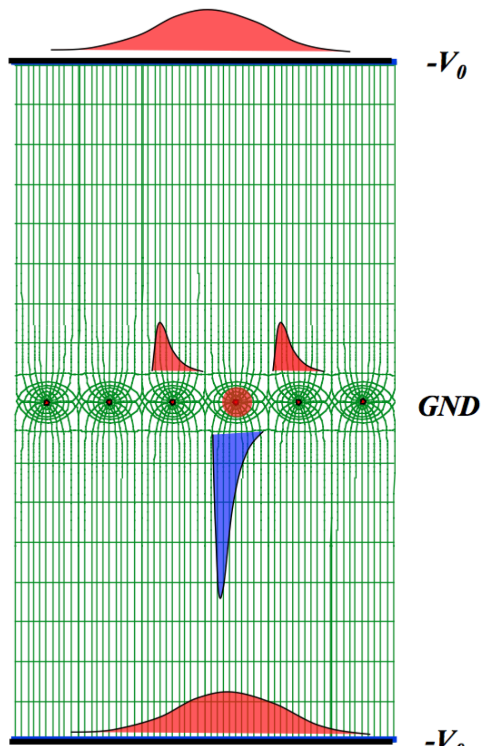

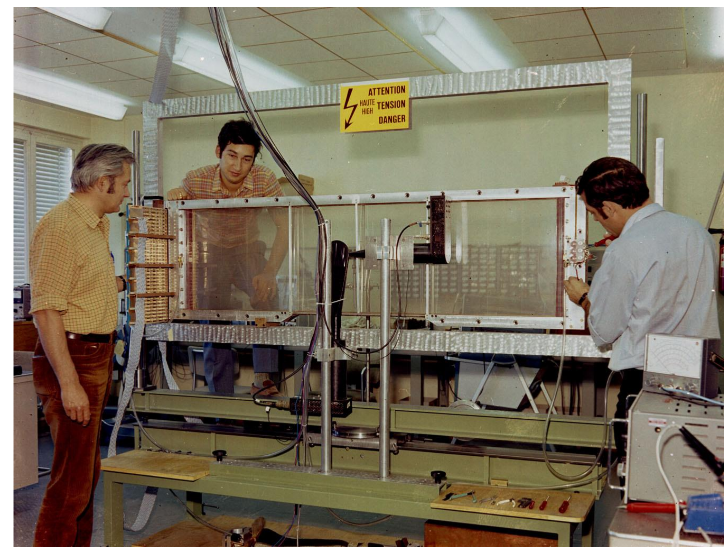

E = 0 : THERMAL DIFFUSION (Ions and electrons):

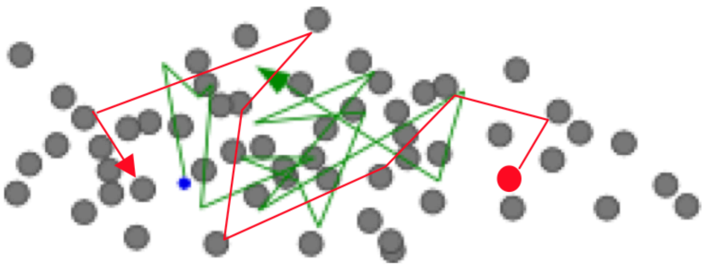

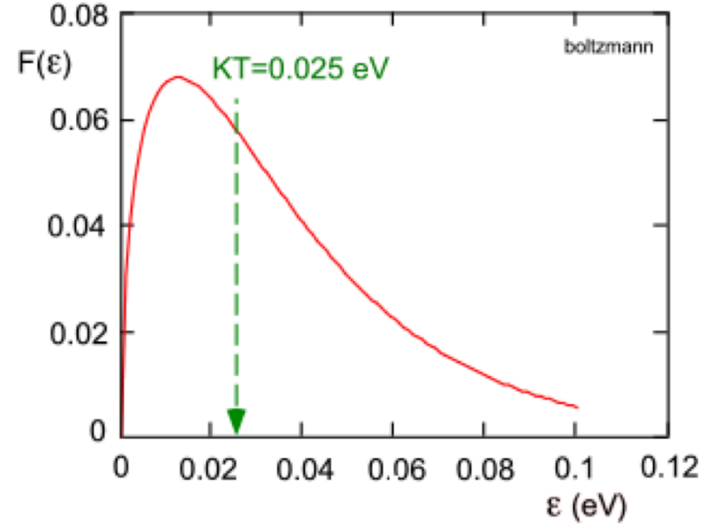

Maxwell energy distribution: $F(\varepsilon) = C\sqrt{\varepsilon}\, e^{-\frac{\varepsilon}{KT}}$

E > 0: CHARGE TRANSPORT AND DIFFUSION

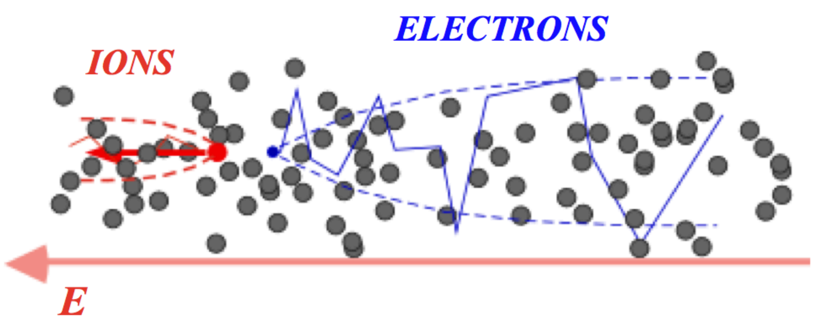

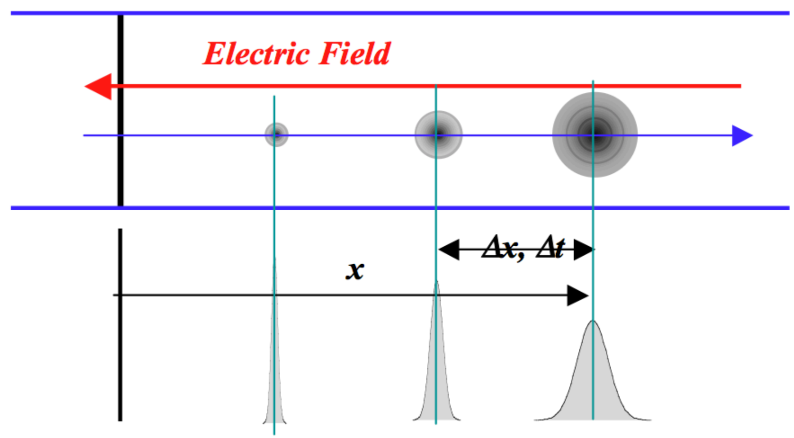

Drift velocity: $w = \frac{\Delta x}{\Delta t}$

Diffusion: $\sigma = \sqrt{2Dt} = \sqrt{2D\frac{x}{w}}$

Distances in gas

Avogadro's number: $6.022\ 10^{23}$ atoms/mole

Atomic weight of Ar: 40 g/mole

Density of Ar: $1.662\ 10^{-3}$ g/cm^3

Number of atoms in 1 cm3 $\rho = 2.7\ 10^{19}$ at/cm^3

Distances between neighbouring Ar atoms $\frac{4}{3}\pi r^3 \times 2.5\ 10^{19} = 1$ d = 4 nm

Cross section of Ar (hard sphere model)

Radius ≈ 70 pm → surface $\sigma = \pi\,(70.10^{-10}\ \mathrm{cm})^2 = 1.5\ 10^{-16}\ \mathrm{cm}^2$

Mean free path for interaction $\lambda_e = 1/\sigma.\rho = 2.7\ \mu\mathrm{m}$

Magboltz: Complete Monte-Carlo program to simulate gas detectors (CERN)

Electron cross section in Ar

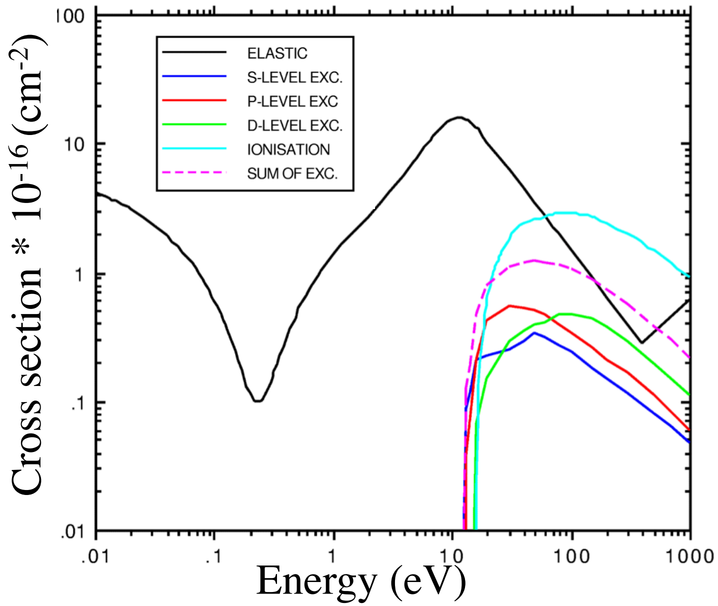

MAIN ELECTRON-MOLECULE INELASTIC PROCESSES:

1)	A+e	⇒	A^{+}+e+e	Ionisation by electronic impact.
2)	A+e	⇒	A^{*}+e	Excitation by electronic impact.
3)	A^{*}+e	⇒	A+e	Deexcitation by electronic collision.
4)	A+hν	⇒	A^{*}	Photo-excitation (absorption of light).
5)	A^{*}	⇒	A+hν	Photo-emission (radiative deexcitation).
6)	A+hν	⇒	A^{+}+e	Photoionisation.
7)	A^{+}+e	⇒	A+hν	Radiative recombination.
8)	A^{+}+B+e	⇒	A+B	Three body recombination.
9)	A^{*}+B	⇒	A+B^{*}	Collisional deexcitation.
10)	A^{*}+B	⇒	A+B^{+}+e	Penning effect.
11)	A^{+}+B	⇒	A+B^{+}	Charge exchange.
12)	A^{+}+B	⇒	A^{+}+B^{+}+e	Ionisation by ionic impact.
13)	A+B	⇒	A^{*}+B	Excitation by atomic impact.
14)	A+B	⇒	A^{+}+B+e	Ionisation by atomic impact.
15)	A+e	⇒	A^{-}	Formation of negative ions.
16)	A^{-}	⇒	A+e	Electrons release by negative ions.
17)	A^{**}+A	⇒	A_2^{+}+e	Associative ionisation.
18)	A^{+}+2A	⇒	A_2^{+}+A	Molecular ion formation.
19)	A^{*}+A+A	⇒	A_2^{*}+A	Excimer formation.
20)	A_2^{*}	⇒	A+A+hν	Radiative excimer dissociation.
21)	$(XY)^{*}$	⇒	X+Y^{*}	Dissociation.
22)	$(XY)^{+}$+e	⇒	X+Y^{*}	Recombinational dissociation

J.Meek and J. D. Cragg, Electrical Breakdown of Gases (Clarendon Press, Oxford 1953)

Electron drift velocity in Ar

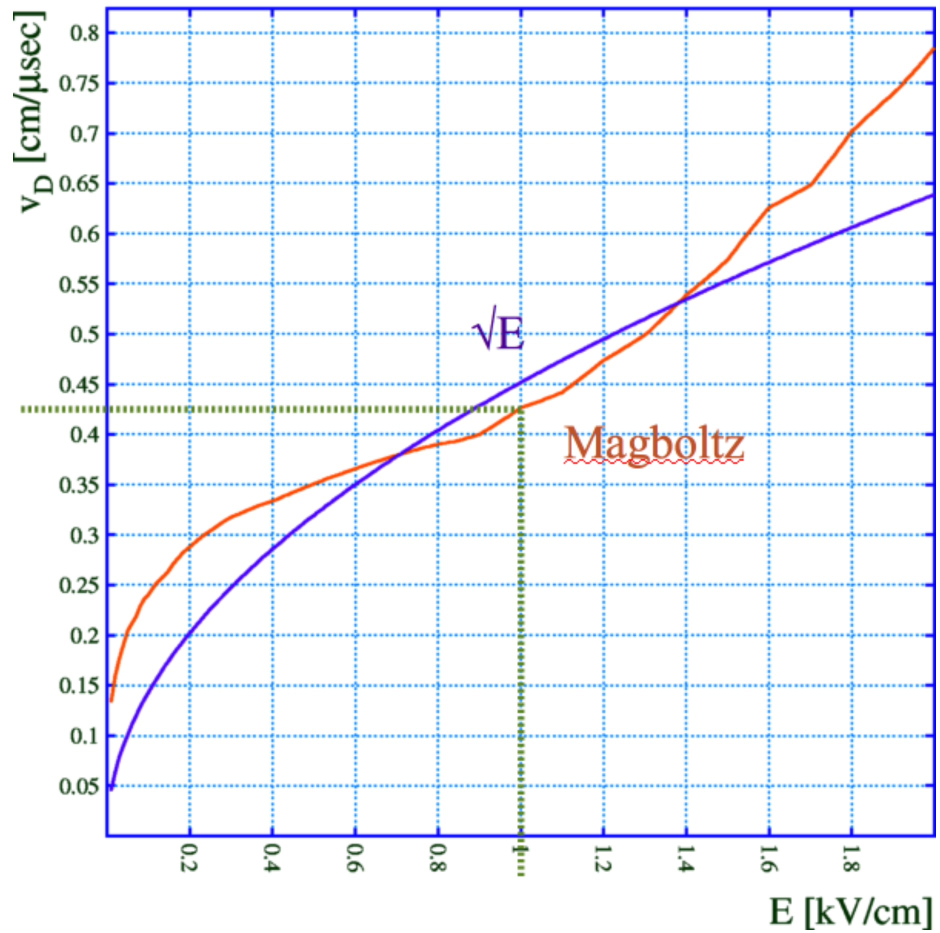

E=1 kV/cm → v = 0.4 cm/μs

Magboltz calculation for Ar+CO2 at 3 bars

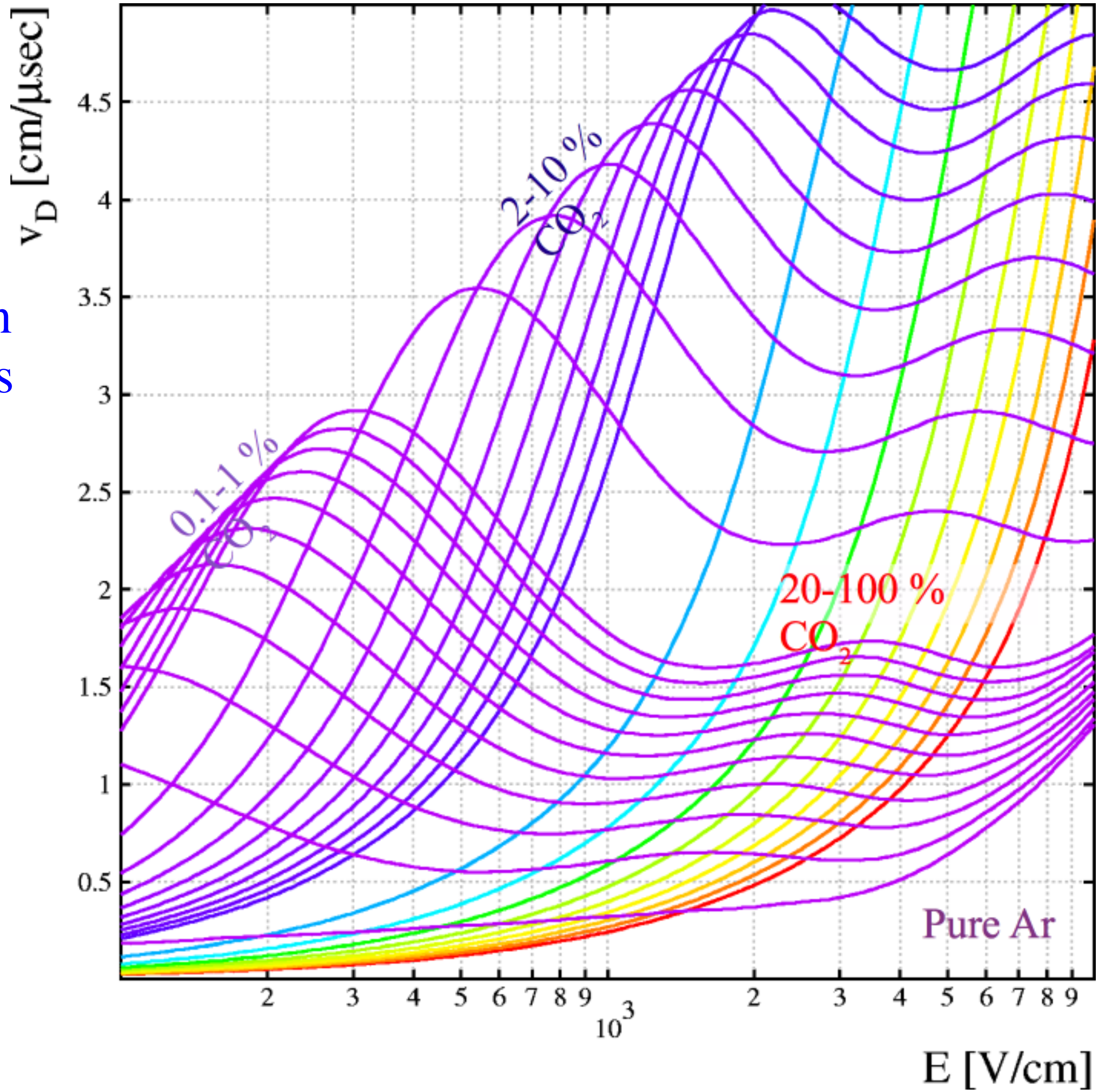

Addition of CO_2 to Ar makes the gas faster

Magboltz calculation for Ar+CO2 at 3 bars

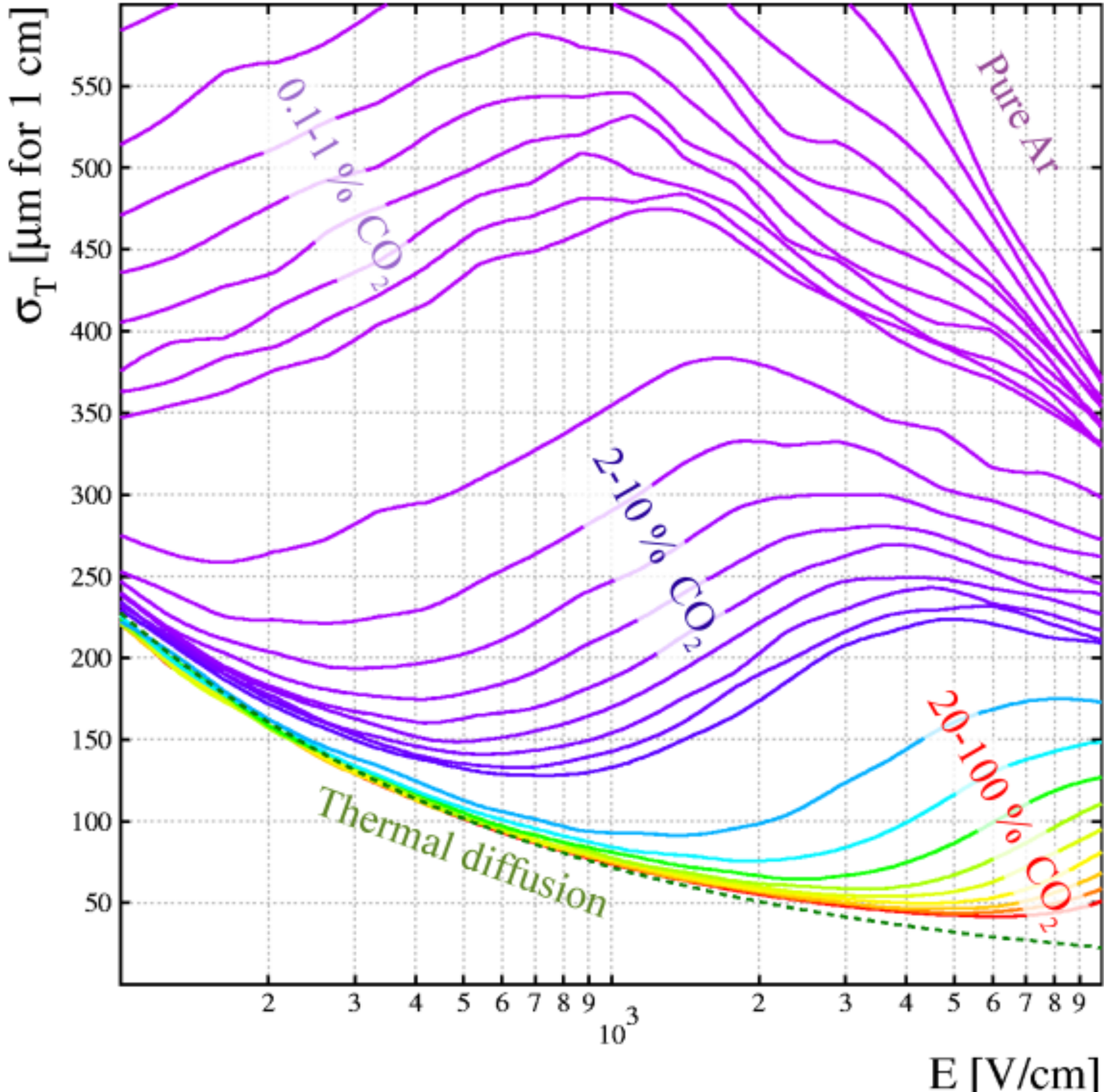

Transverse diffusion is reduced by CO2

Effect of increasing the electric field

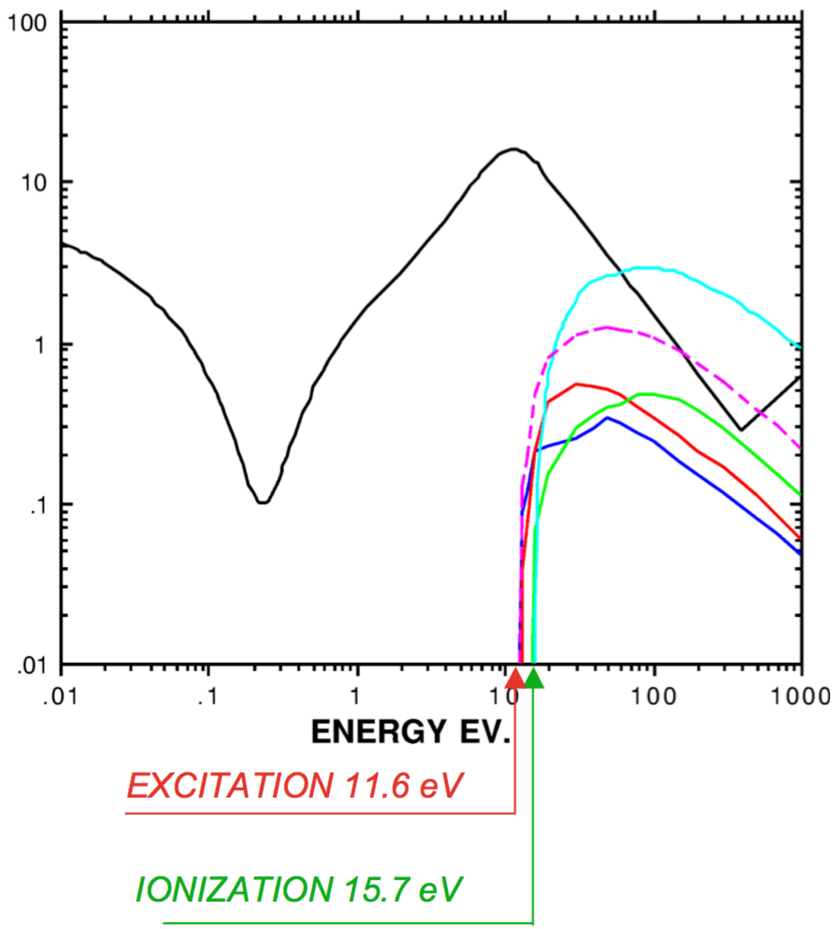

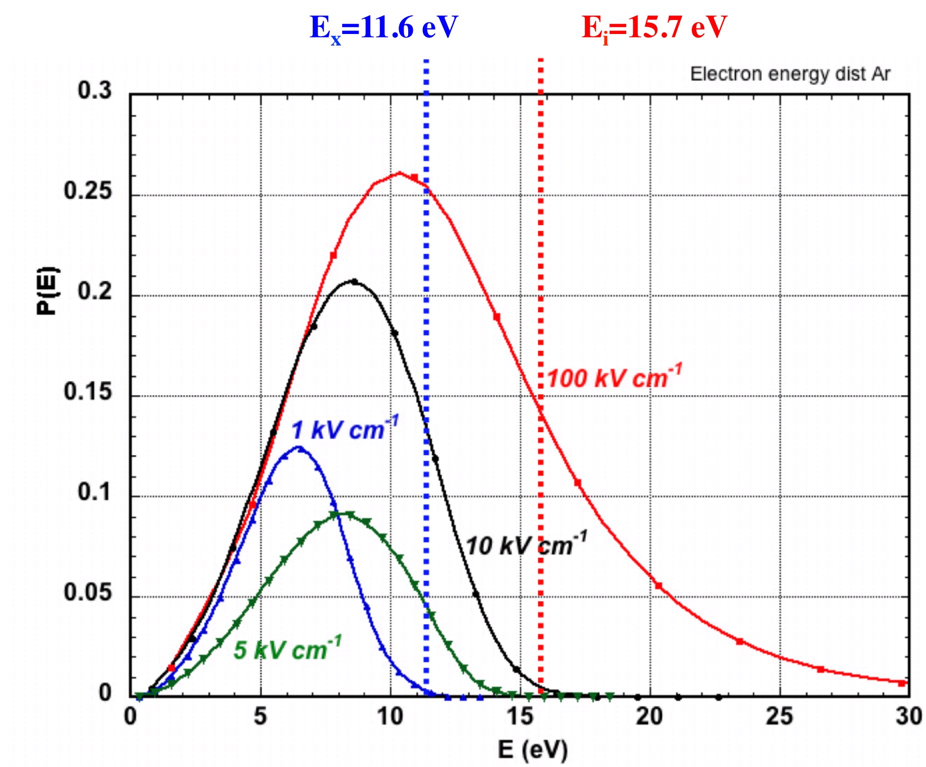

Electrons energy distribution in Argon
at increasing electric fields

Effect of changing the gas

EQUAL FIELD, DIFFERENT GAS:

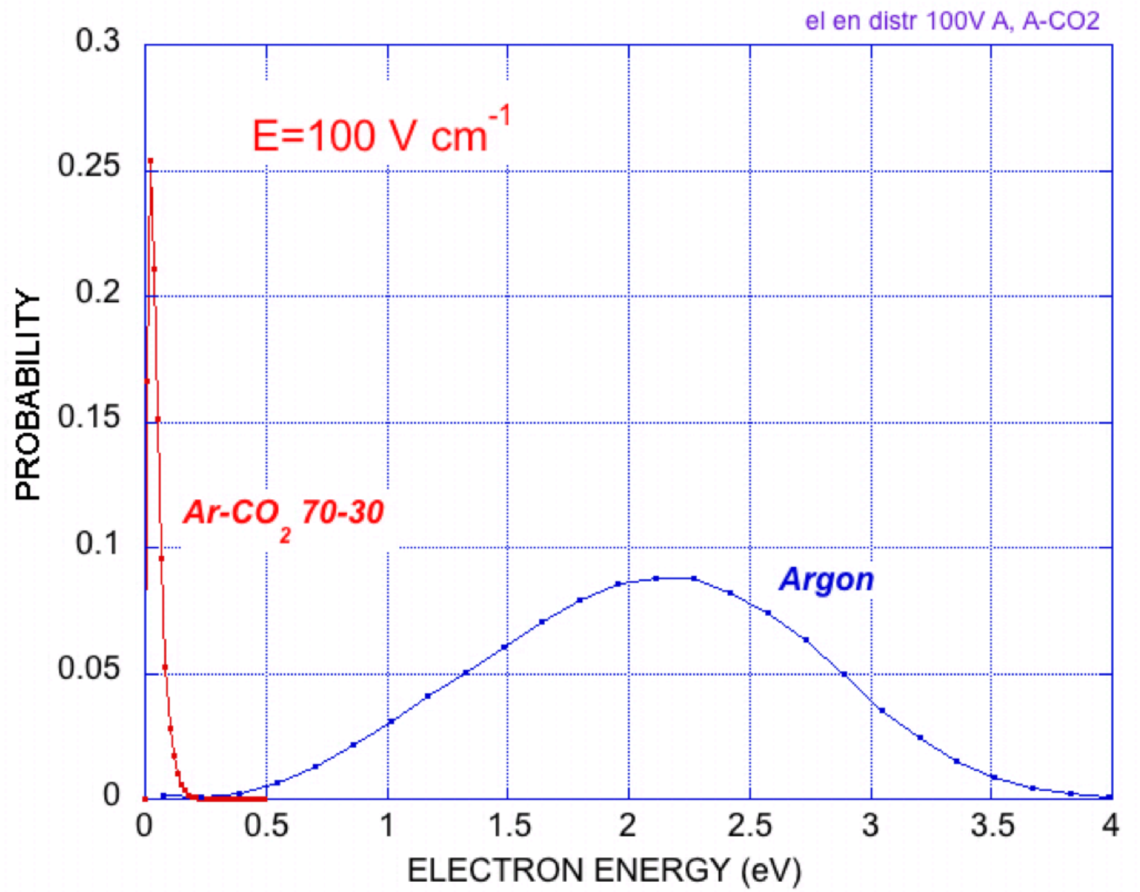

Charge multiplication in a uniform E (simple model)

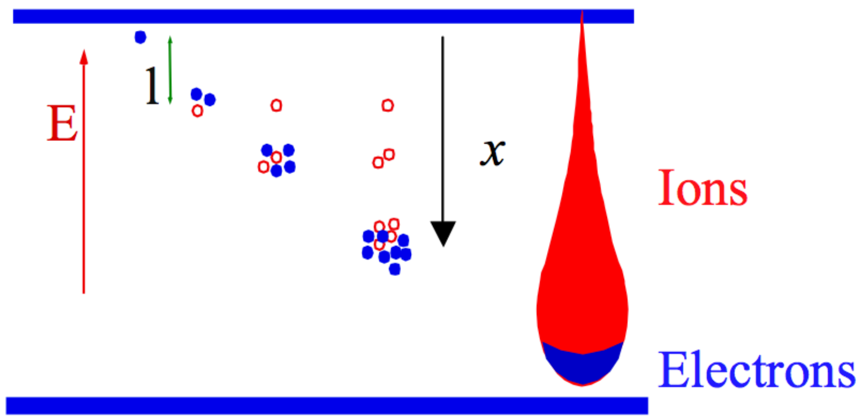

Mean free path for ionization

$$\lambda = \frac{1}{N.\sigma}$$

N = density of molecules per cm3
σ = ionization cross section

Number of collisions per cm $\alpha = \frac{1}{\lambda}$ ‣ α is called Townsend coefficient $\frac{\alpha}{P} = f\left(\frac{E}{P}\right)$

Incremental increase of the number of charges in the avalanche : dn(x) = n(x).α(x).dx

Multiplication factor (Gain) M = n(x)/n(0) = $e^{\int_0^x \alpha(y)\,dy}$

TOWNSEND COEFFICIENT FOR Ar, CH_4 and Ar-CH_4:

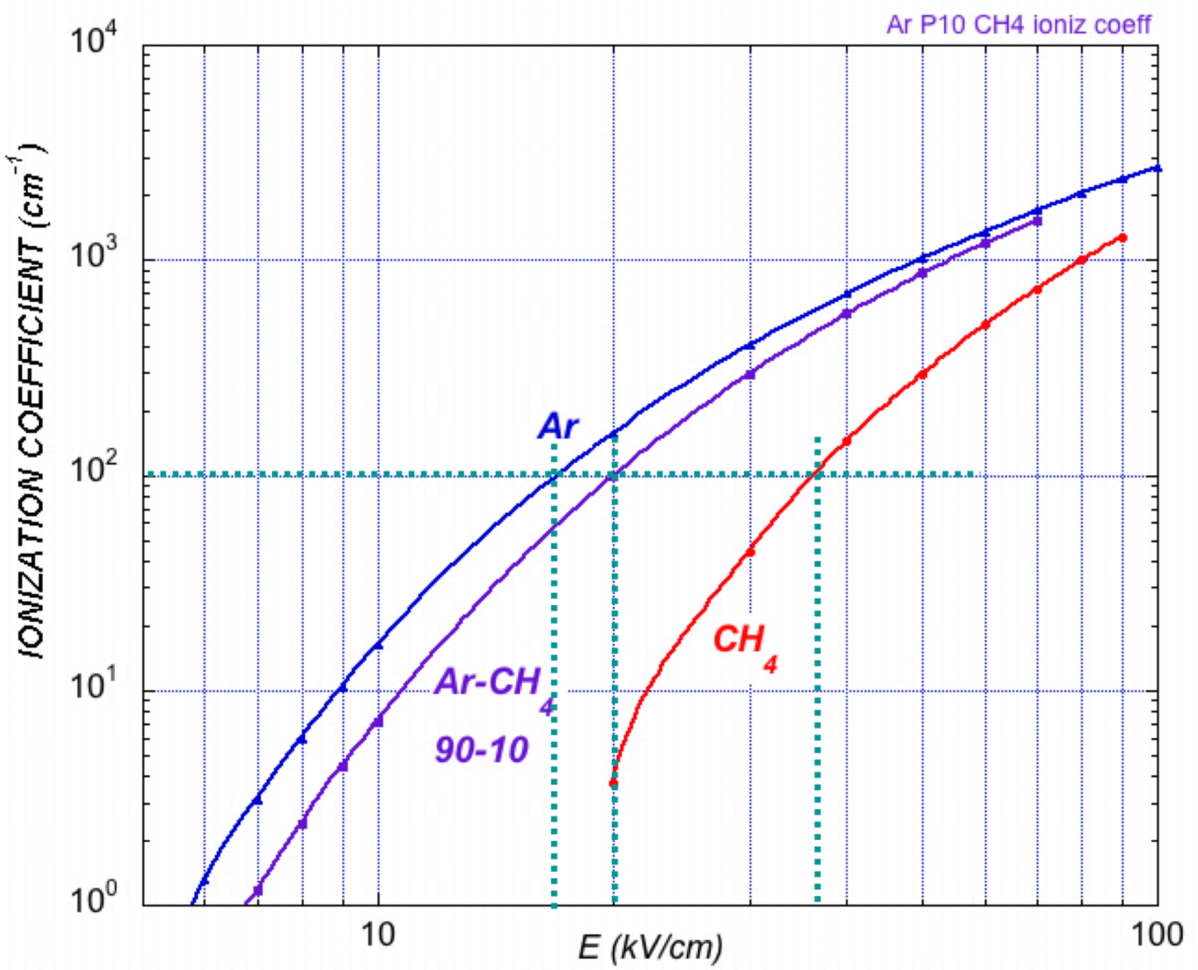

Gas amplification strongly depends on the gas mixture

Cylindrical proportional counter

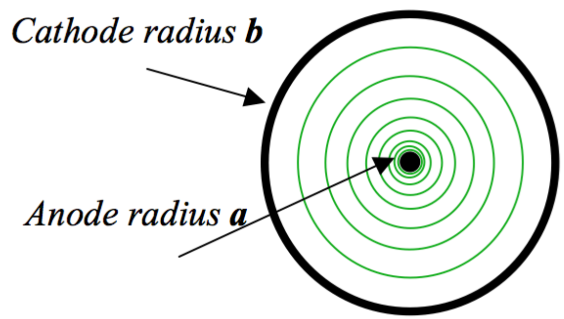

ELECTRIC FIELD AND POTENTIAL:

$$E(r) = \frac{CV_0}{2\pi\varepsilon_0}\frac{1}{r}$$

$$V(r) = \frac{CV_0}{2\pi\varepsilon_0}\ln\frac{r}{a}$$

$$C = \frac{2\pi\varepsilon_0}{\ln(b/a)}$$ capacitance per unit length

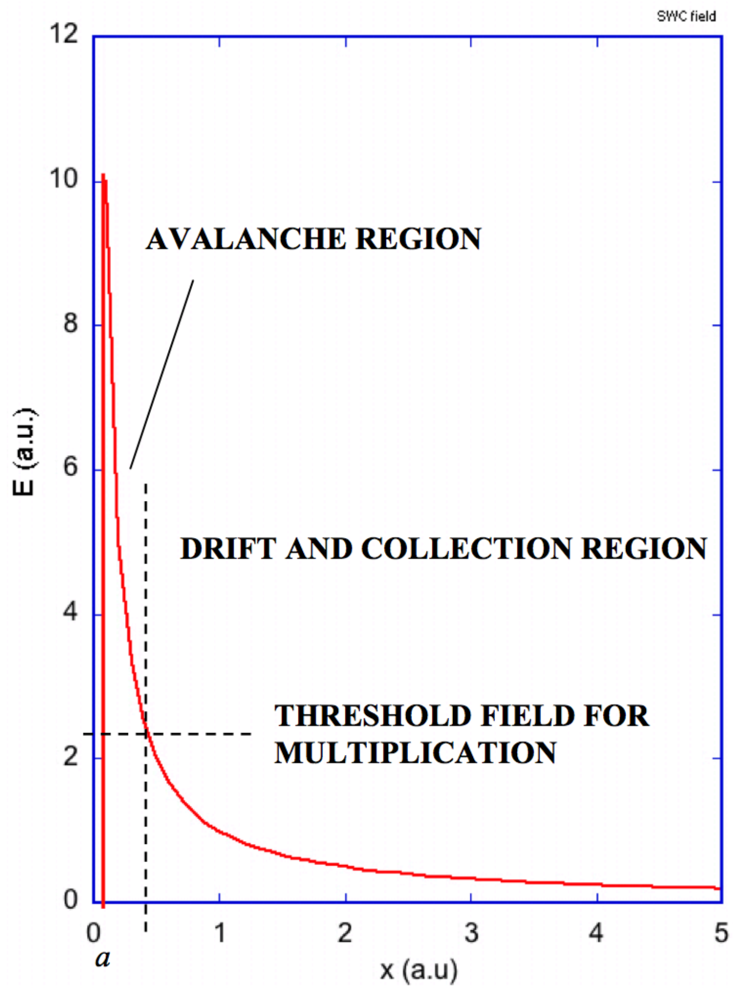

The avalanche process in a proportional counter

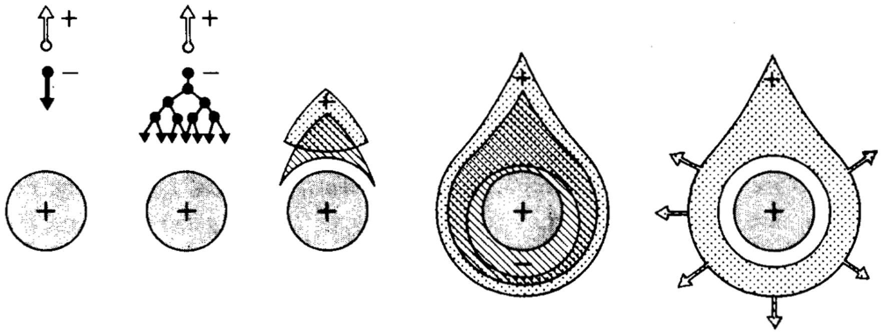

1/ Primary electrons drift toward the anode and primary ions to the cathode

2/ When the electrons reach the high E field around the anode, they are sufficiently accelerated between collision to ionize other molecules of gas

3/ Each primary electron induces a process of charge multiplication (avalanche). The amplification gain is the average number of secondary electrons produced.

4/ Due to lateral diffusion, a drop-like avalanche surrounding the wire, develops. Electrons are collected in around 1 ns.

5/ a cloud of positive ions slowly migrate toward the cathode without memory of the primary charge location

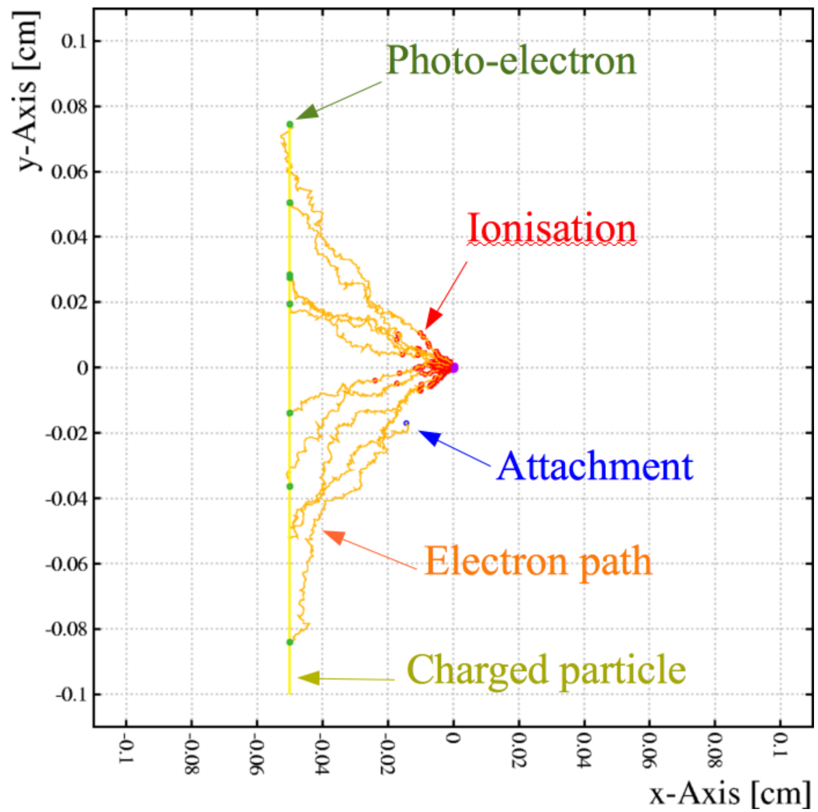

Signal induction

CHARGE SIGNAL INDUCTION:

$$q^- = \frac{Q}{V_0}\int_a^{a+\lambda}\frac{dV}{dr}dr = -\frac{QC}{2\pi\varepsilon_0}\ln\frac{a+\lambda}{a}$$

$$q^+ = \frac{Q}{V_0}\int_{a+\lambda}^{b}\frac{dV}{dr}dr = -\frac{QC}{2\pi\varepsilon_0}\ln\frac{b}{a+\lambda}$$

$$q = q^- + q^+ = -\frac{QC}{2\pi\varepsilon_0}\ln\frac{b}{a} = -Q$$

λ: distance of avalanche start

$$\frac{q^-}{q^+} = \frac{\ln(a+\lambda)-\ln a}{\ln b - \ln(a+\lambda)} \approx 0.01$$

99% of signal due to positive ions

$$q(t) = -\frac{QC}{2\pi\varepsilon_0}\ln\left(1+\frac{\mu^+ CV_0}{2\pi\varepsilon_0 a^2}t\right) = -\frac{QC}{2\pi\varepsilon_0}\ln\left(1+\frac{t}{t_0}\right) \qquad (t \leq T^+)$$

CHARGE SIGNAL: POSITIVE ION TAIL

RC differentiation for faster response

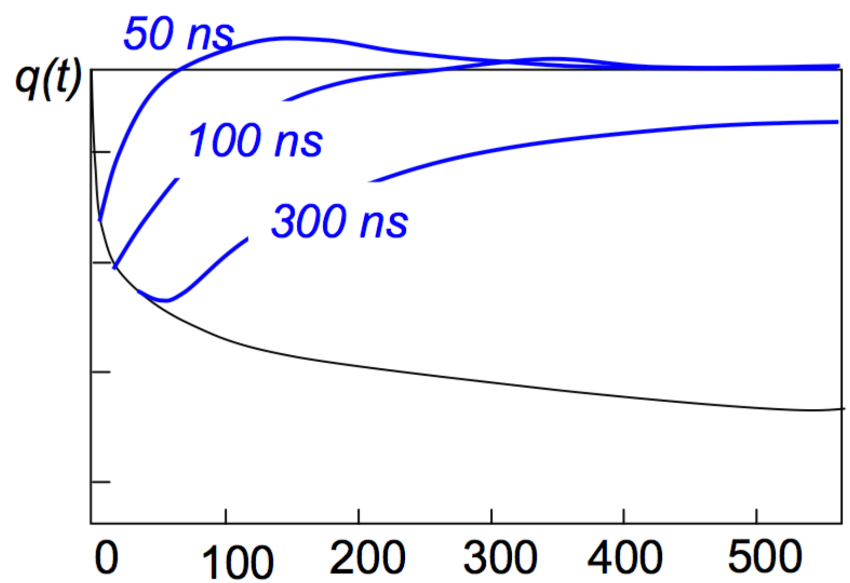

Gas detectors measure the current signal induced by the moving positive ions.

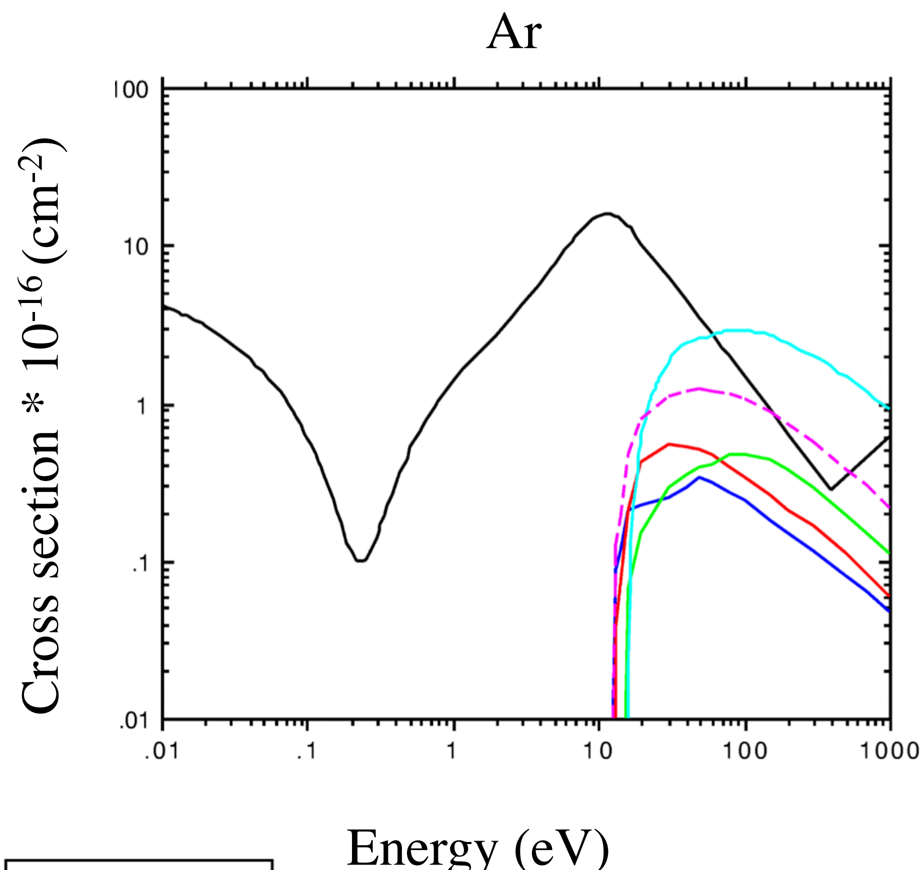

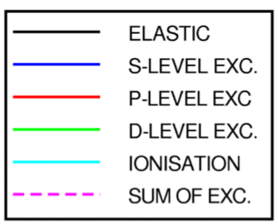

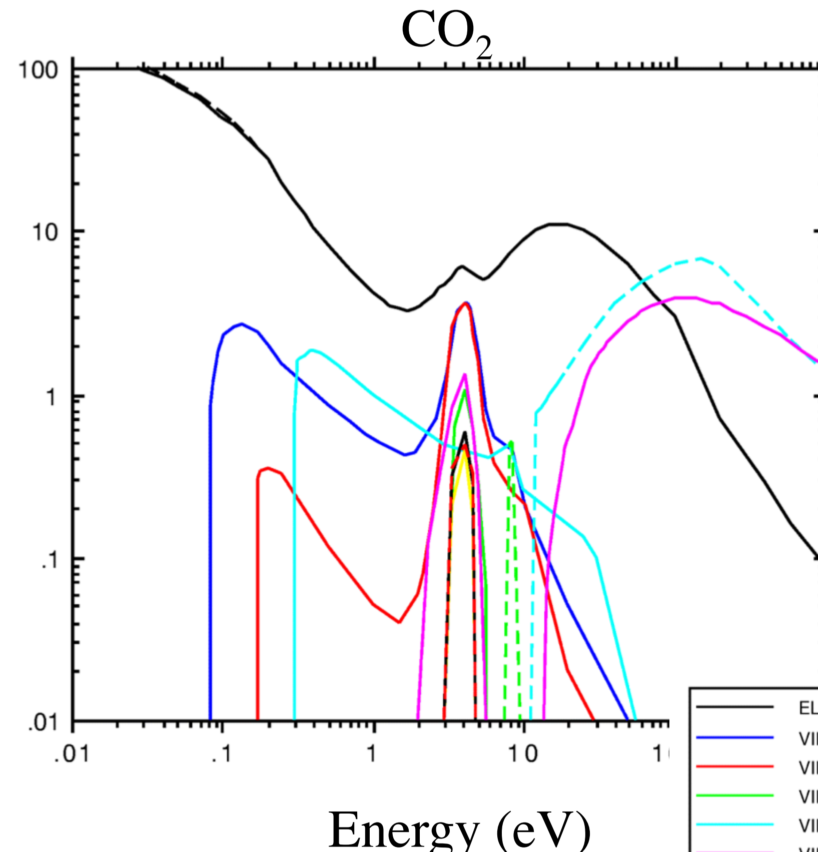

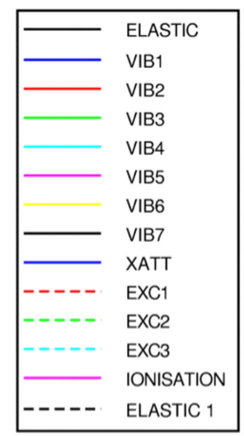

The addition of some quenching gas is needed to reach high gain operation in particular to avoid electron feedback induced by UV photons emitted during the avalanche

The G(V) curve

By operating the detector in the proportional mode, each avalanche is created independently from others → the signal produced is proportional to the energy liberated by the particle.

Needed for gamma discrimination in neutron detectors.

Choice of the gas :

Low working voltage

High gain operation

High arte capability

Long lifetime

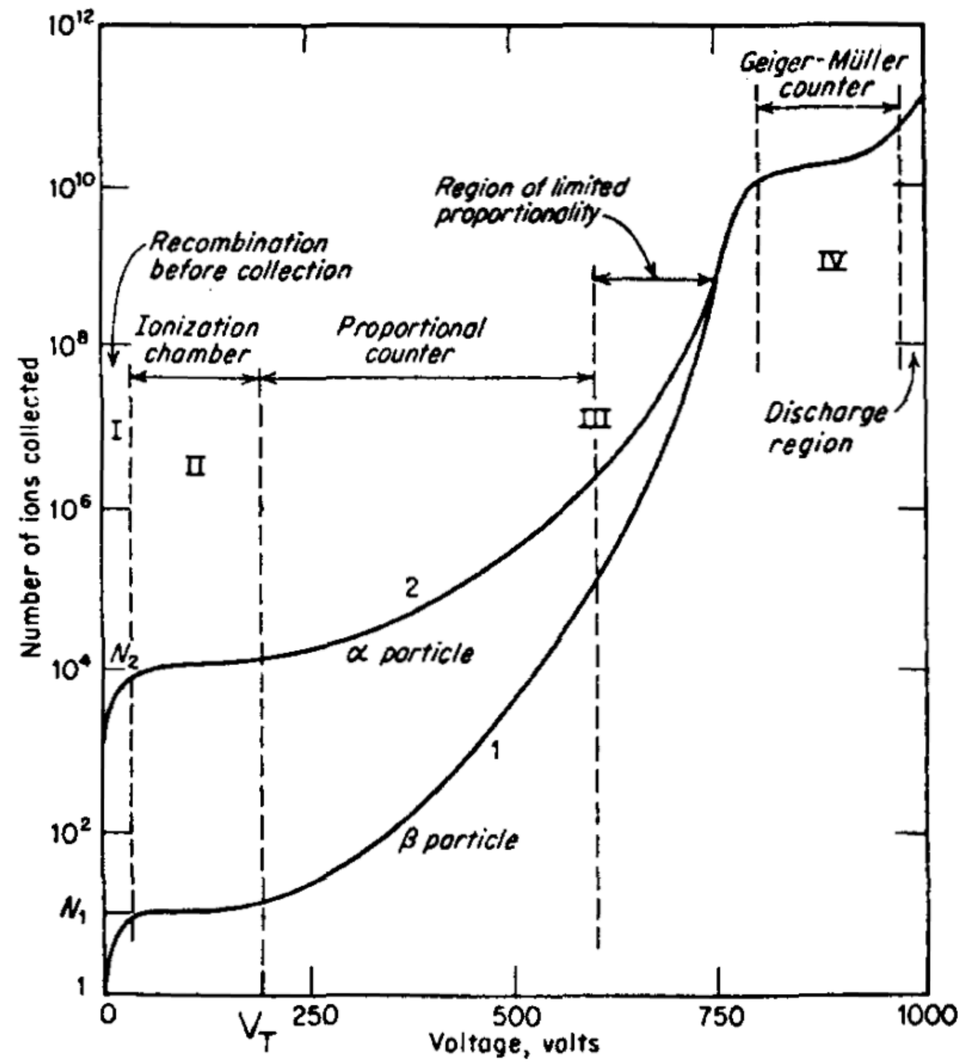

Fig. 50 Gain-voltage characteristics for a proportional counter, showing the different regions of operation (from W. Price, see bibliography for Sections 2 and 3).

^{3}He proportional counters

$^3He + n \rightarrow p + {^3H} + 764$ KeV
5333 barns @ 1.8 angstroms (25 meV)

Main features
- Good gamma discrimination
- high detection efficiency
- mixed with a stopping gas

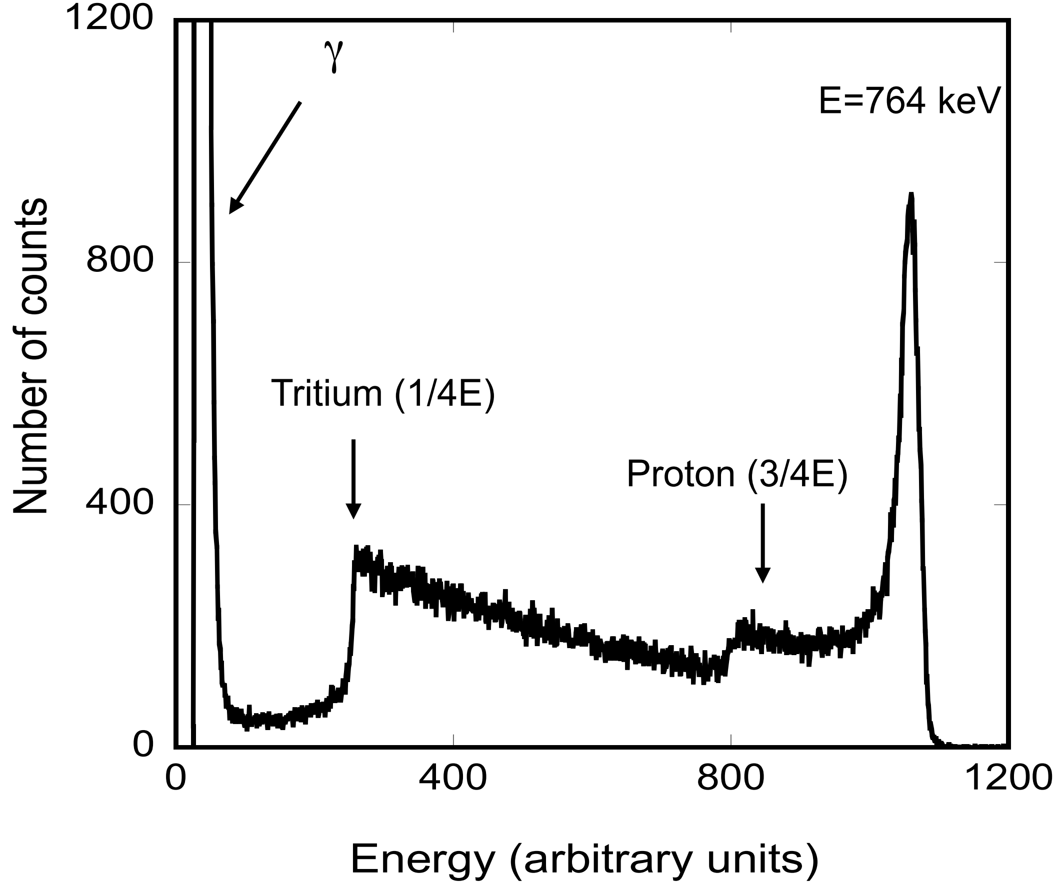

Pulse height spectrum measured with a single ^{3}He counter and a low noise FET pre-amplifier

Electron attachement du to electro-negative impurities in the gas

Attachment cross section of Oxygen

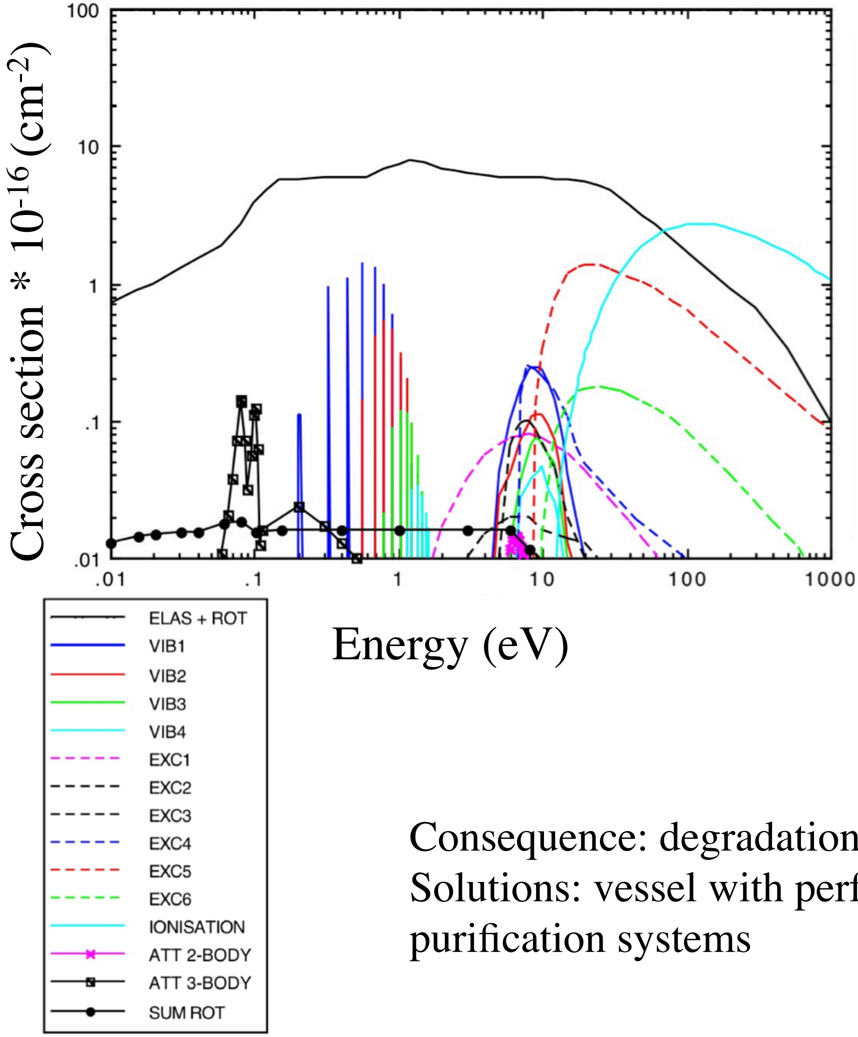

ELECTRONS SURVIVING AFTER 20 CM DRIFT
(E = 200 V/cm):

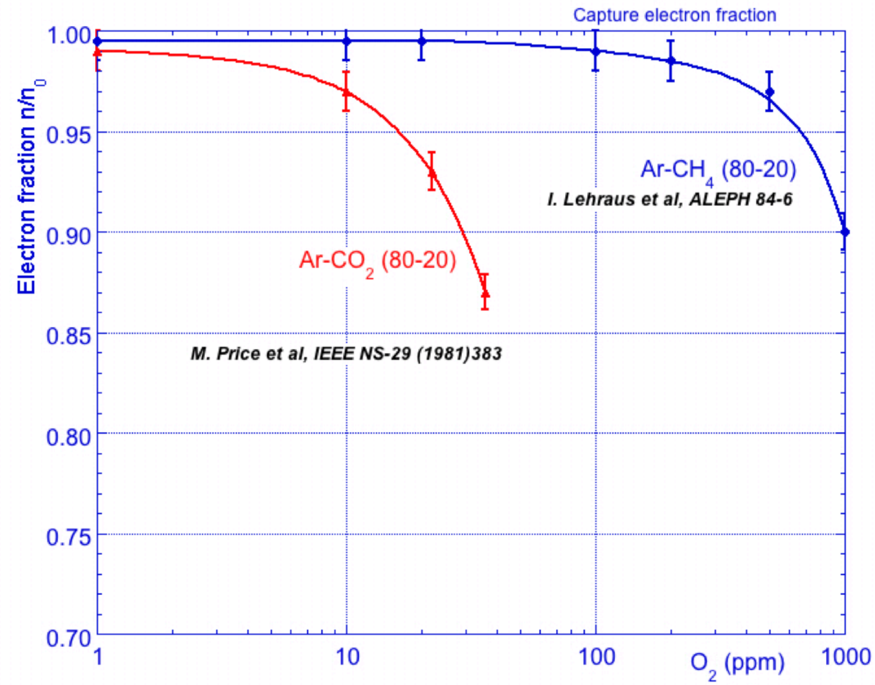

Consequence: degradation of the energy resolution
Solutions: vessel with perfect gas tighness, continuous gas flushing, purification systems

Gamma sensitivity

Neutrons instruments are exposed to an intense gamma field to which the detector should be non sensitive.
Solutions:
- Shielding : high Z material in front of the detector
- low Z gas to lower the absorption probability
- discrimination threshold adjusted according to the gamma PH on the instrument

ABSORPTION LENGTH IN GASES (STP) VS PHOTON ENERGY

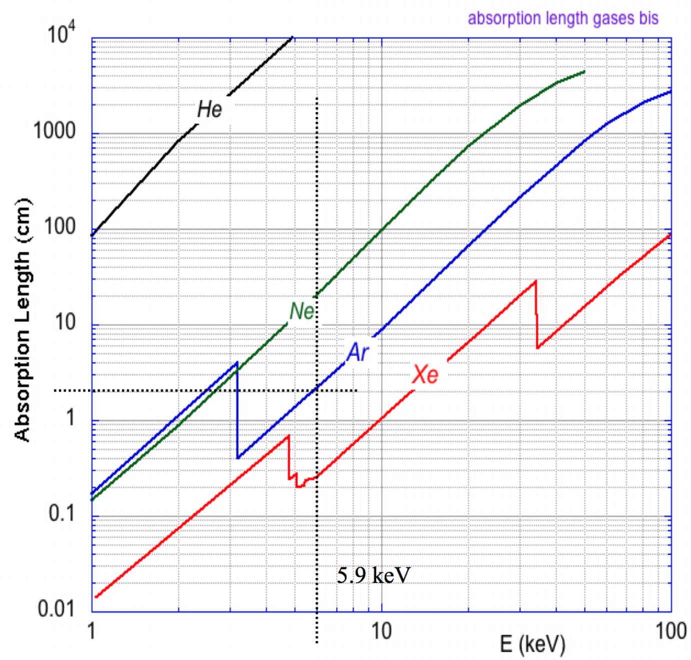

Space charge effect

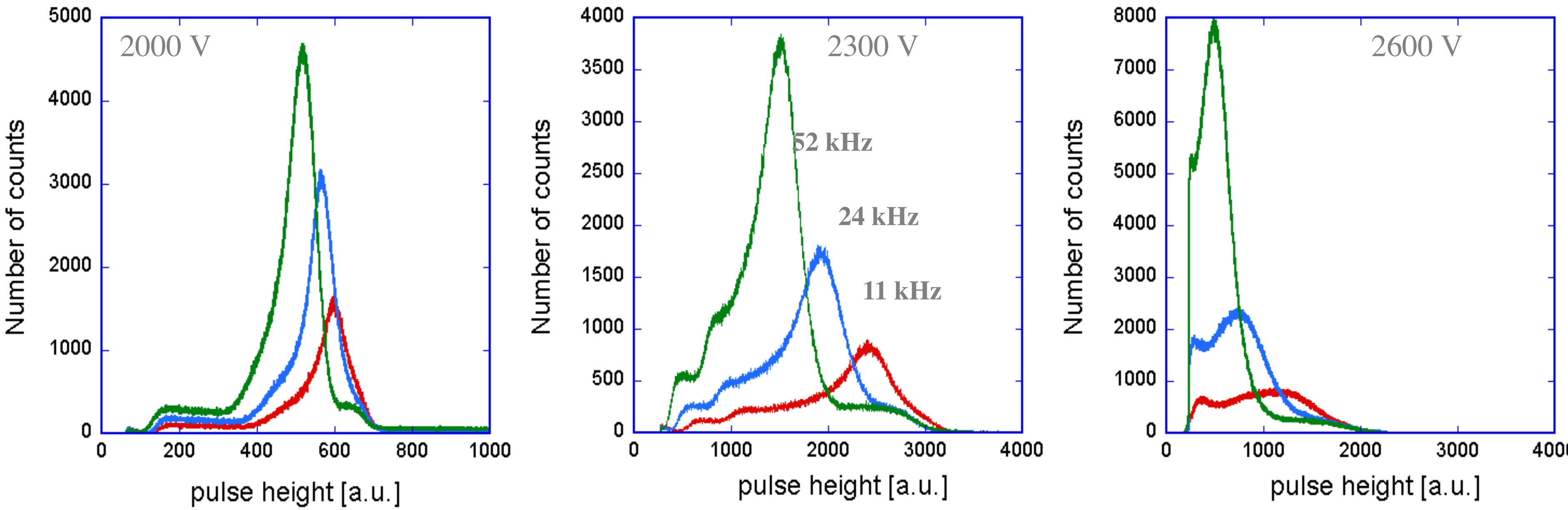

Variation of the detector response at different gain and count rate

The Centre of Gravity shift

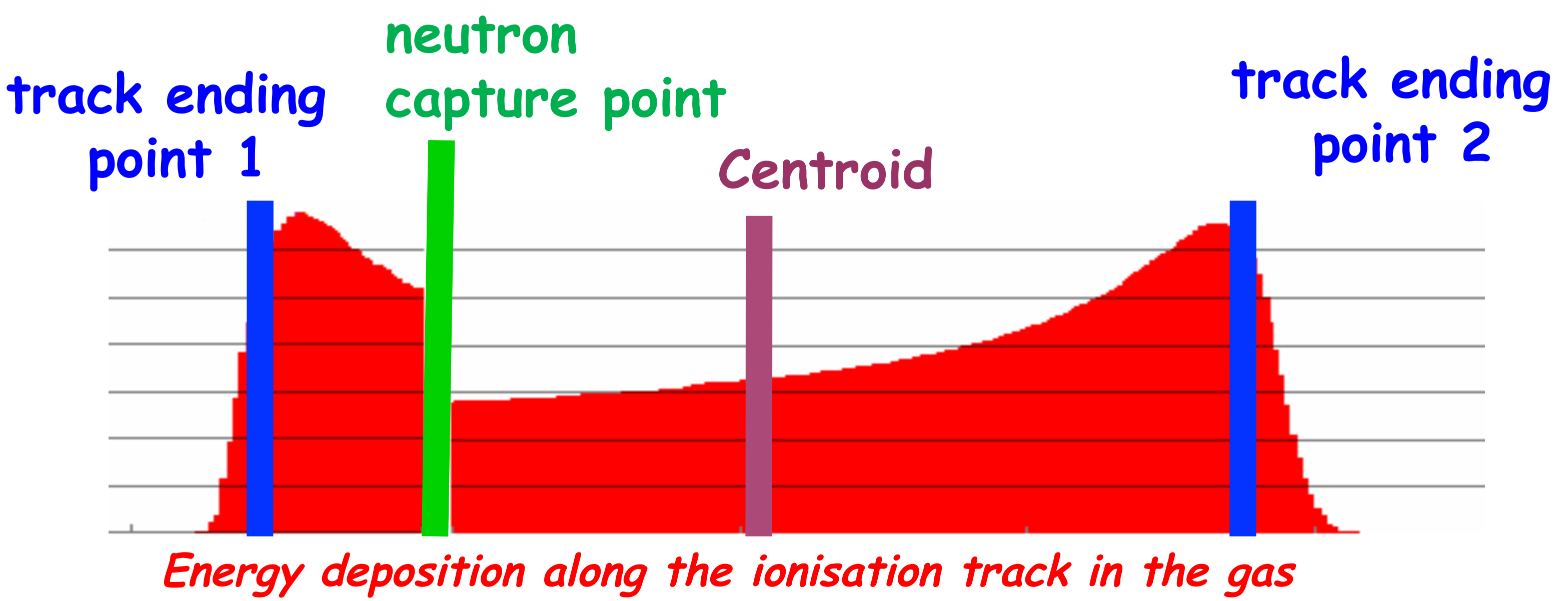

Case 1:
gas convertor

1/ TPC
Track reconstruction + particle identification → capture point
Requires a lot of information + processing

2/ FAS (First Active Signal)
The result depends on the amplifier shaping time:
Fast → 1 of the 2 ending points
Slow → Max of the charge → centroid

3/ TOT (Time Over Threshold Signal)
Max TOT or Center of Gravity of the TOT→ centroid

5/ The barycenter shift

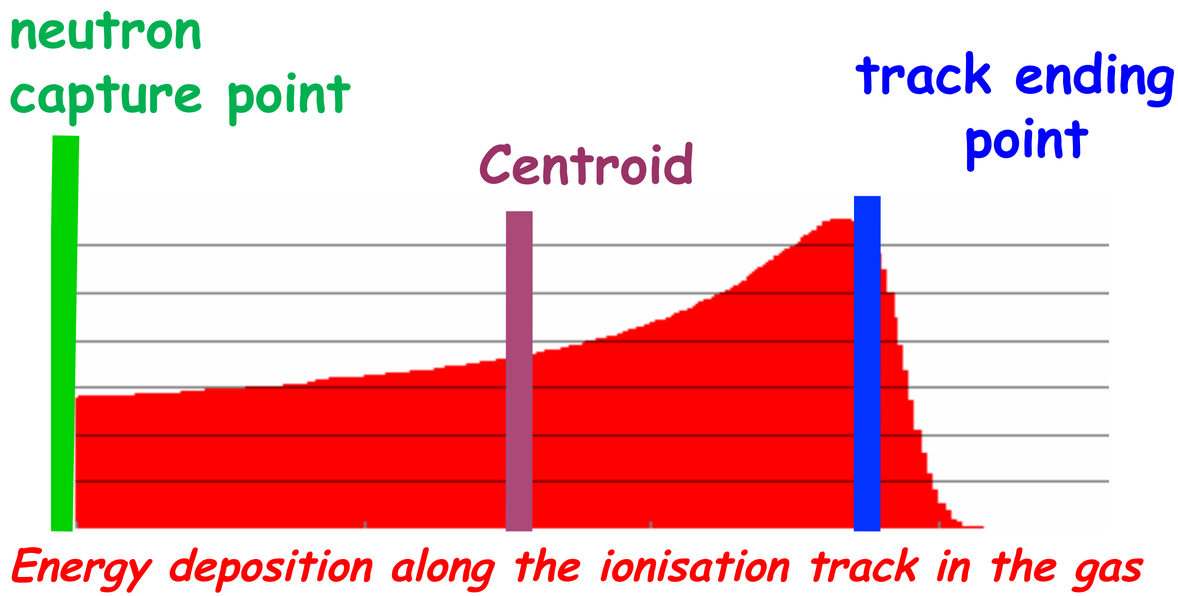

Case 2:
Solid convertor
in gas

The convertor film is coated on a substrate facing the amplifying electrode
→ the FAS is not a good localization estimator

1/ LAS (LastActive Signal) → interaction point
accessible with parallel readout electronics ; not practical with thin film convertors due to the high number of readout channels

2/ TOT (Time Over Threshold Signal)
Max TOT or Center of Gravity of the TOT→ centroid

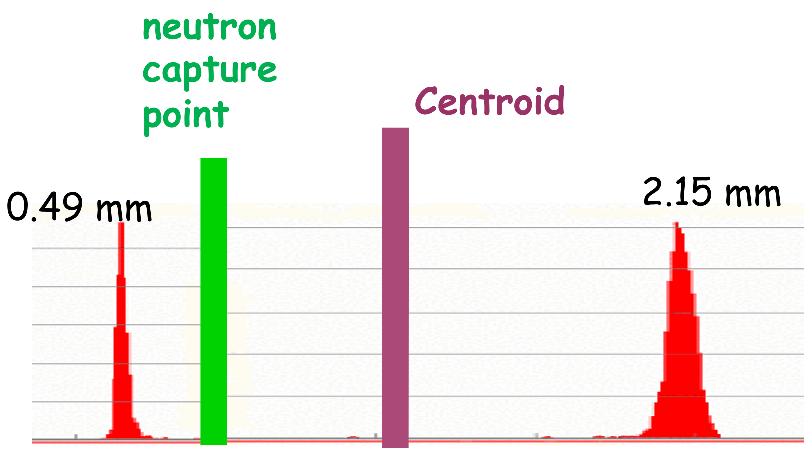

Particle ranges (proton and tritium) in 2 bars of CF4

Calculated with http://www.srim.org/

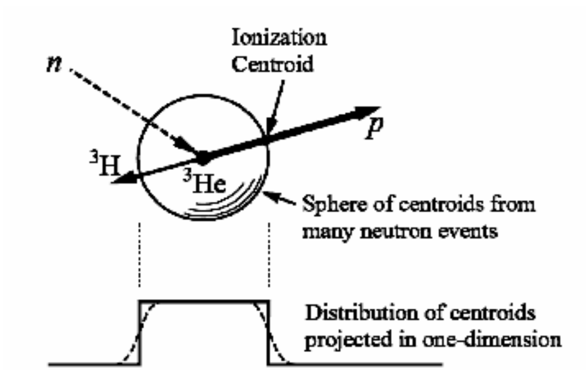

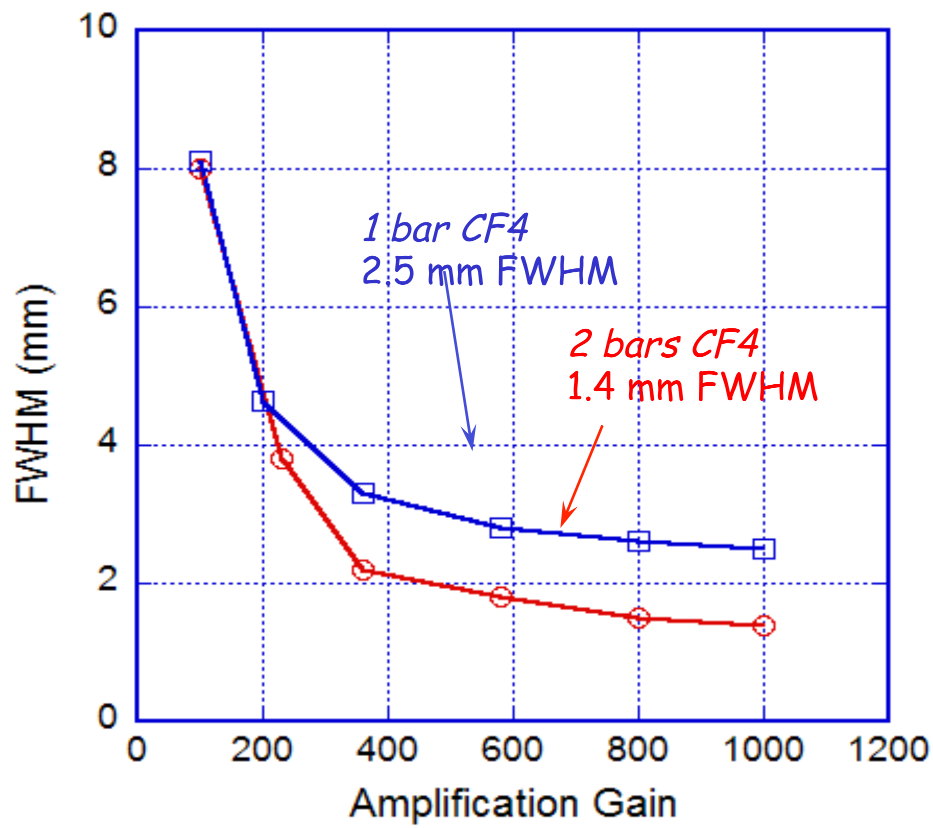

Position resolution versus amplification gain and stopping gas pressure

The centroid is distributed on a sphere with a diameter = **70% the proton range**
The projection of the sphere on each localization axis is a rectangle

6/ Parallax error

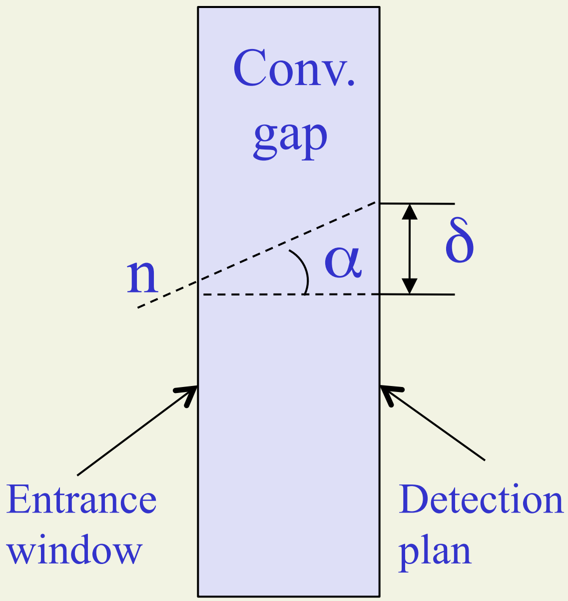

Example

- L2 (sample to detector) = 50 cm
- Gap = 1 cm

→ δ = 3 mm @ 15 cm from the detector center

Detection efficiency versus Gas pressure

$\varepsilon = \exp[-\mu_{al} * ep_W] * (1 - \exp[-\mu_{3He} * ep_{Gap}])$

$\mu = \rho * \sigma$ *absorption coef*
ρ *material density*
σ *interaction cross-section*

ε= 14% @ 1 cm.bar

Typical value used: 10 cm.bar

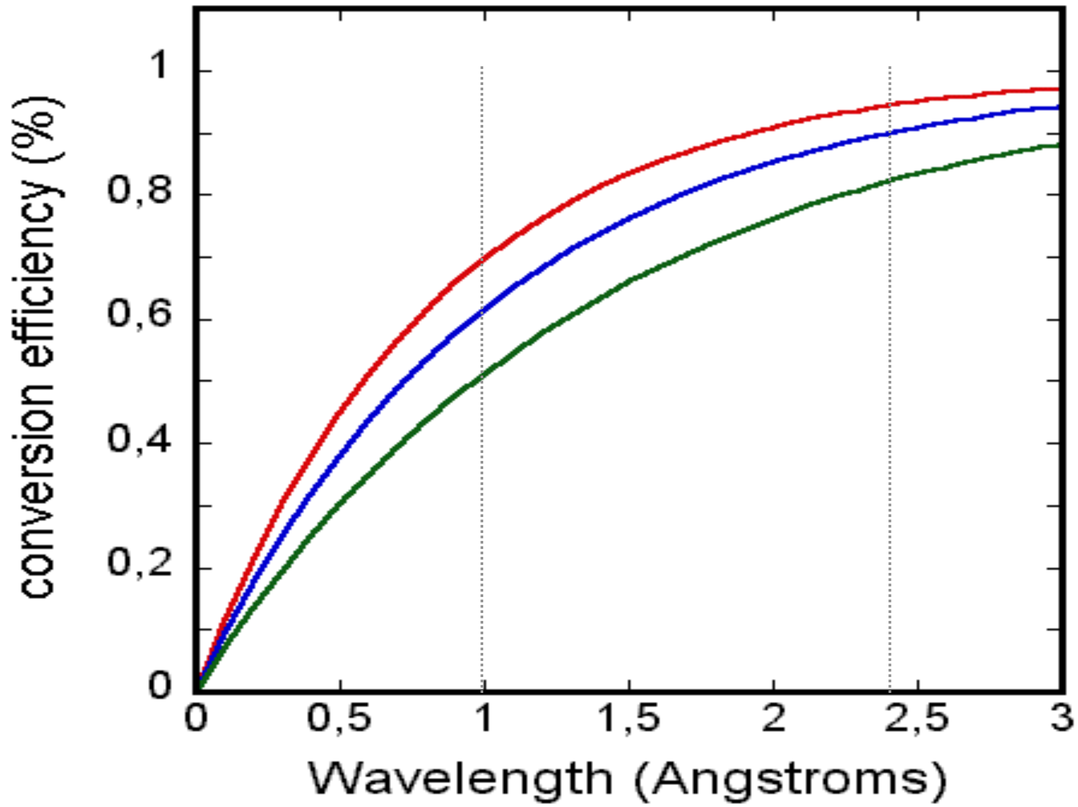

Capture probability in 3 cm of ^3He for 3,4,5 bars of pressure

Detection efficiency measurement

Beam characterization with a Multi-counter, 3bar ^3He + 1bar CF_4

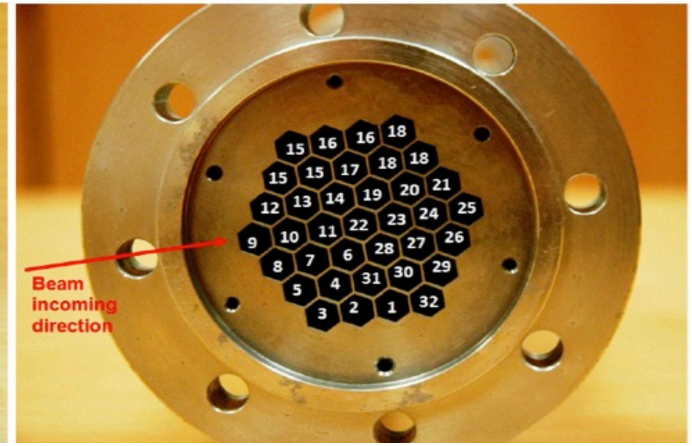

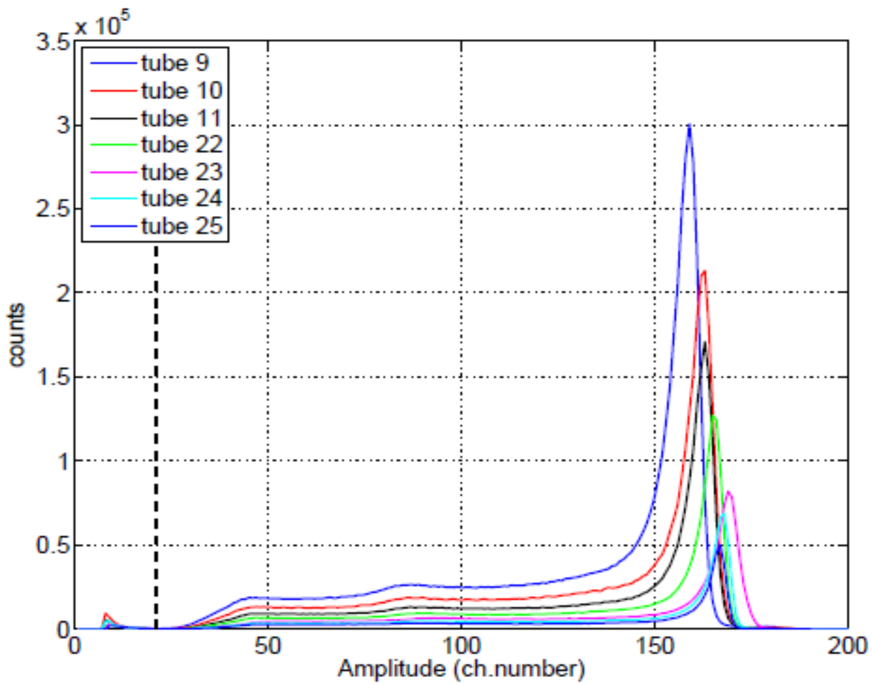

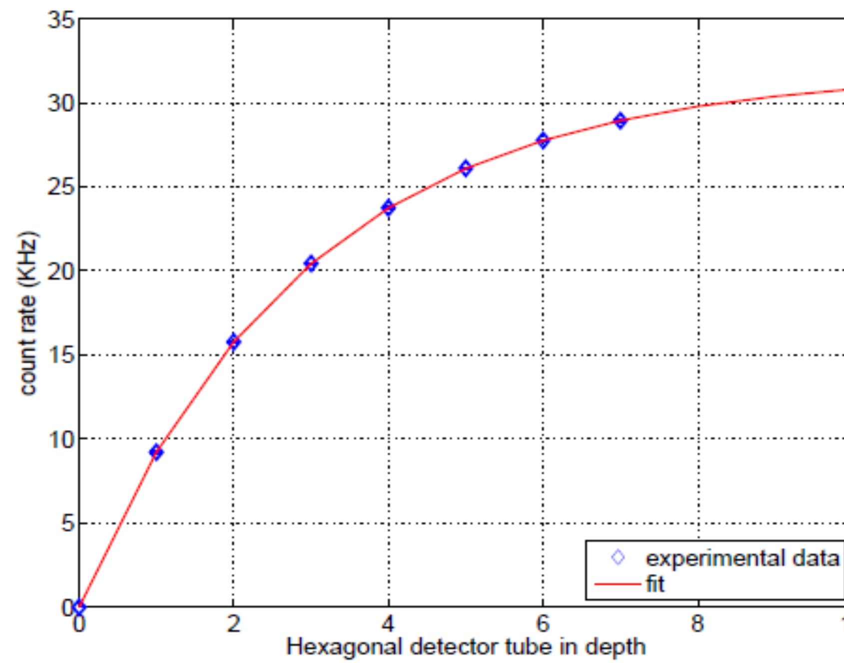

Scattering & absorption measured @ 2.5 Å, with a position sensitive counter tube, and a sample of Aluminium (5083), 5 mm thick

Measured attenuation : 5.92% (abs. + scatt.)

Calculated absorption = 1.72 %

➔ scattering = 4.2%

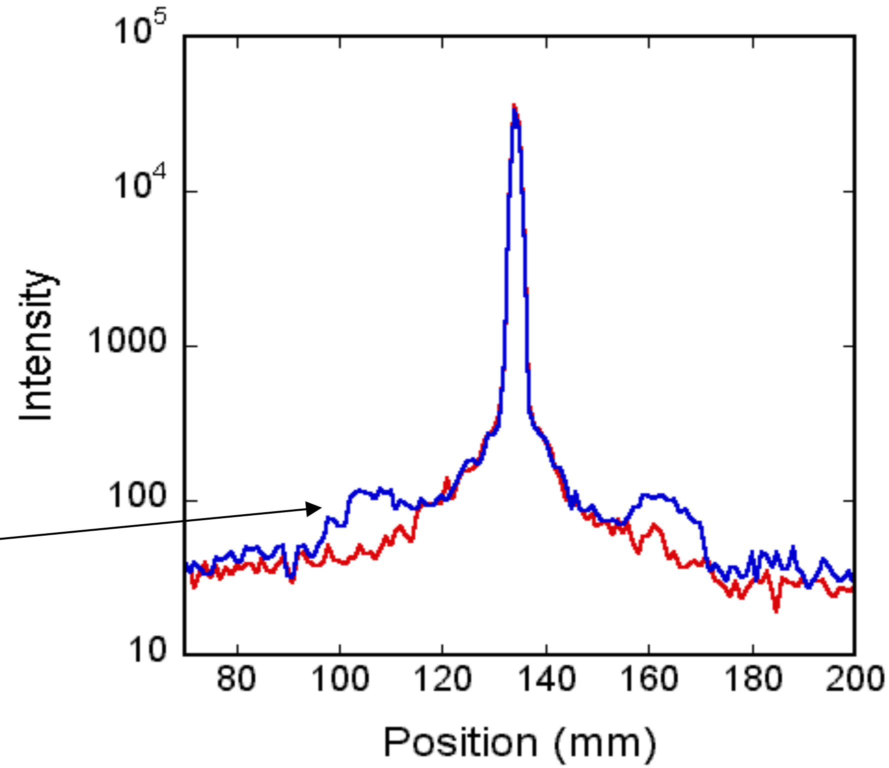

Beam attenuation $$att = e^{-\mu_{al} \times d_{wind}}$$

Choice of the gas for a 3He detector

What is the (3He-CF4) gas mixture do we have to put in a detector of 5 mm conversion gap to get 80% detection efficiency (for 2.5 Å) and to reduce the contribution of the gas to 1 mm FWHM in the spatial resolution ?

^{3}He pressure for 80% efficiency

Absorption cross-section at 2.5 Å

$$\sigma_{2.5} = \sigma_{1.8} \times \frac{2.5}{1.8} = 5333 \times 1.39 = 7406 \text{ barns}$$

Conversion efficiency $$\varepsilon = 1 - e^{-\rho \times \sigma_{2.5} \times d_{gap}}$$

$$\rho = \frac{P \times N_{av}}{V_{mol}}$$

$$V_{mol} = 22.4 \times 10^3$$

$$P = \frac{-Ln(1-\varepsilon) \times V_{mol}}{\sigma \times N_{av} \times d_{gap}} = 16 \text{ bars}$$

SRIM calculation to evaluate the added CF4 pressure required to achieve a proton range of 1mm/0.7 = 1.42 mm

1.5 bars of CF_4 + 16 bars ^3He → 1.5 mm

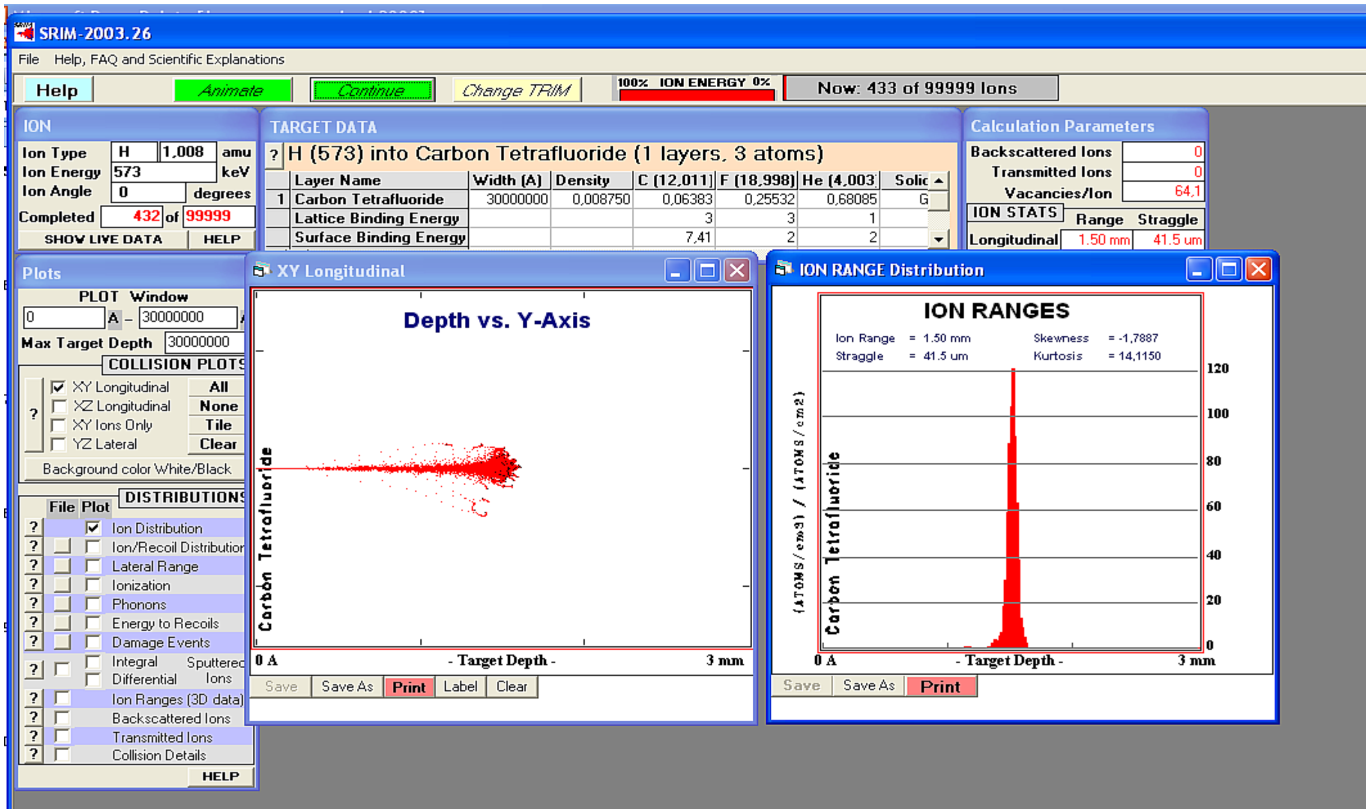

MWPC design constraints

Precise position measurement require precise and small wir spacing

Geometric tolerances cause gain variations

Large chambers need high mechanical tension to minimize sagging

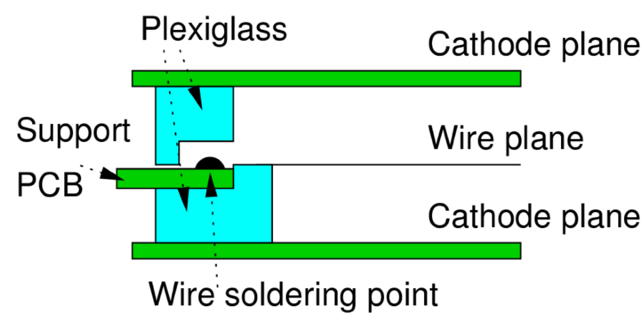

Comparison between a MWPC and an image plate detector

Lysosyme protein crystal 8 mm^3

Image Plate detector (rotated by 180° for the measurement with the bidim26

Bidim26 (distance to sample: 57 cm)

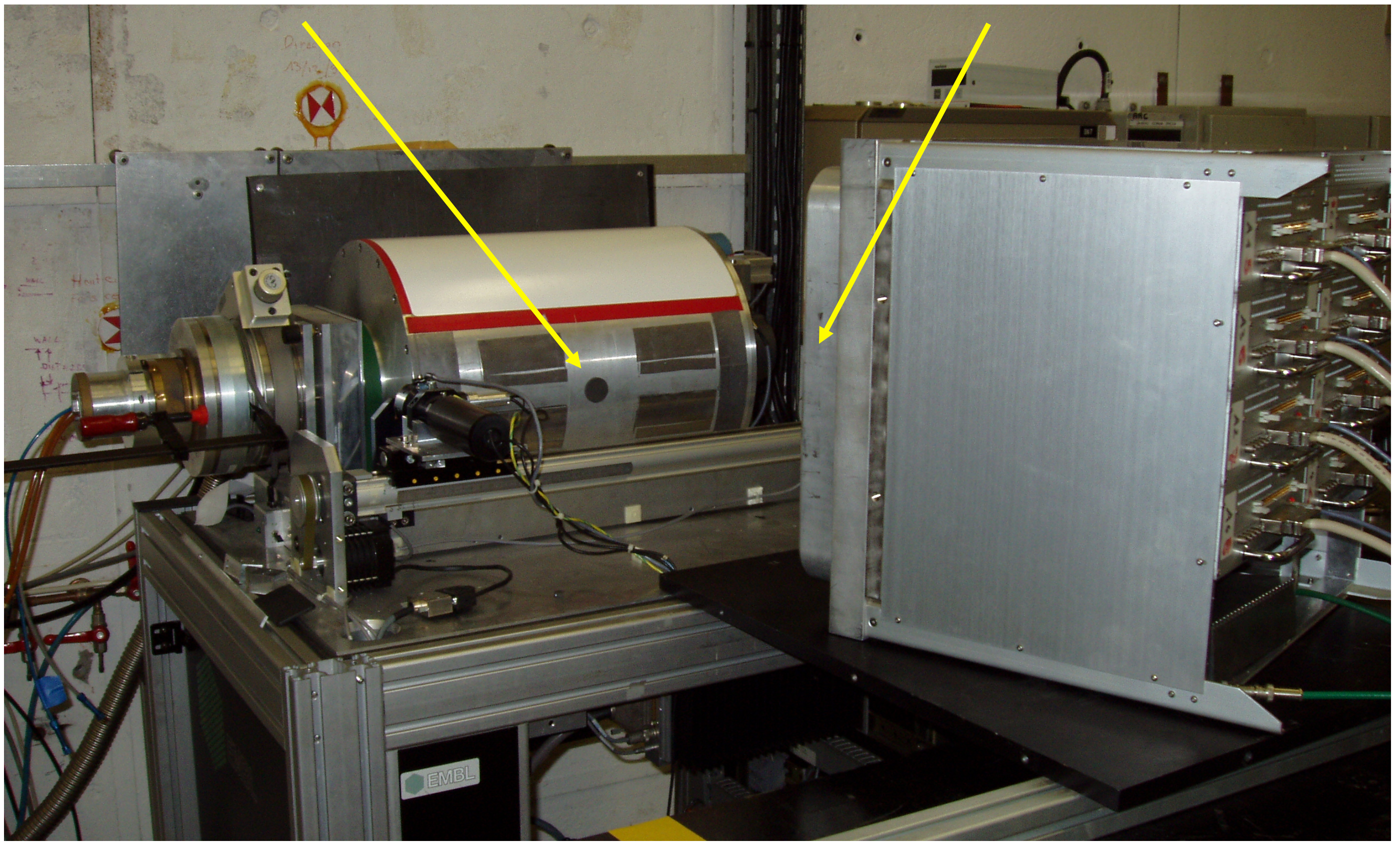

Test on LADI Instrument

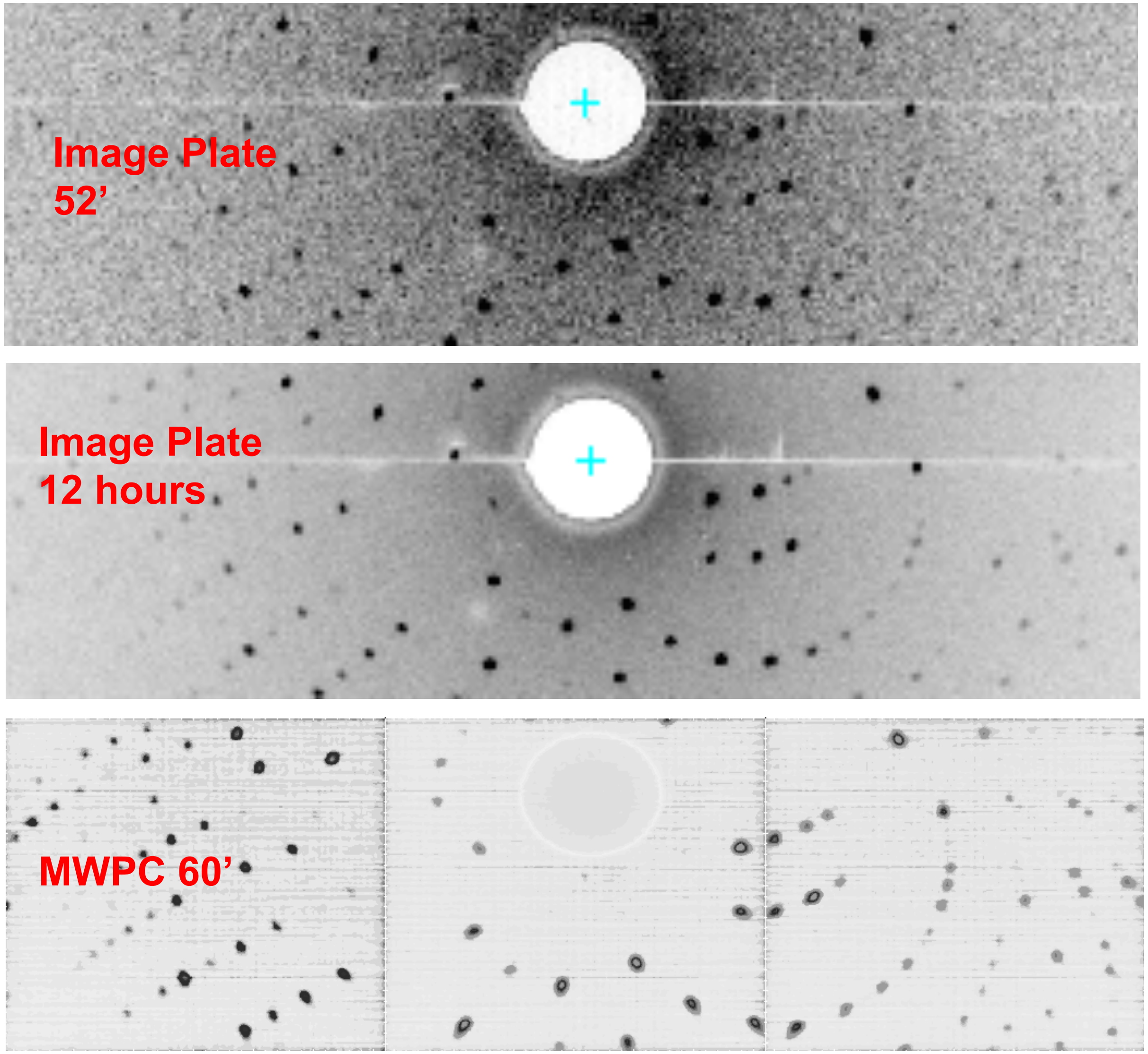
Image Plate
52’
Image Plate
12 hours
MWPC 60’

Main limitations of MWPCs: Radiation hardness and counting rate

→ Development of Micro-pattern Gas Detectors (MSGC, GEM, Micromegas)

MSGC (1988, A. Oed)

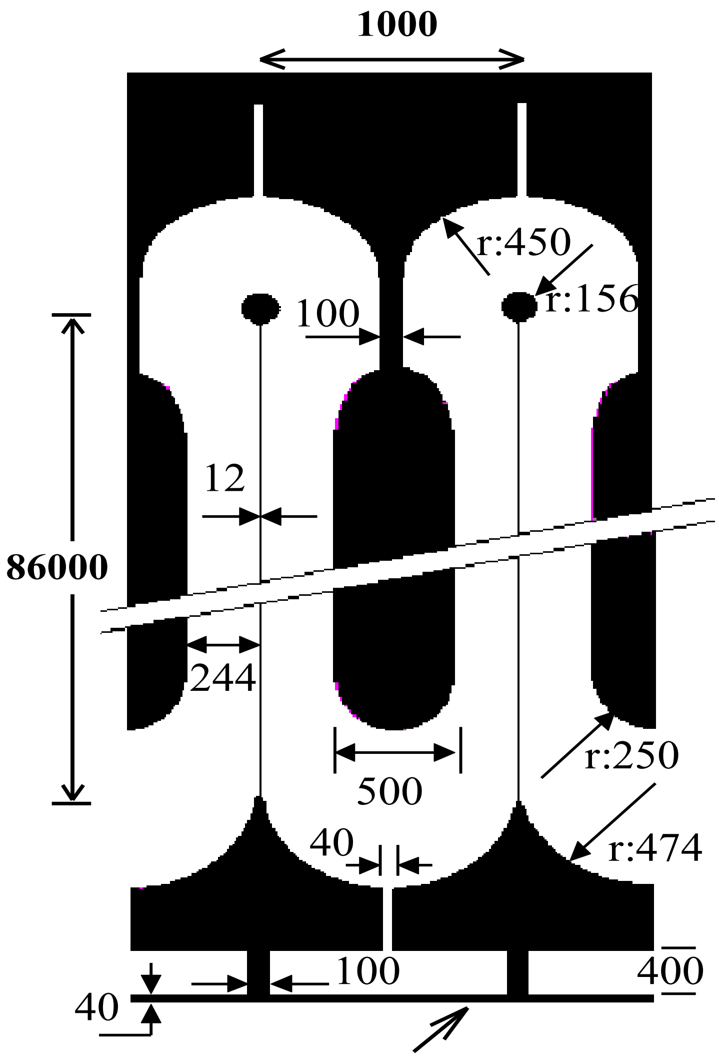

GAS ELECTRON MULTIPLIER (GEM)

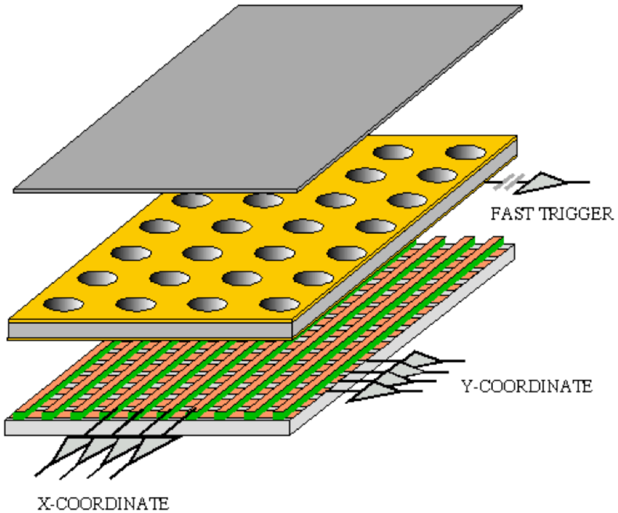

(F. Sauli)

MICROMEGAS and GRIDPIX

(I. Giomataris & G.Charpak)

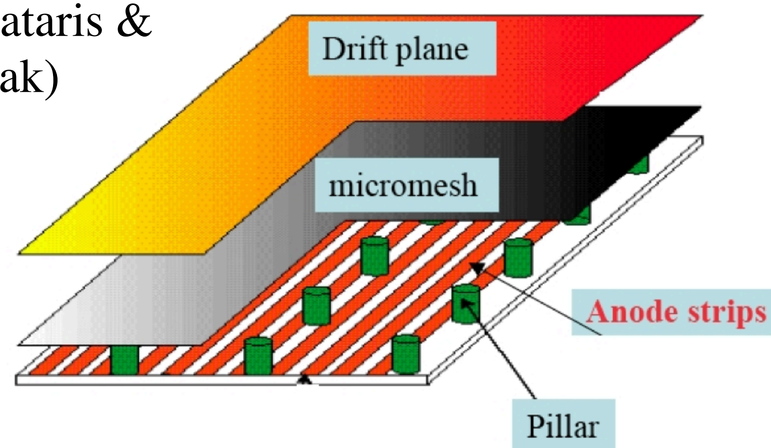

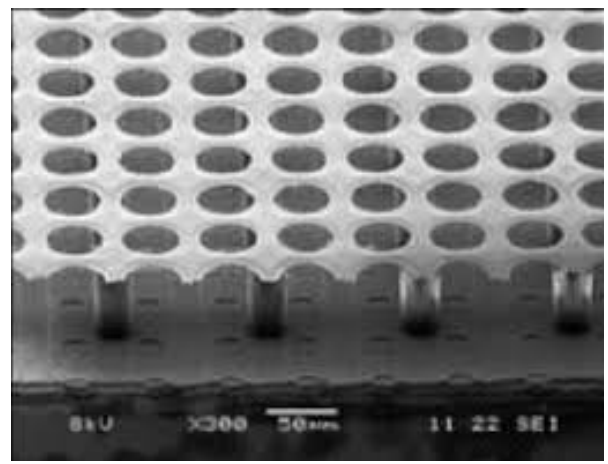

Thermal neutron gas detectors : examples from the ILL

PSD for Small Angle Neutron Scattering

From standard MWPC …

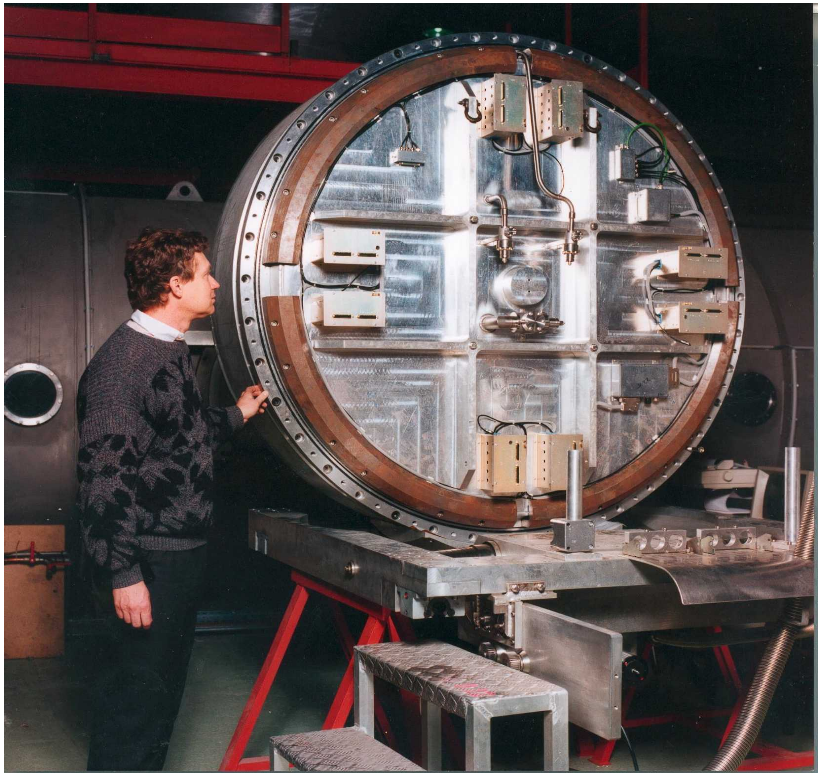

XY measured by coincidence of 2 orthogonal wire frames (max count rate 200 KHz)

To Multi-PSD

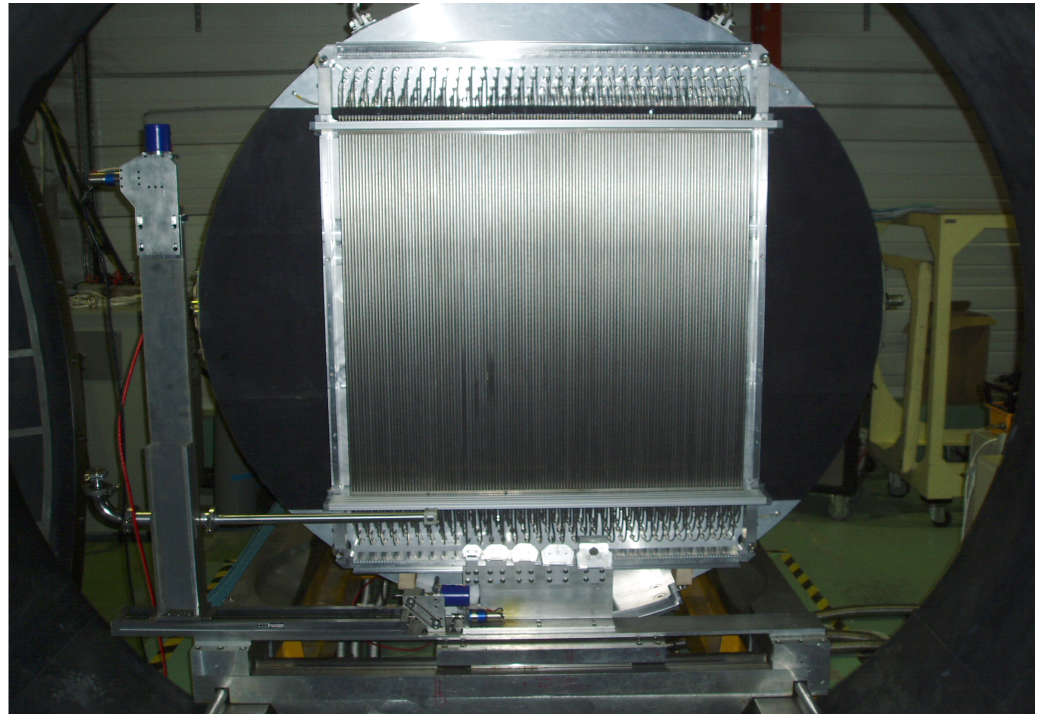

128 PSD covering 1 m^2 of sensitive area.
Position measurement by charge division
Tube diam.: 8 mm. Pressure: 15 bars
Efficiency: 75 % @ 5 Angstroms

Parallel charge division readout of independent detection elements combine the advantages of good spatial resolution in 1D together with high global counting rate

No deviation from linearity at 3 MHz

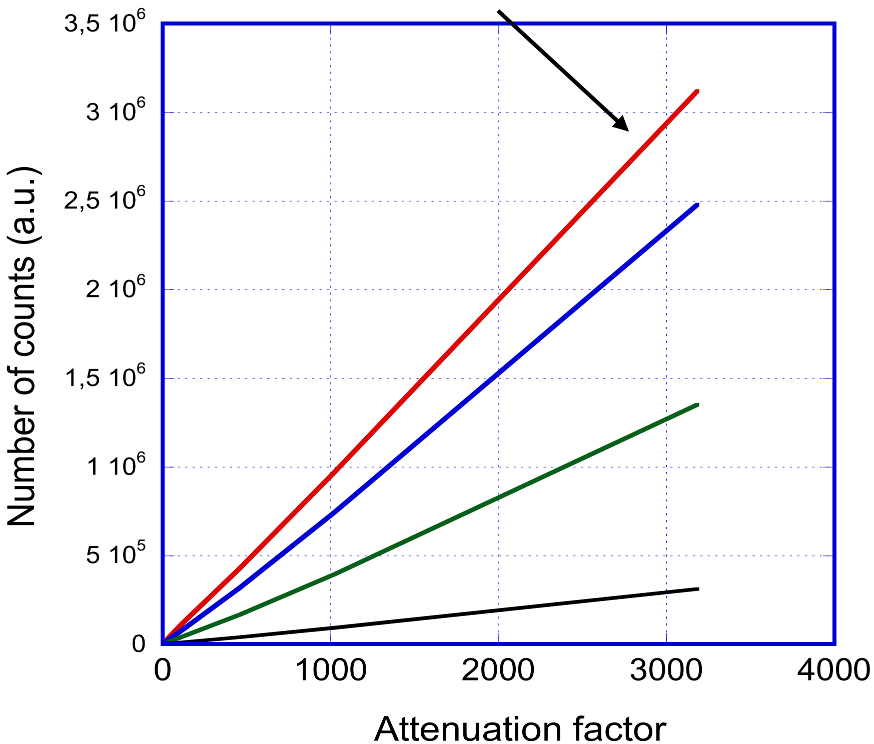

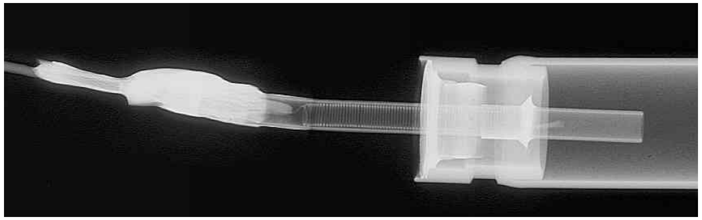

2001: Reuters Stokes started the development of a 1 m long, 8 mm diam. PSD for D22
2004: end of the D22 project
Hundreds of these detectors are used in several facilities.

- counting rate capability increased by 50 compared to previous MWPC.
- better time resolution and lower noise background
- lower parallax error

Aluminium Multitube for SANS and reflectometers

Improved efficiency, uniformity, and robustness

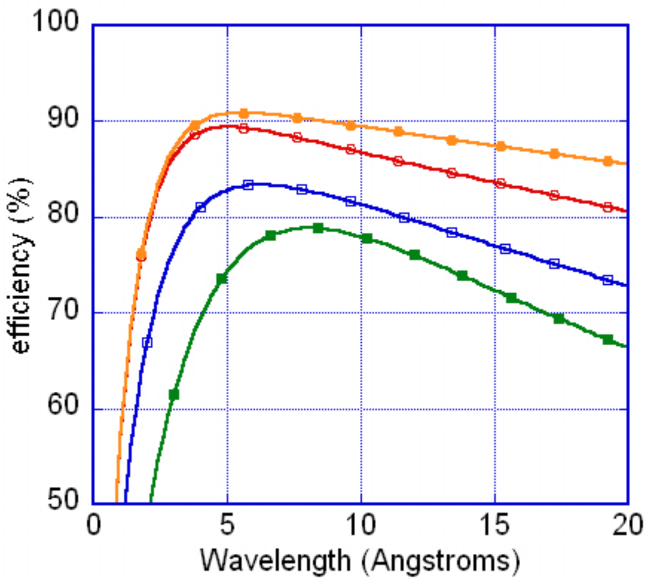

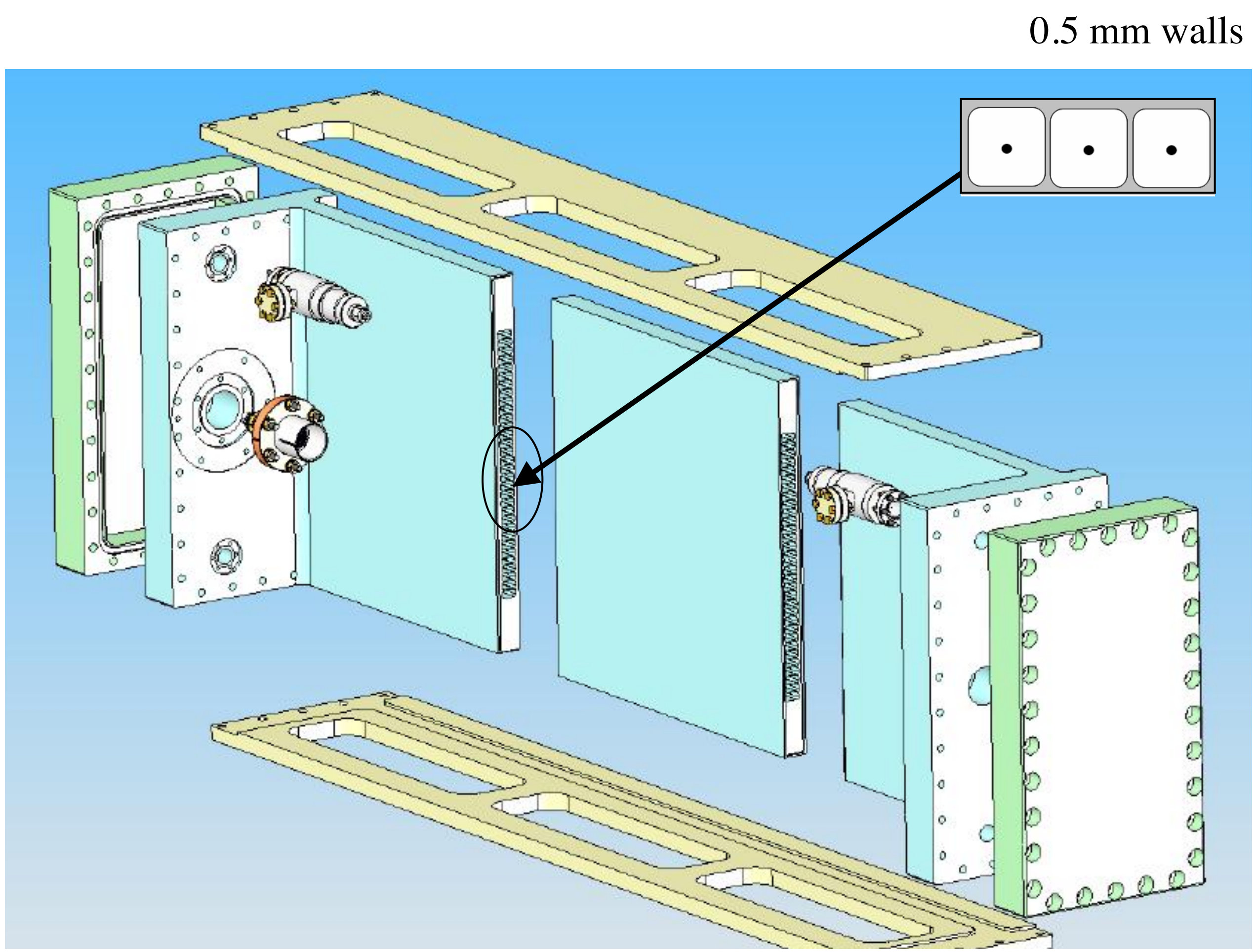

Green: MWPC 15 mm alu window, 750 mbars 3He, 60 mm gap (commercially available detector)

Blue: multi-PSD tubes diameter 8 mm ext x 7.5 mm int. every 8 mm, 15 bars 3He (D22)

Multitube, 15 bars 3He, 7.5 mm square tubes every 8 mm with 3 mm thick aluminium window (**orange**) and 5 mm window (**red**)

Monoblock Multitube

for SANS (D33) and
reflectometers (Figaro, D17)

Resolution: 8 mm x 1.5 mm
Det eff: 50 % @ 2 A
72 % @ 5 A

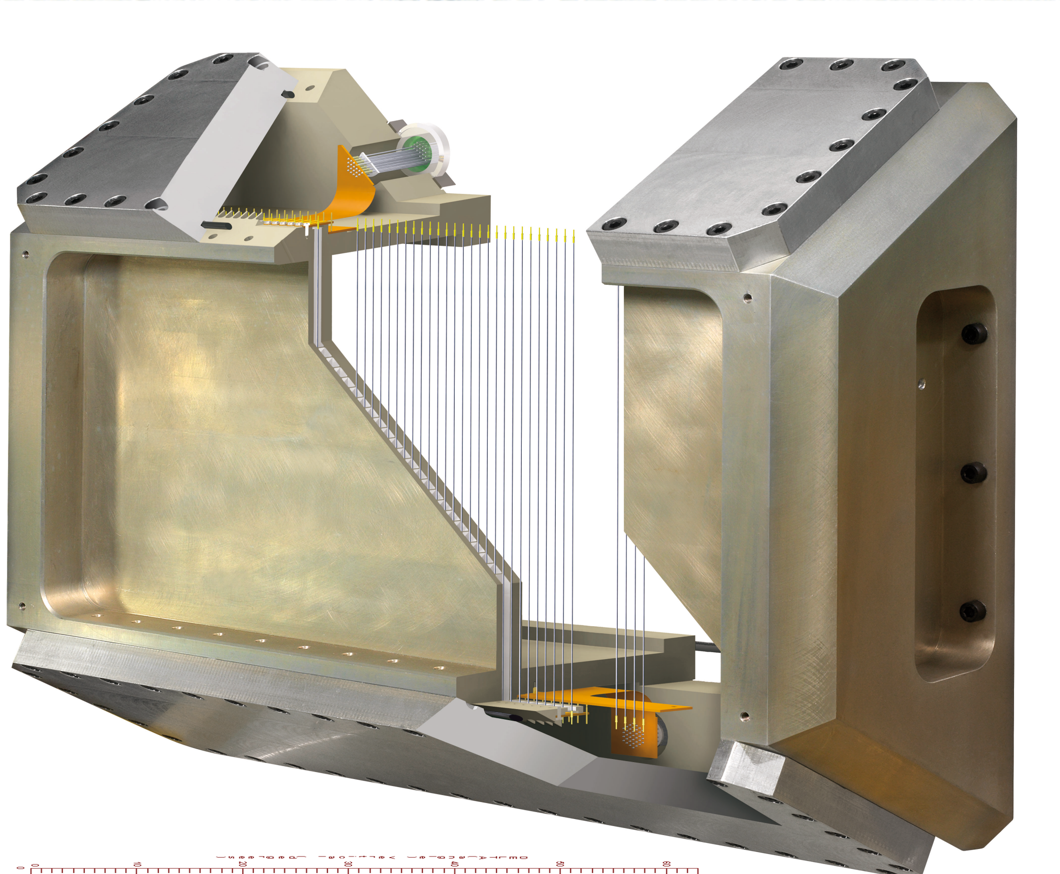

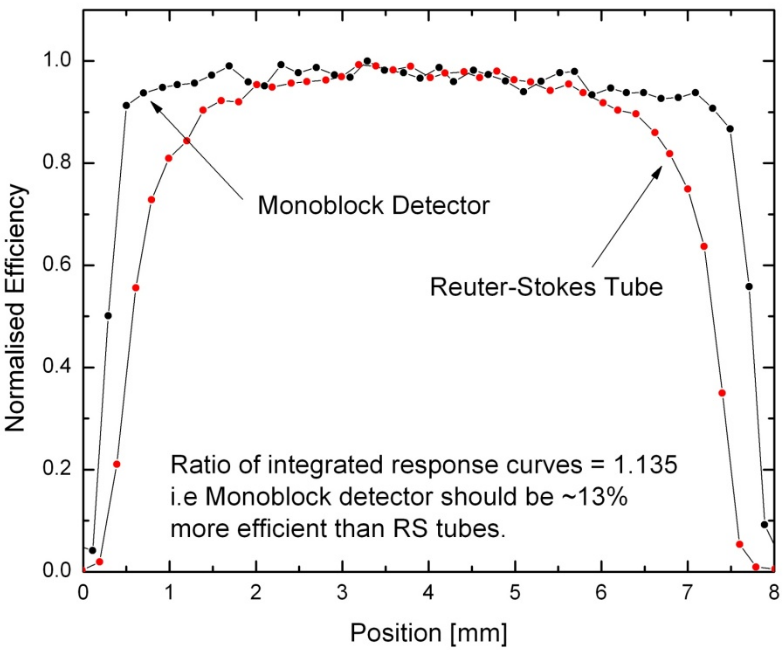

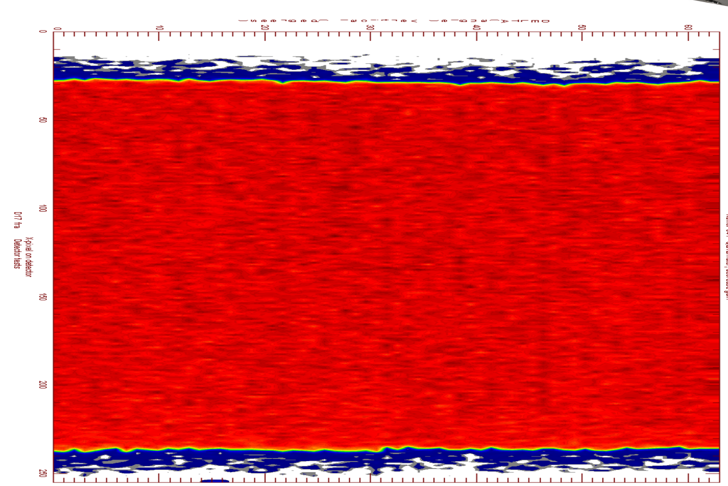

Curved 1D MSGC for the D20 Powder Diffractometer (2000)

NEUTRONS FOR SCIENCE

D20 powder diffractometer
1D localisation
48 MSGC plates (8 cm x 15 cm)
Angular coverage : 160° x 5,8°
Readout pitch : 2.57 mm (0,1°)
5 cm conversion gap
1.2 bar CF4 + 2.8 bars 3He
Efficiency 60% @ 0.8 Å

Curved 2D MWPC for the D19 Single Crystal Diffractometer (2005)

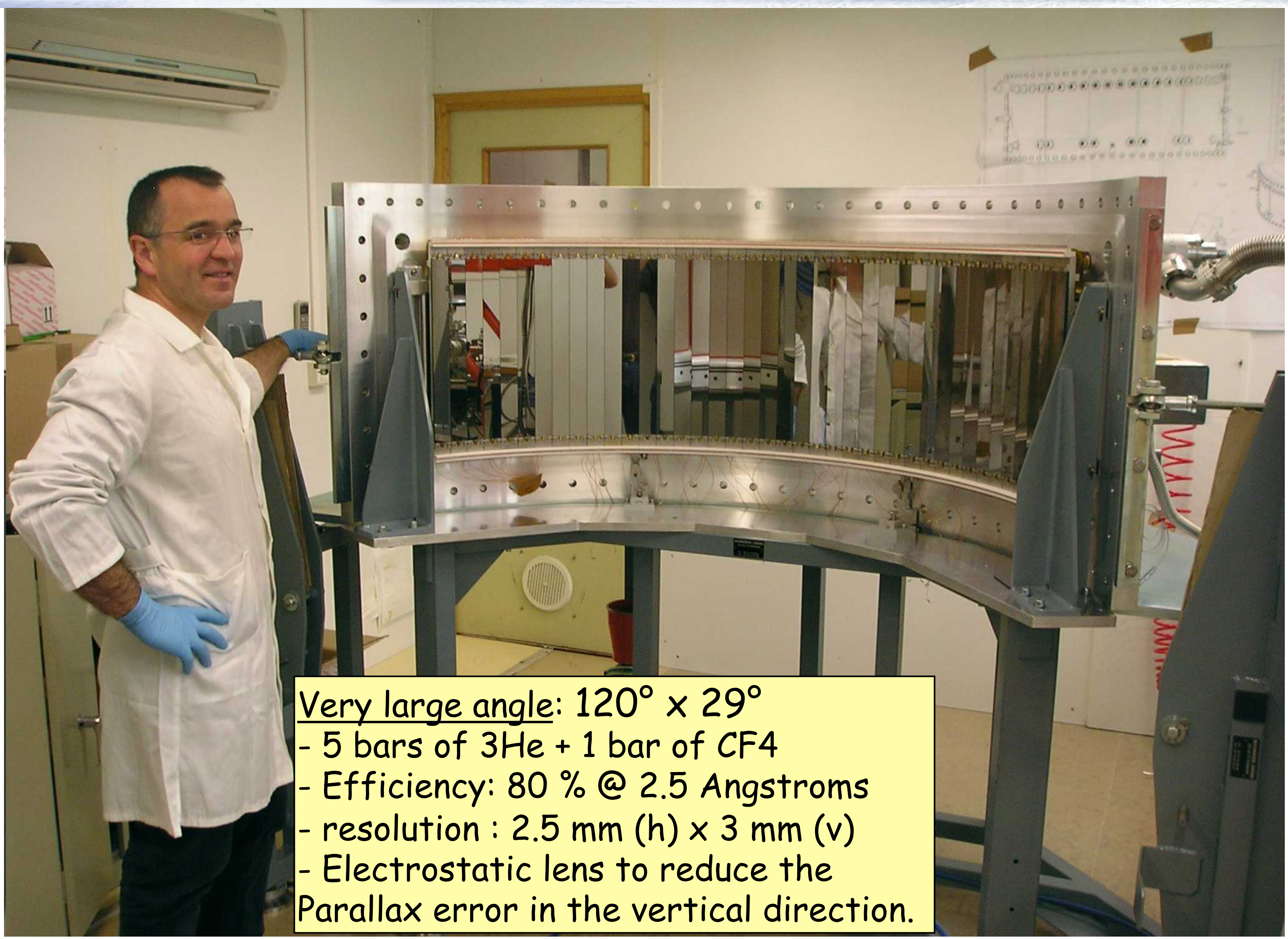

Very large angle: 120° x 29°
- 5 bars of 3He + 1 bar of CF4
- Efficiency: 80 % @ 2.5 Angstroms
- resolution : 2.5 mm (h) x 3 mm (v)
- Electrostatic lens to reduce the Parallax error in the vertical direction.

Curved 1D MWPC for the D1B Powder Diffractometer (2011)

Window thickness : 7mm
Conversion gap 22mm
Gas : 5 bar ^{3}He + 1 bar CF_4
Detection efficiency @ 2.52Å : 83%
Anode pitch : 0.1° (2.6 mm at 1.5m)
1280 * 15μm gold plated W-Re wires
Aperture : 128°
Operating voltage : $V_a = 2050V$, $V_C = 410V$

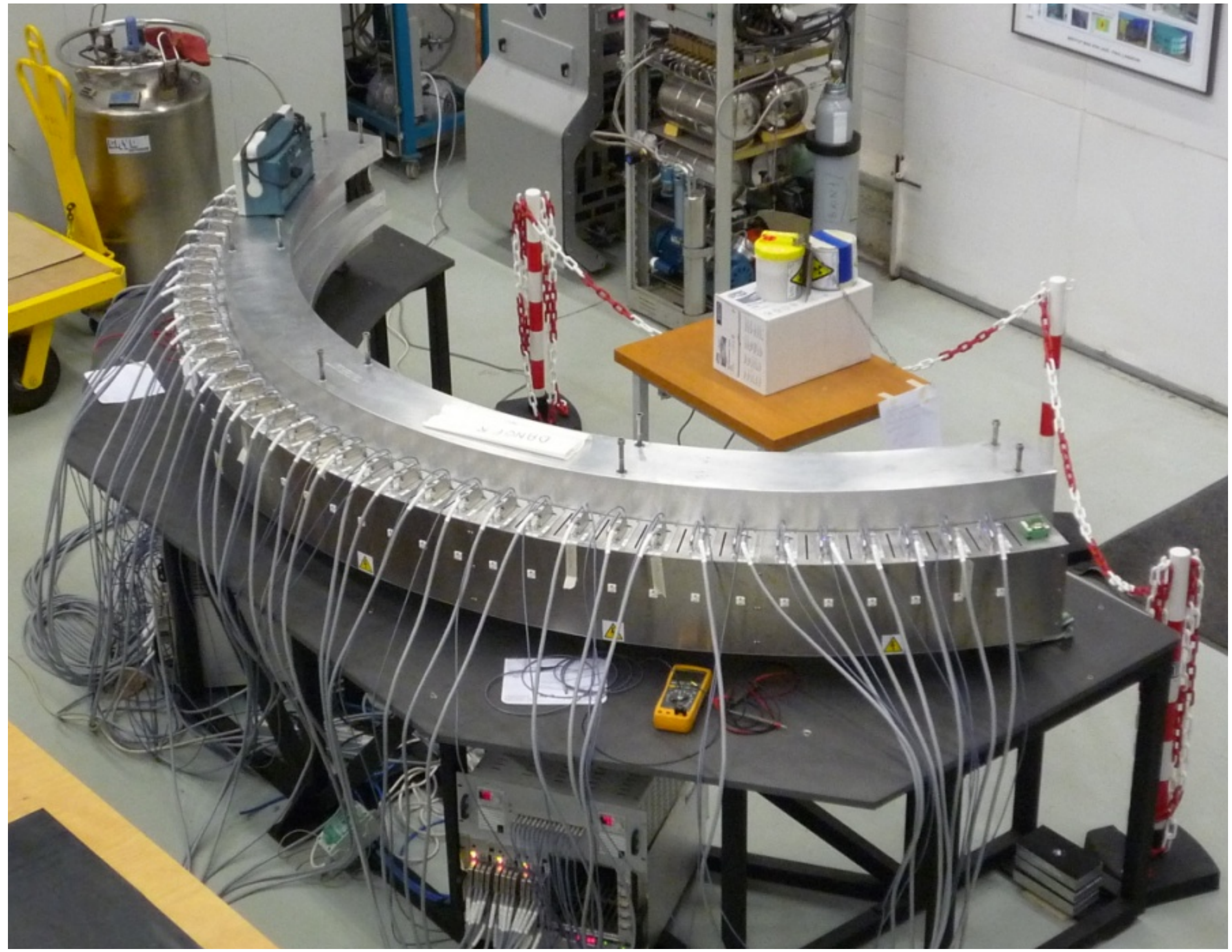

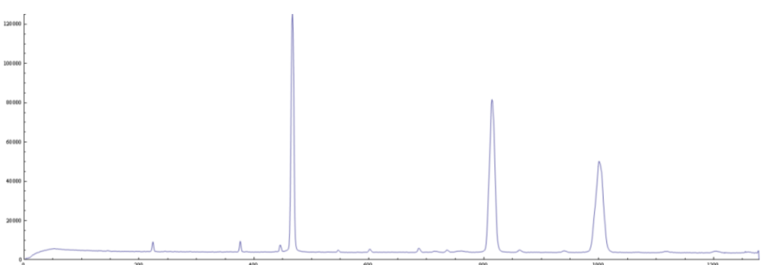

diffraction curve from a
Silicon sample

MILAND (FP6/NMI3 2004 - 2008)

- 32 cm x 32 cm sensitive area
- 1 mm readout pitch (640 channels)
- 5 mm conversion gap (+ 20 mm optional)
- 15 bars gas pressure (13.5 ^{3}He + 1.5 CF4)
- TOT (Time-Over-Threshold) processing

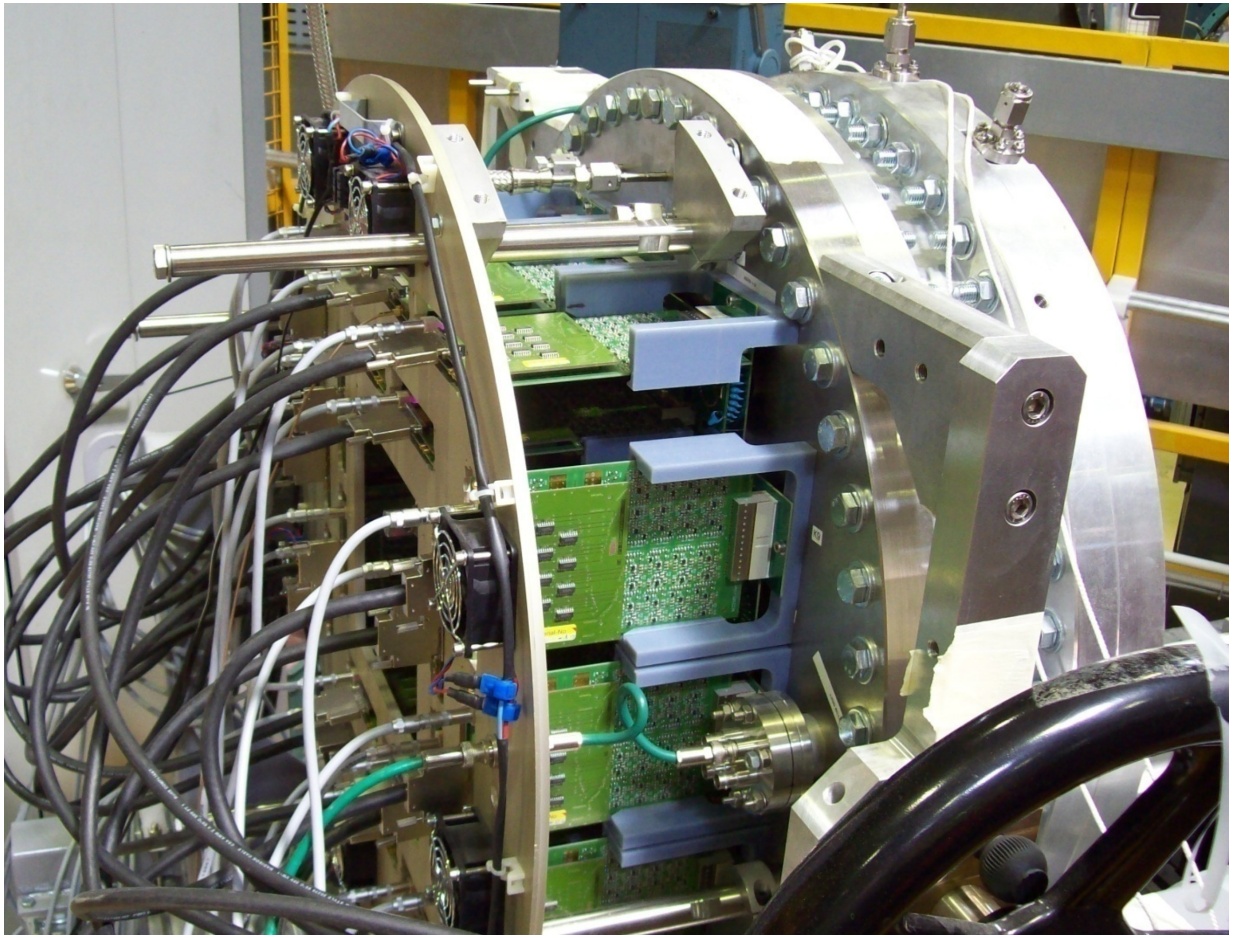

BNC
Tokyo University
ESRF
SNS
ILL

LLB
ISIS
GKSS
FRM-II
LIP

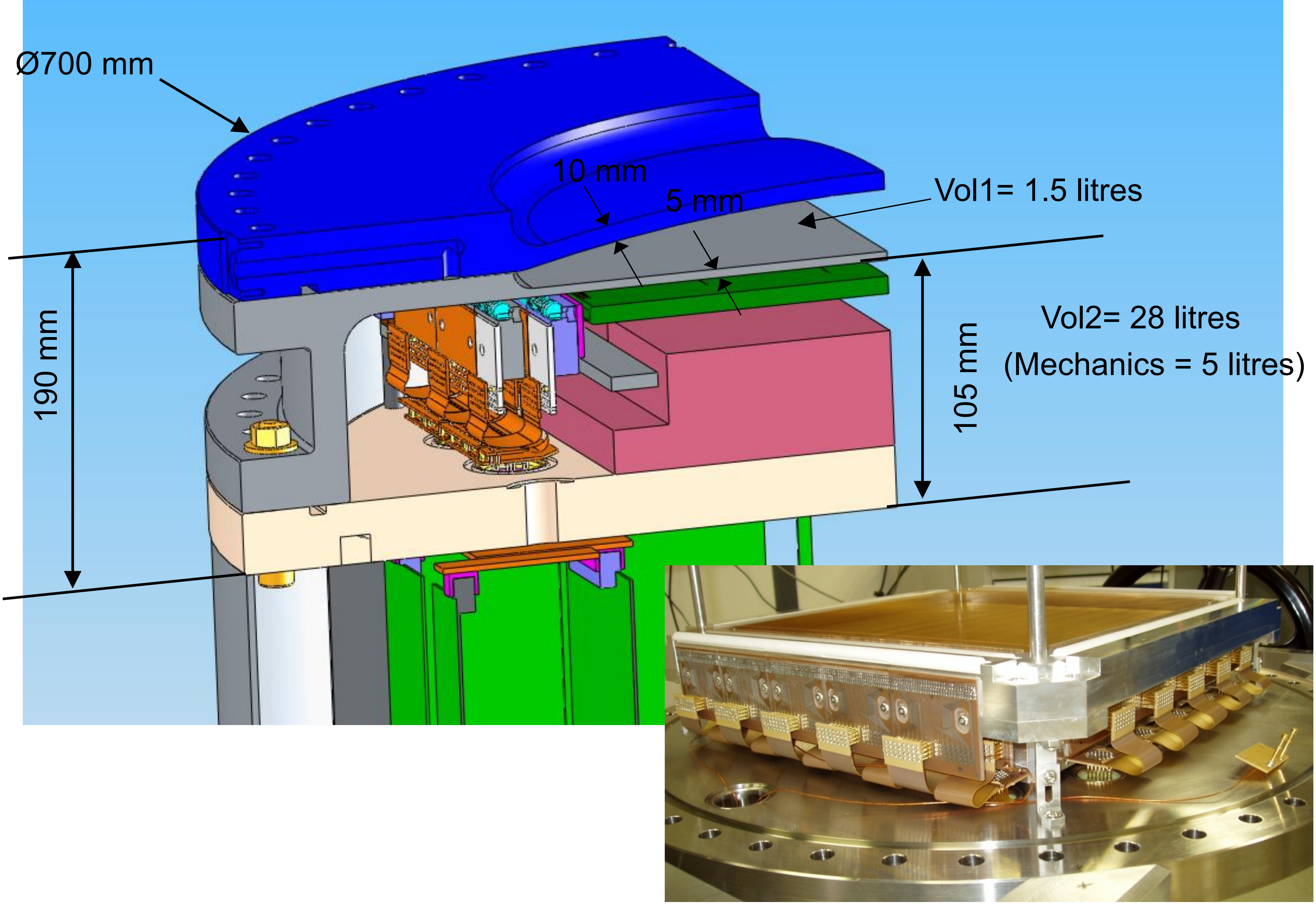
Ø700 mm
10 mm
5 mm
Vol1= 1.5 litres
190 mm
105 mm
Vol2= 28 litres
(Mechanics = 5 litres)

pressure vessel fabrication

TIG welding of 20 HV 37pts feedthroughs connectors and gas feedthroughs

Gas tightness control

Pressure test (0 to 21.5 bar)

Temperature pressure compensation

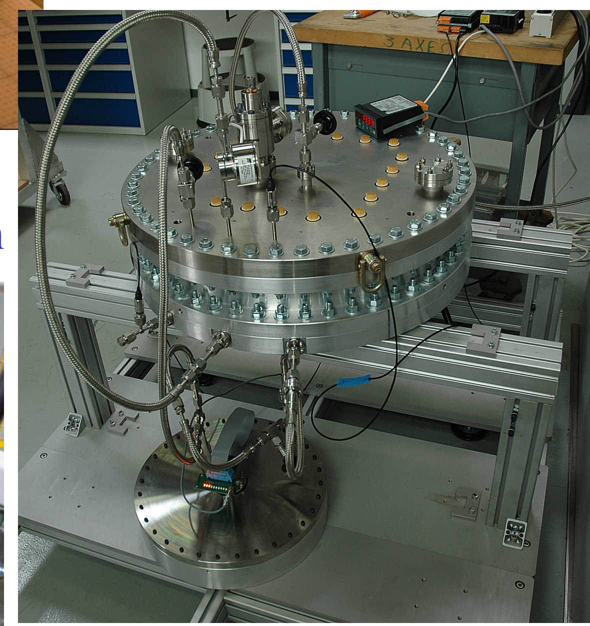

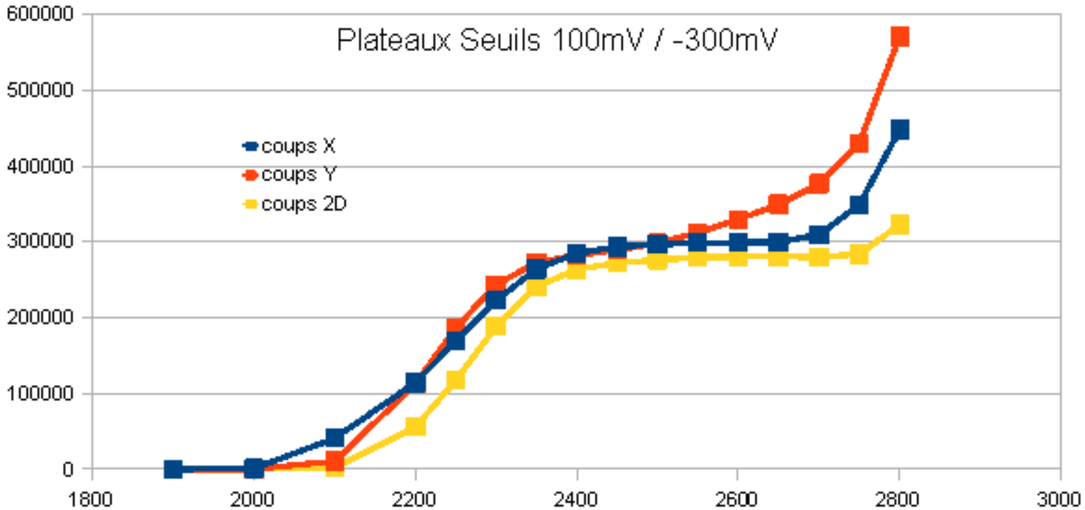
Plateaux Seuils 100mV / -300mV
coups X
coups Y
coups 2D
600000
500000
400000
300000
200000
100000
0
1800
2000
2200
2400
2600
2800
3000

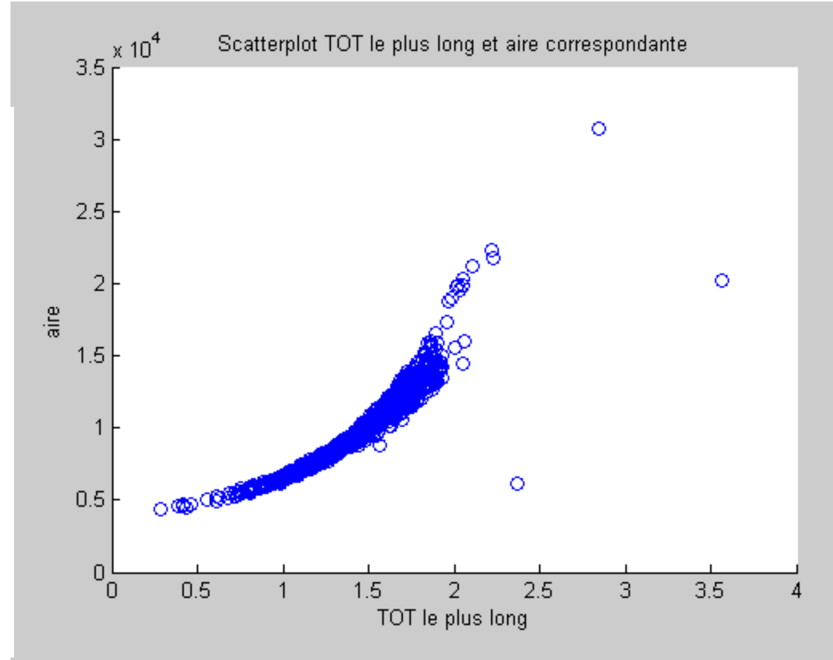
Scatterplot TOT le plus long et aire correspondante
x 10^4
aire
TOT le plus long
3.5
3
2.5
2
1.5
1
0.5
0
0
0.5
1
1.5
2
2.5
3
3.5
4

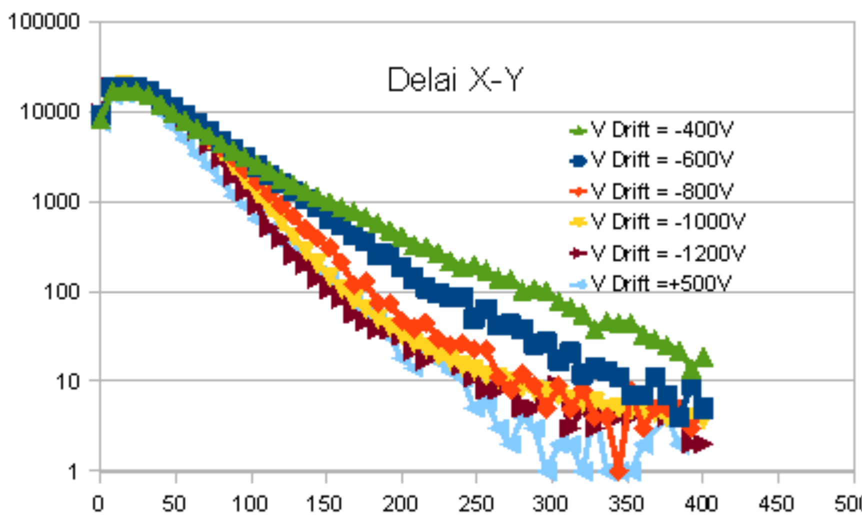
Delai X-Y
V Drift = -400V
V Drift = -600V
V Drift = -800V
V Drift = -1000V
V Drift = -1200V
V Drift =+500V
100000
10000
1000
100
10
1
0
50
100
150
200
250
300
350
400
450

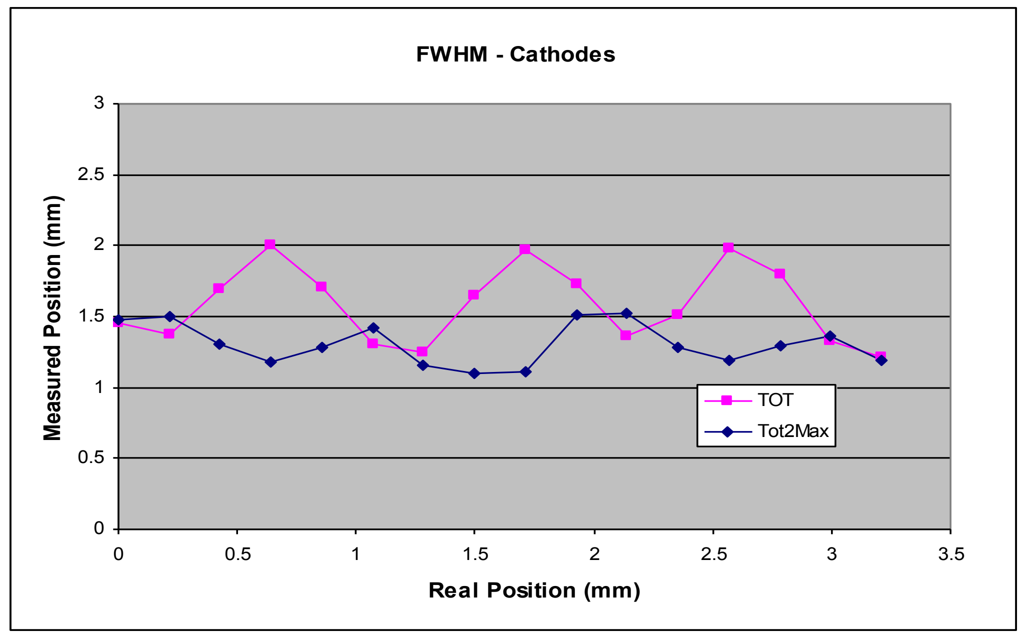
FWHM - Cathodes
Measured Position (mm)
Real Position (mm)
TOT
Tot2Max
3
2.5
2
1.5
1
0.5
0
0
0.5
1
1.5
2
2.5
3
3.5

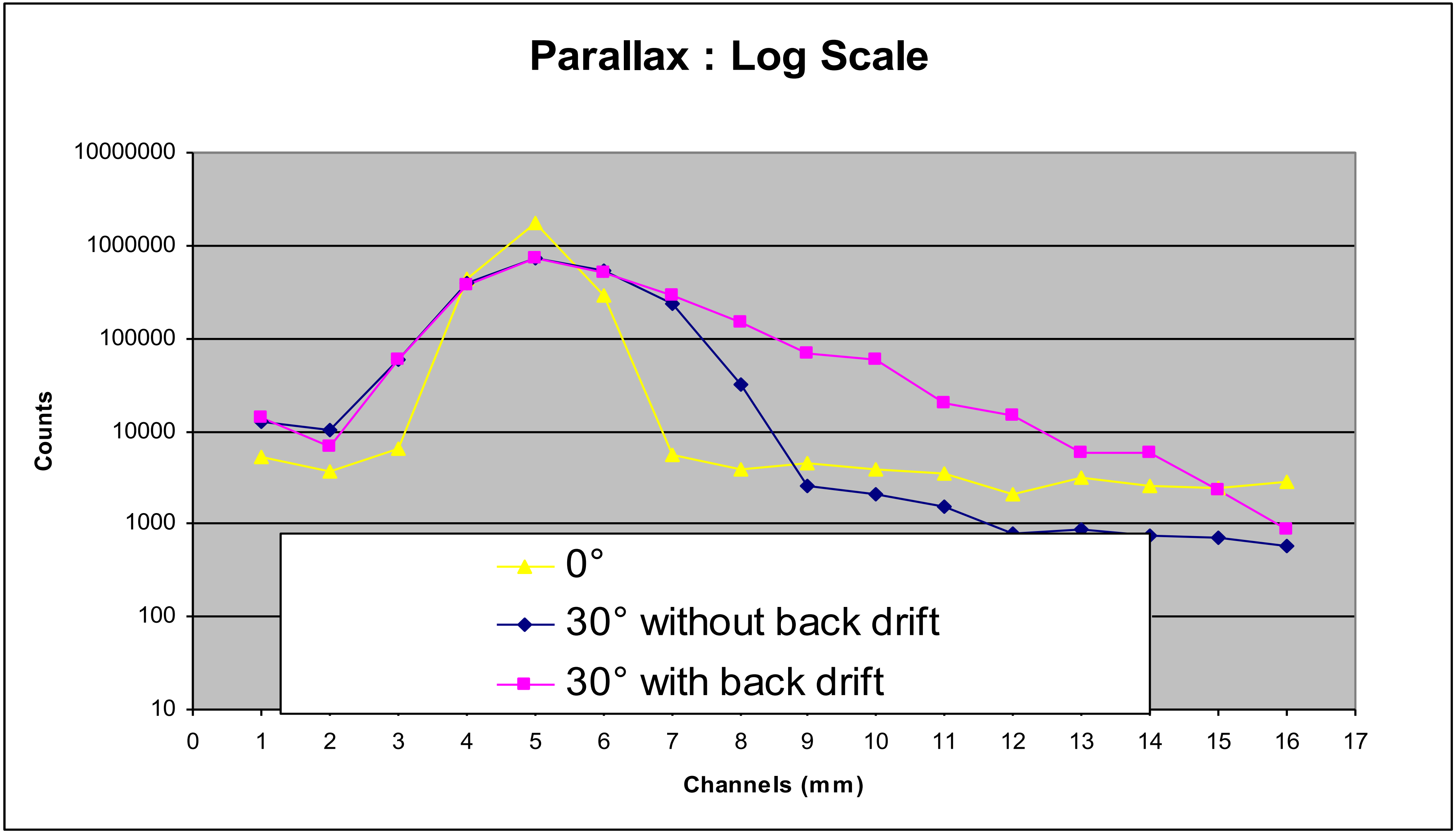

Parallax : Log Scale
10000000
1000000
100000
10000
1000
100
10
Counts
0
1
2
3
4
5
6
7
8
9
10
11
12
13
14
15
16
17
Channels (mm)
0°
30° without back drift
30° with back drift

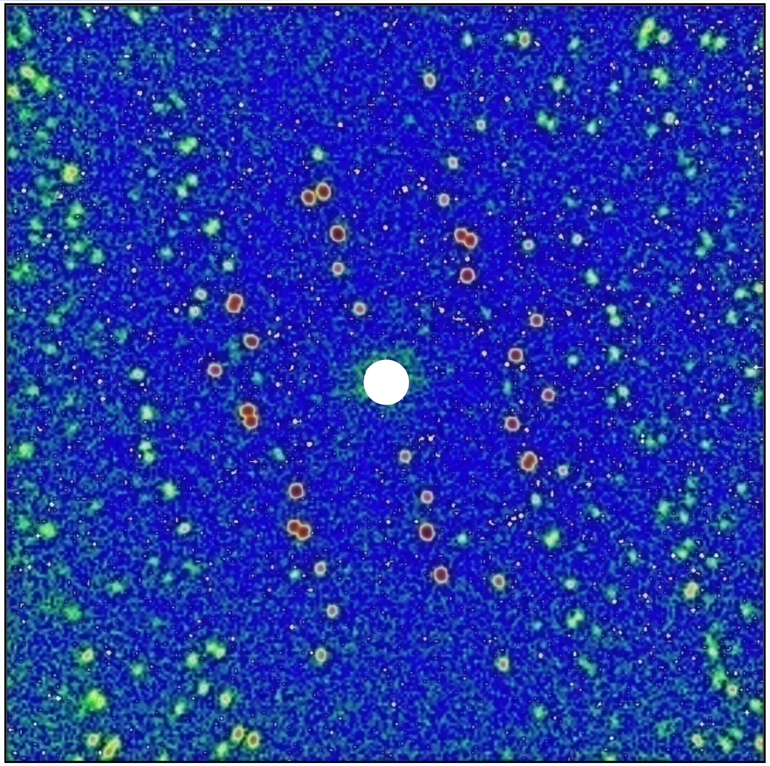

Image obtained on the D16 instrument with a **lysozyme** crystal, by superimposing images obtained during an angular scan. The detector was mounted at 35 cm from the sample. The neutron flux on the sample was 4 * 10^4 n/sec, and the total acquisition time 16 hours.

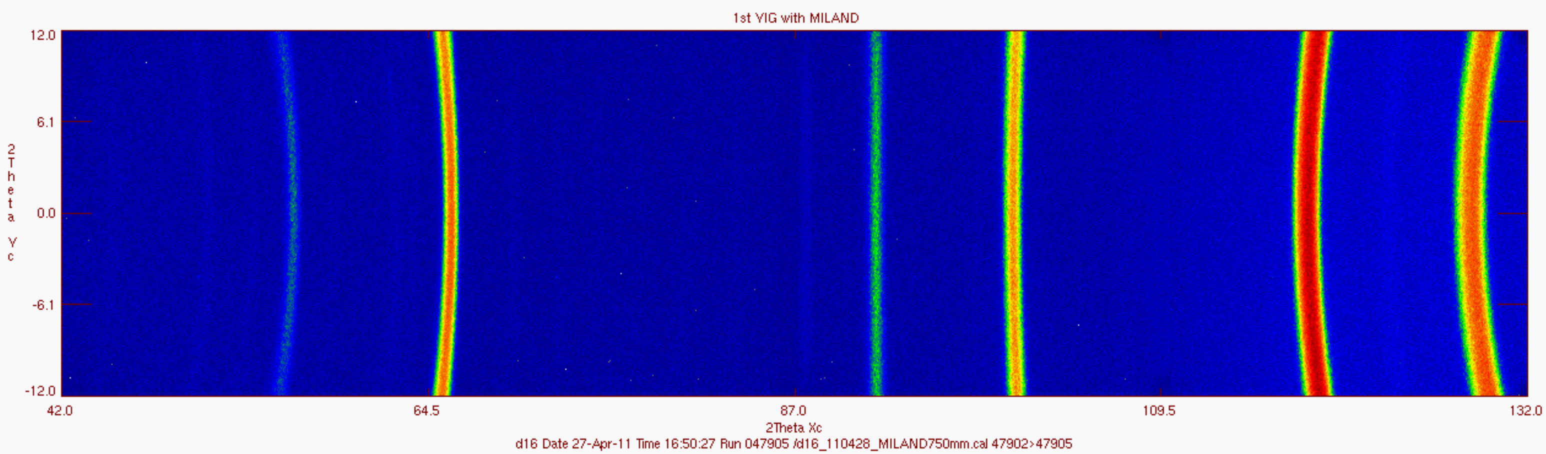

YIG

MILAND results

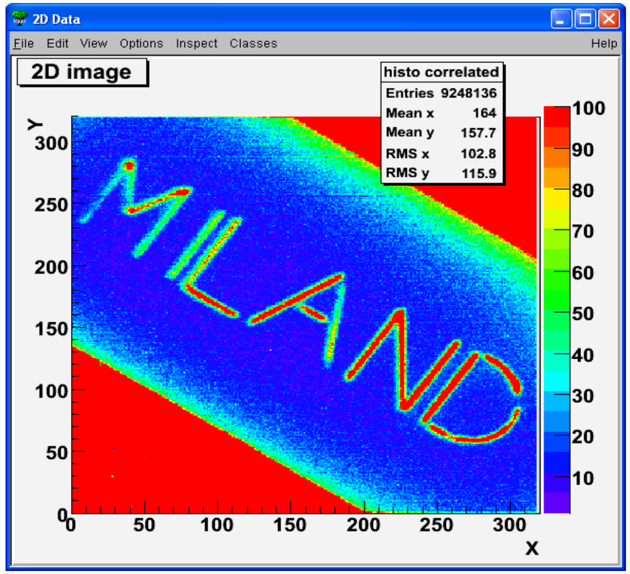

- ✓ Detection efficiency 70% @ 2.5 Angstroms
- ✓ Spatial resolution: 1 mm FWHM (1.2 mm)
- ✓ Reduced Parallax error 5 mm gap + High pressure (15 bars)
- ✓ Global counting rate τ : 0.7 MHz @ 10% neutron lost

- ✓ Gamma sensitivity < 10-8
  Sensitivity of the measurement to cosmic neutrons → replacement of 3He by 4He
- ✓ Counting uniformity : variance <= 5% (6% cathode; 1% anode)
- ✓ Counting stability (variation < 10-4 / hour)

2D MWPCs: 192X/192Y, 1 mm (in project)

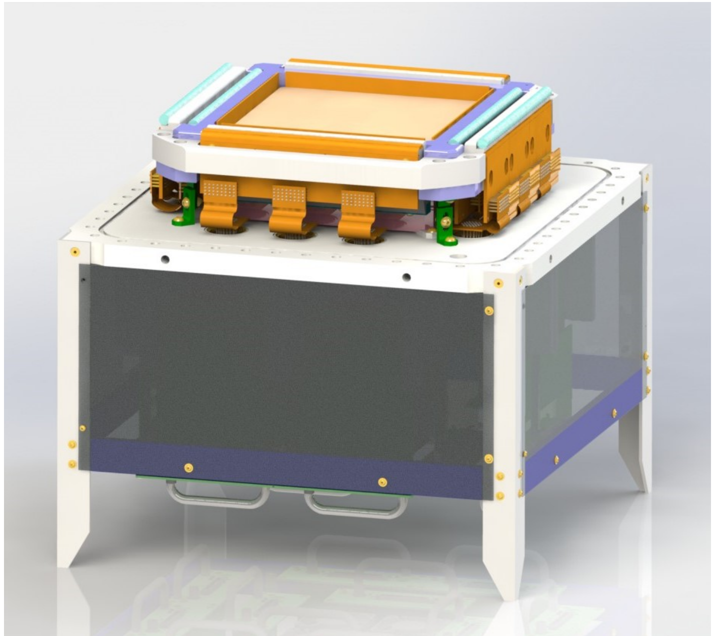 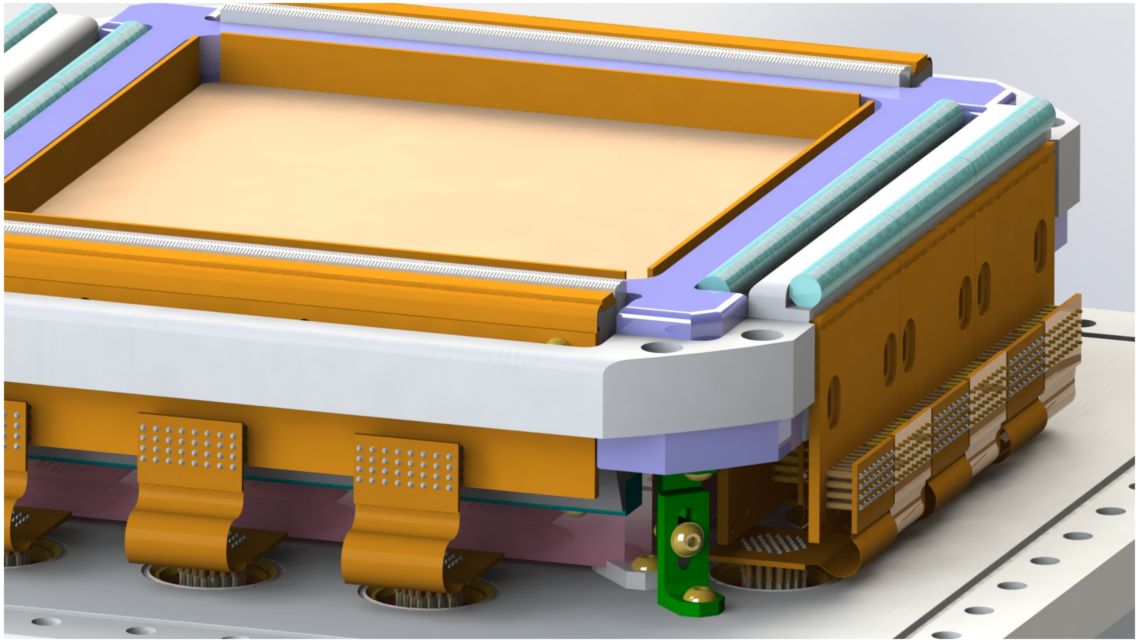

Design based on the MILAND detector

GSPC (Gas Scintillating Proportional Chamber)

Measuring the light produced during the avalanches

NMI3/WP22 (2008 – 2012)

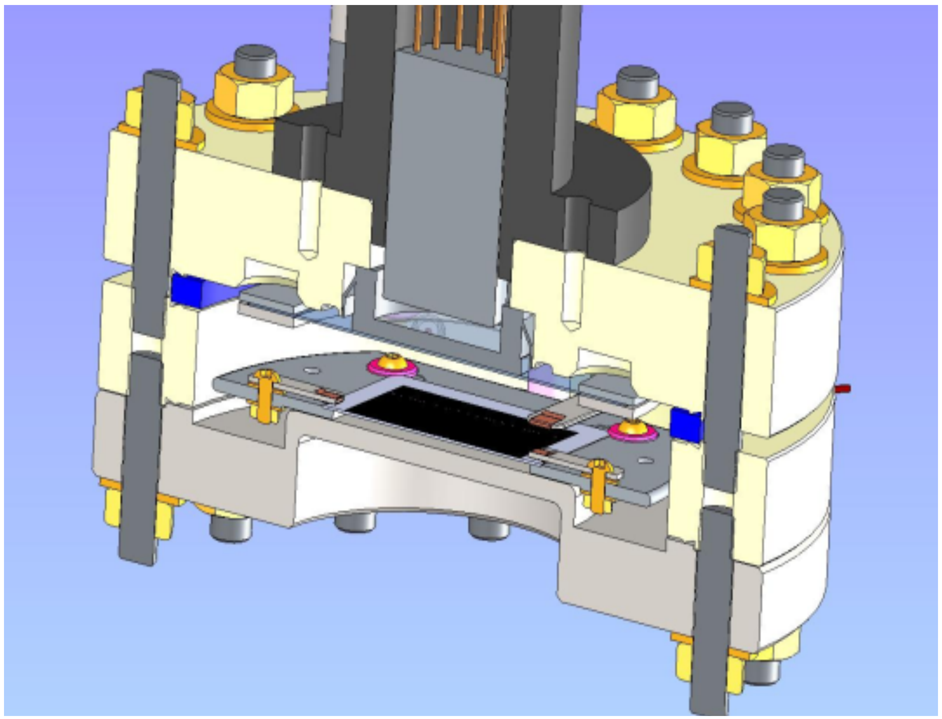

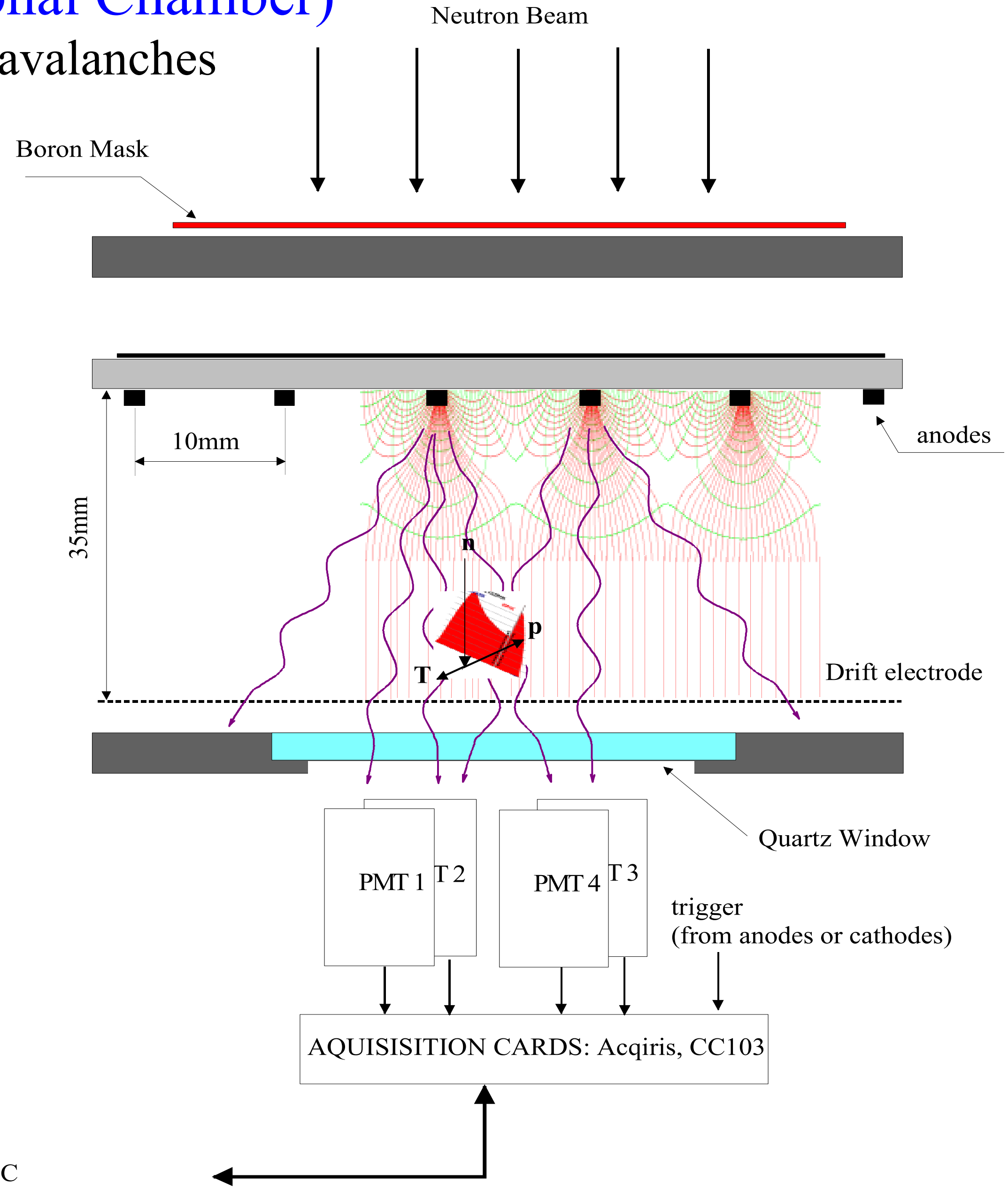

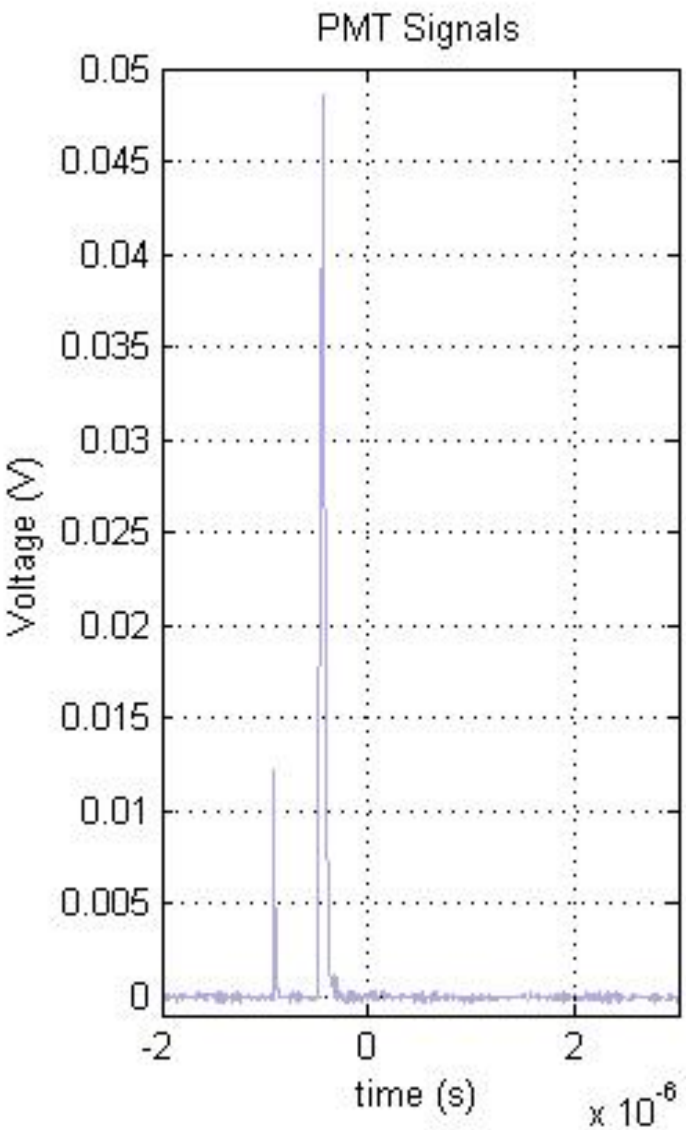

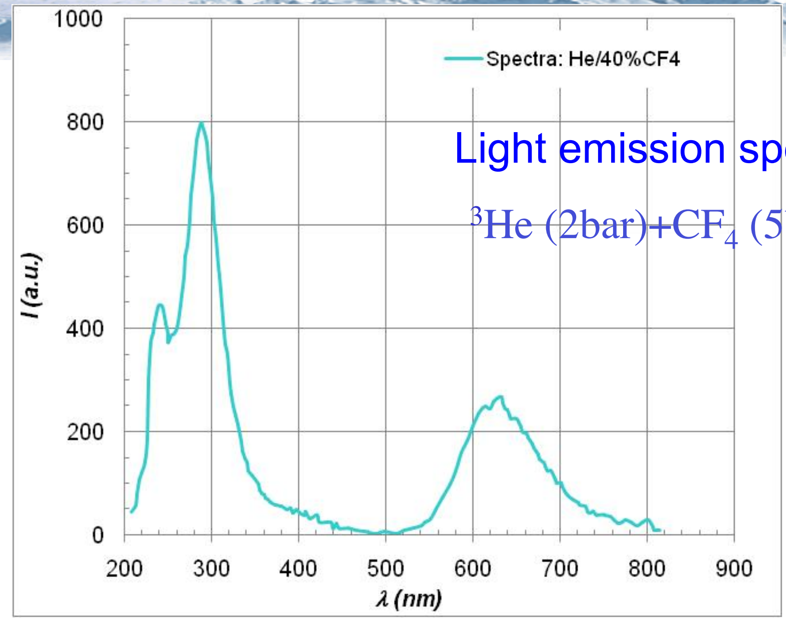

Light emission spectrum

^{3}He (2bar)+CF_4 (5bar)

Material	λ max. emission (nm)	Light Yield (photons/neutron)	Decay (ns)
Li glass (Ce) (GS20)	395 nm	~7,000	75
LiI (Eu)	470	~51,000	1400
ZnS (Ag) - LiF	450	~160,000	>1000
CF_4 gas amplification	300 - 600	G*2000 (G: detector gain)	25

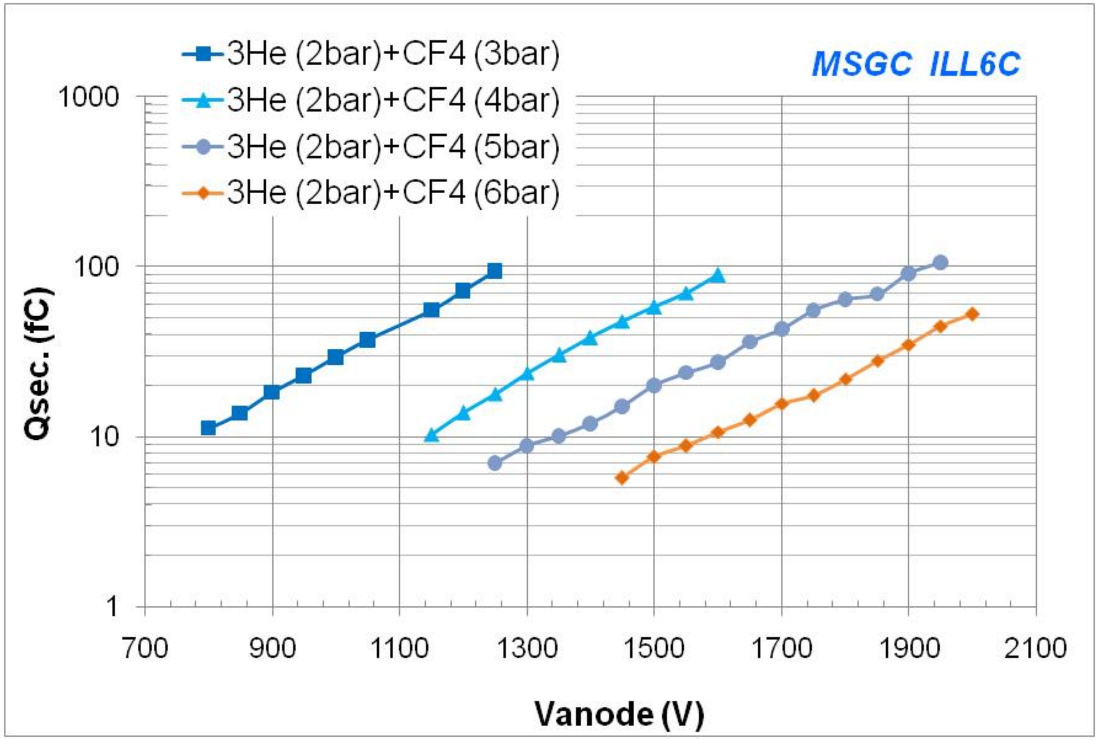

Scintillation light decay time

primary light: 15 ns

Second. light : 25 ns

Typically 100 ns total dead time taking into account the track charge collection time

→ 1 MHz counting rate @ 10% dead time correction

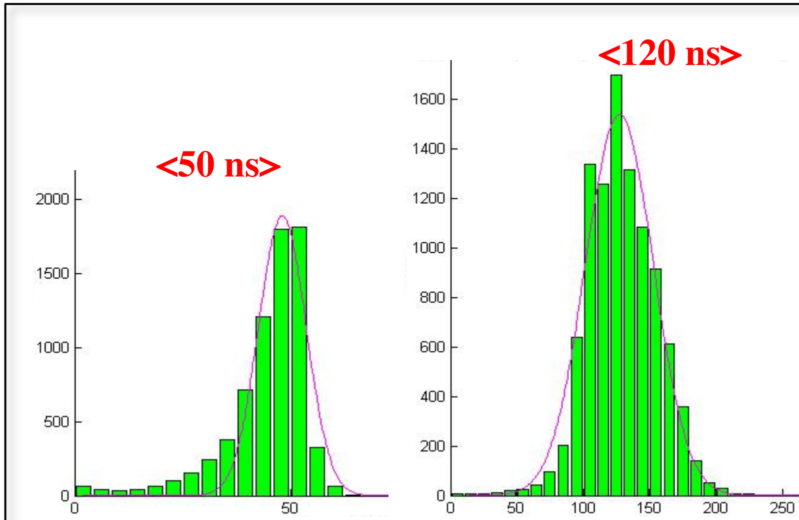

Primary (left) and secondary (right) light pulse TOT distribution

Conditions to reach 0.5 mm FWHM position resolution ?

→ 6 bars of CF_4

→ amplification gain =1000

MSGC is unique in the fact that it can be operated at High pressure of CF_4

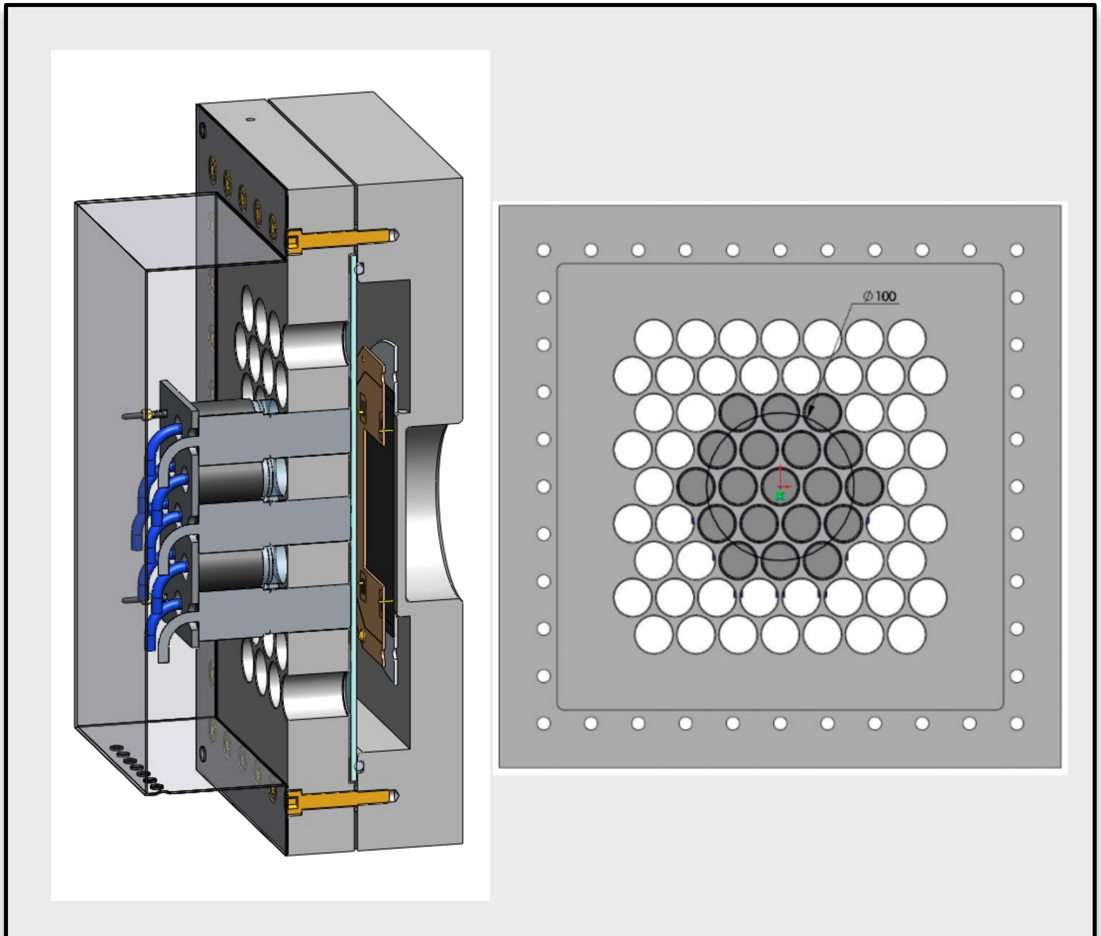

GSPC19 (window: 10 cm diam)

0.7 mm resolution measured

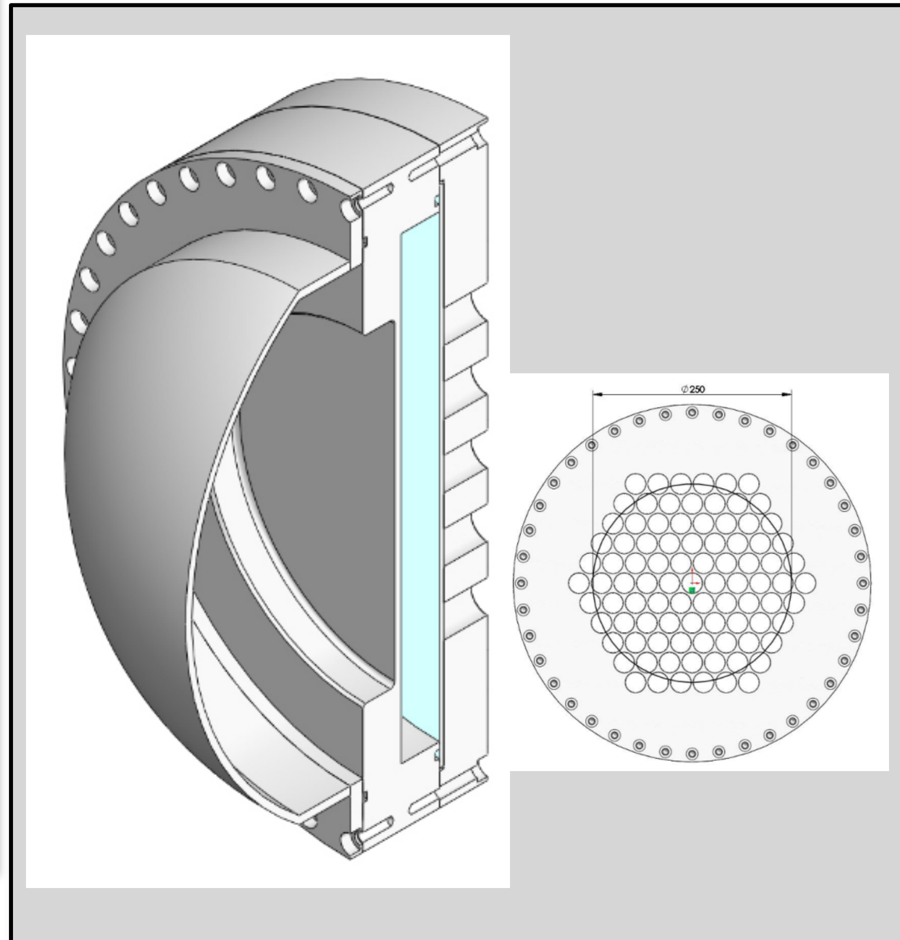

GSPC91 (not fabricated)

Window: 25 cm diam

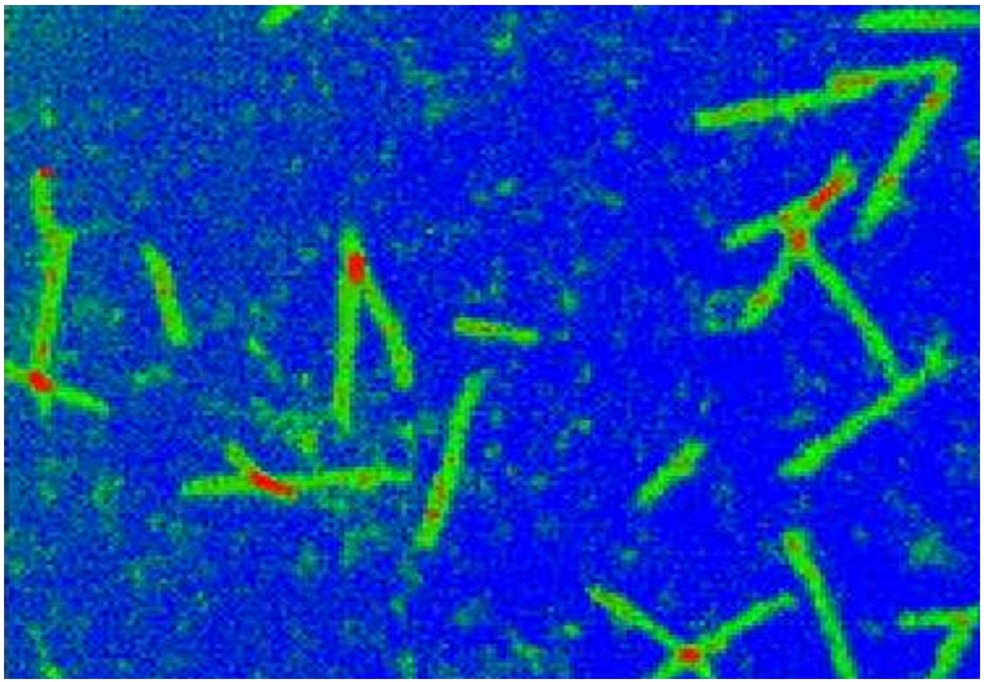

secondary light emitted in a GEM chamber, readout with a CCD camera

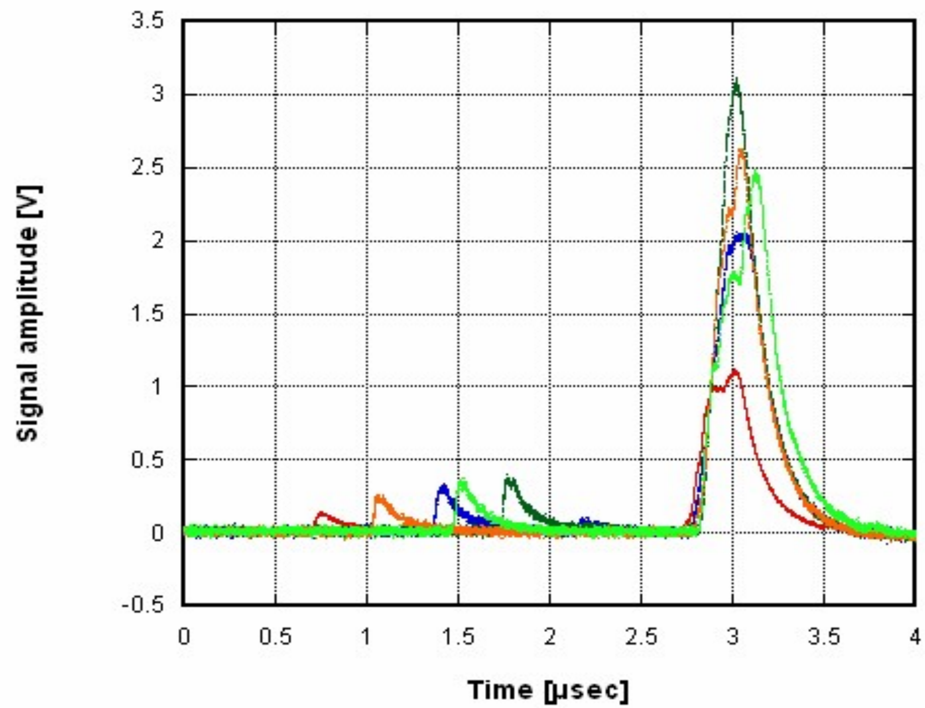

Primary and secondary light measured with a PMT

Multi-events recognition with a triple readout electrode MWPC

Sensitive area = overlap of 3 wire frames mounted at an angle of 60°

The number of readout channels is multiplied only by 1.8 compared to a standard detector with similar sensitive area and spatial resolution

several simultaneous neutrons are localised with a fast processor without any ambiguity.

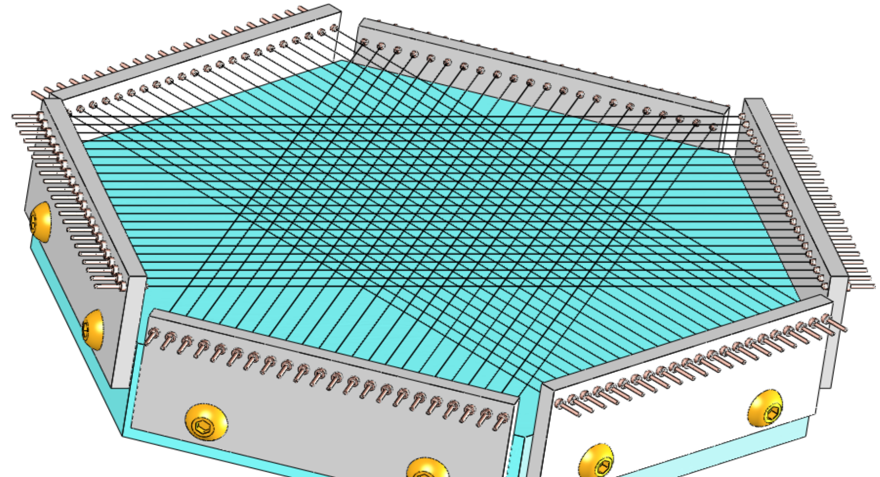

Prototype Wire pitch : 2 mm
64 wires in each plane

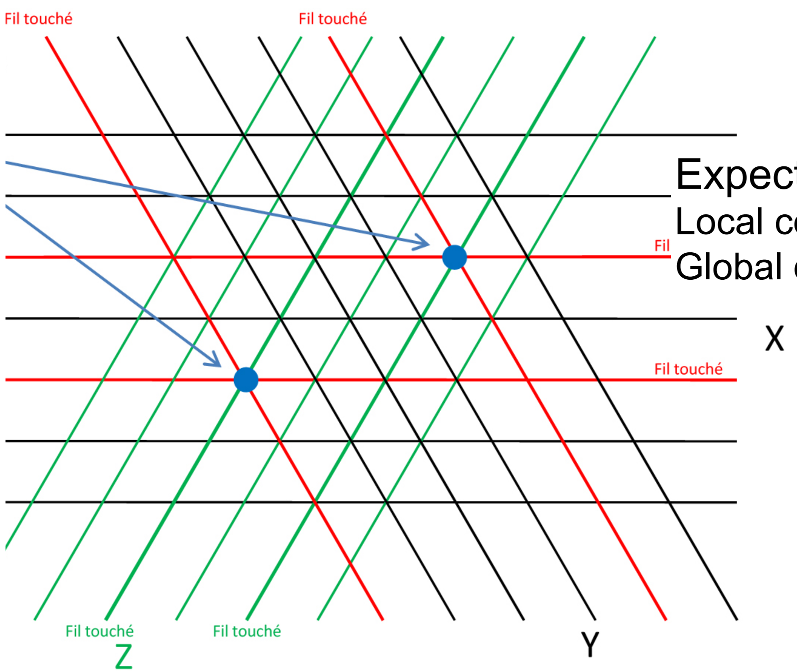

Expected performances
Local count rate 50 KHz/pixel
Global count rate > 1 MHz

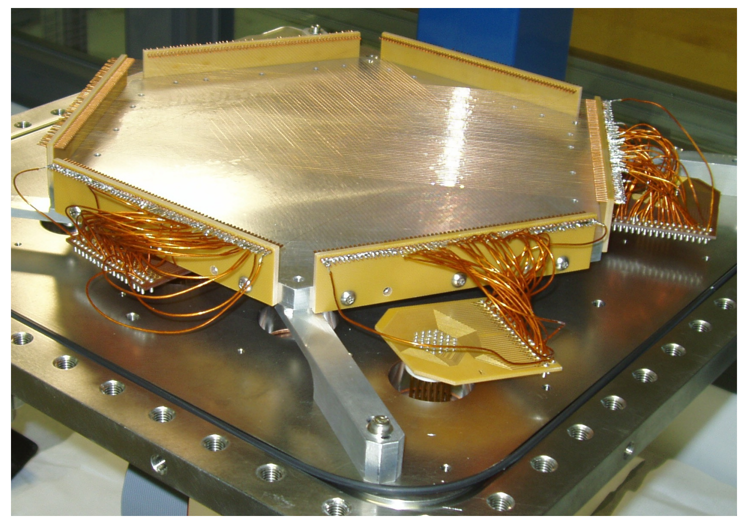

Measurement with the parallel charge division MSGC200

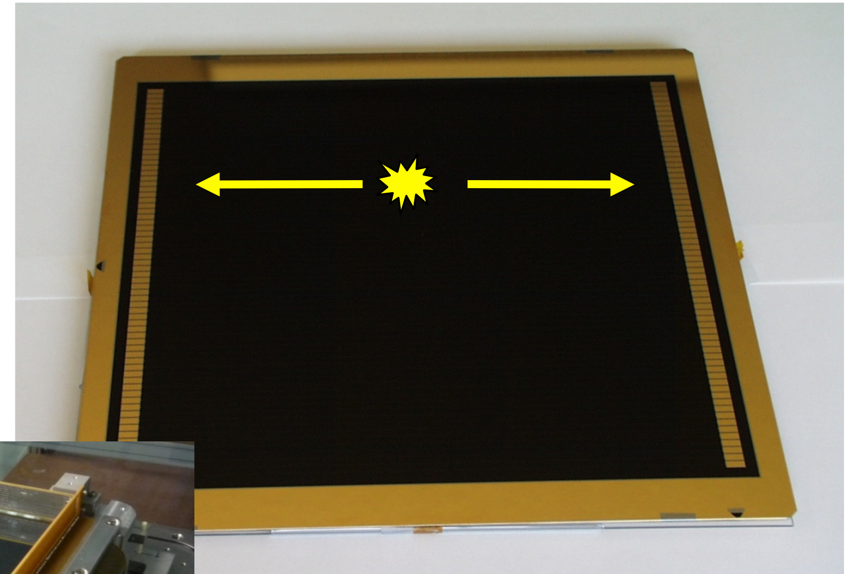

Principle

Each anode is readout individually on both ends for position measurement

Possible applications

- Resolution of 0.5 mm needed in one direction
- Very high counting rate
- Limited sensitive area (20 cm x 20 cm)

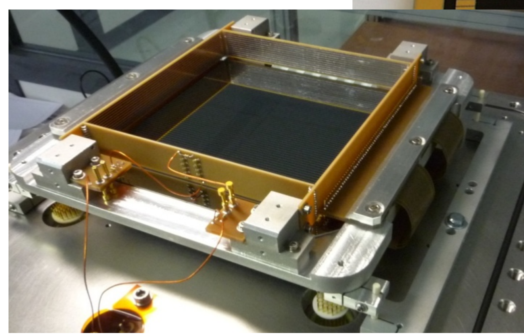

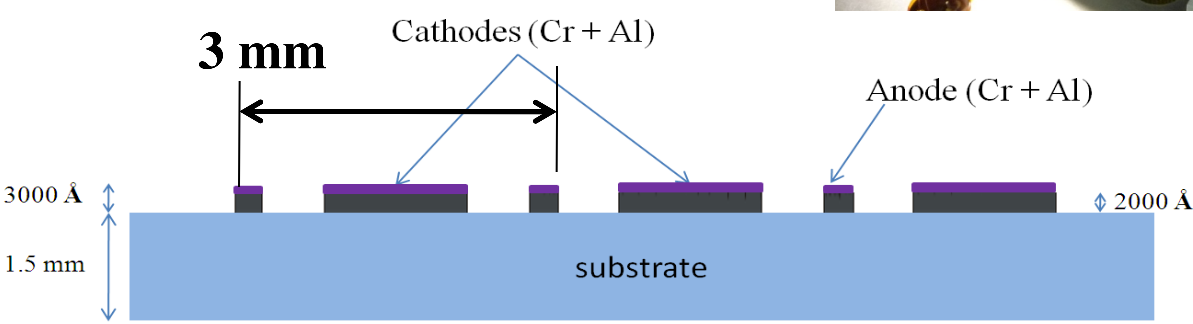

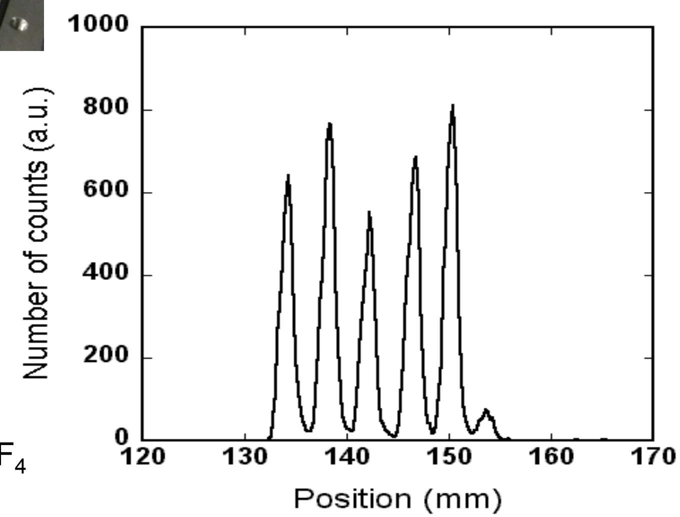

Resolution: 1.3 mm FWHM corresponds to the limit of the stopping gas: 2 bars CF_4

Resolution below 1 mm can be achieved !

On-going development in SINE2020

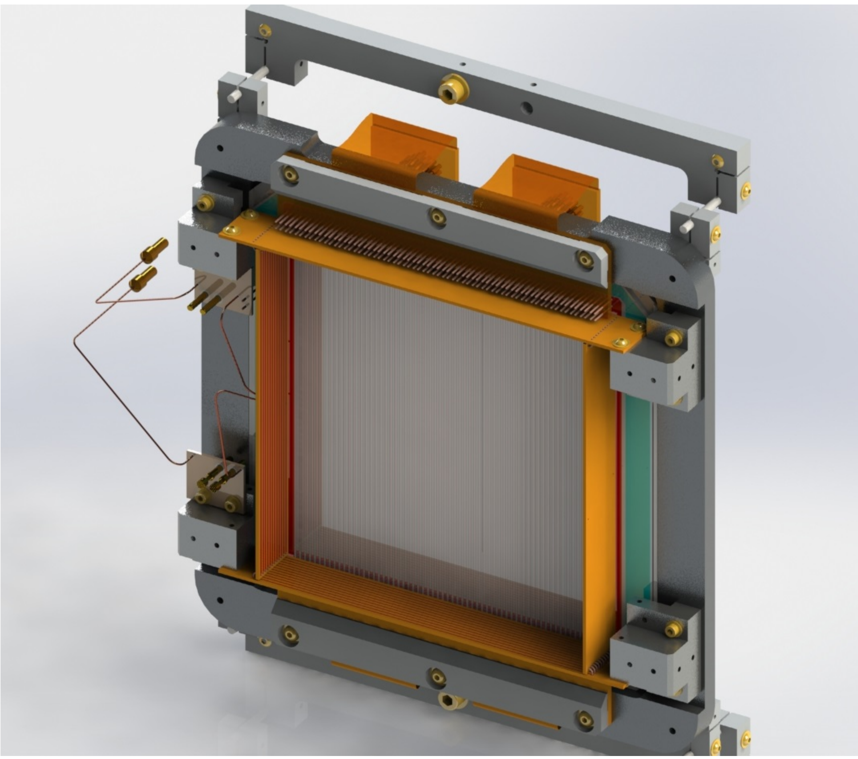

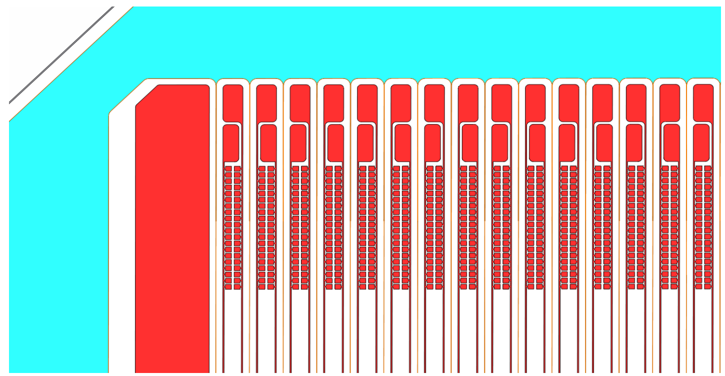

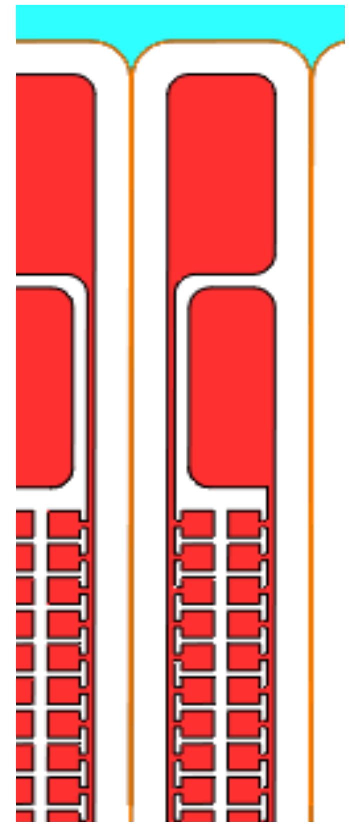

TASK 9.3: Development of a 3He based microstrip gas with a novel 2D readout

The microstrip gas chamber is intrinsically a 1D position sensitive device

- **The proposal is to make it 2D position sensitive by laying down resistive cathodes**

Operation with BF3

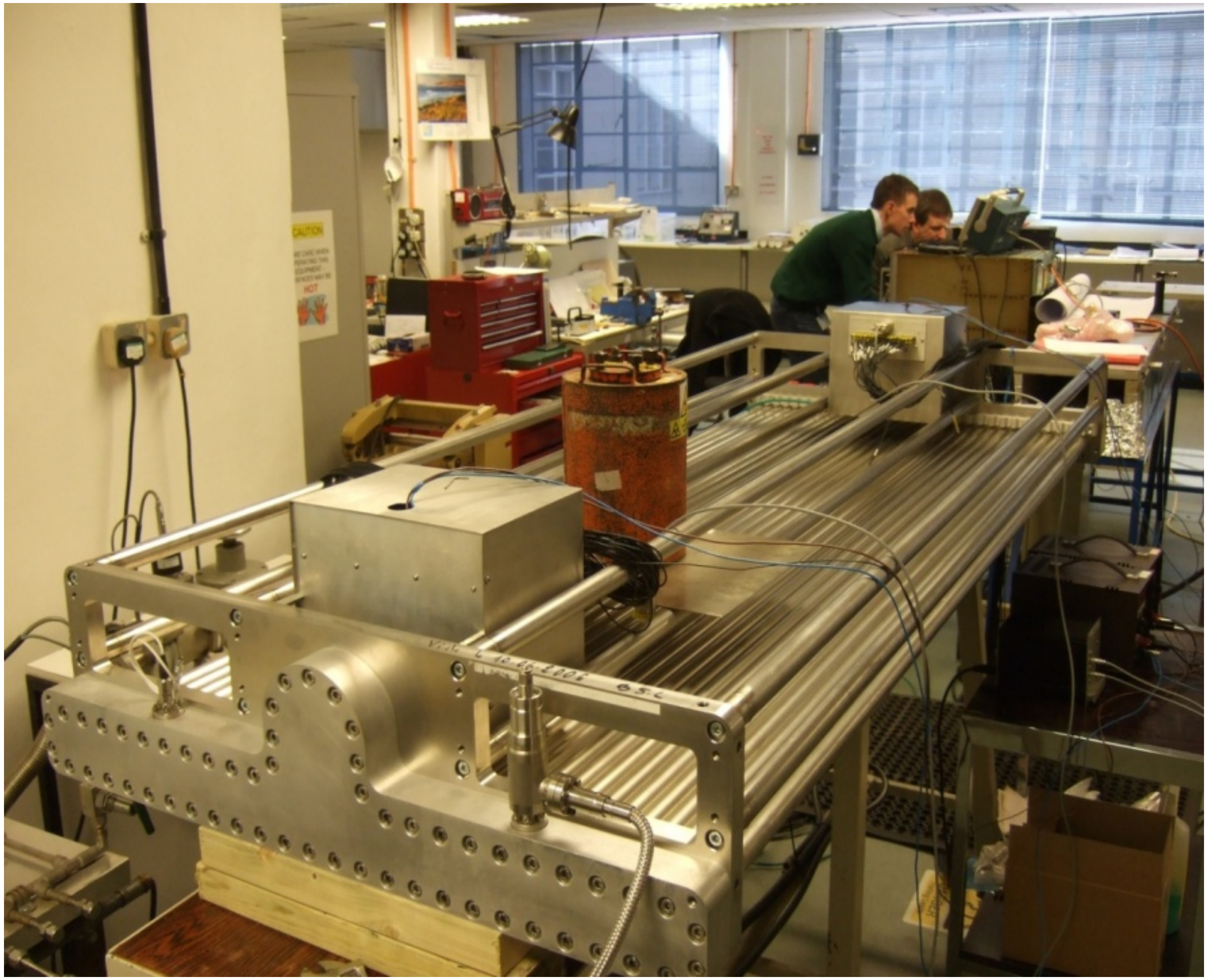

Test of an IN5 Multitube filled with BF3

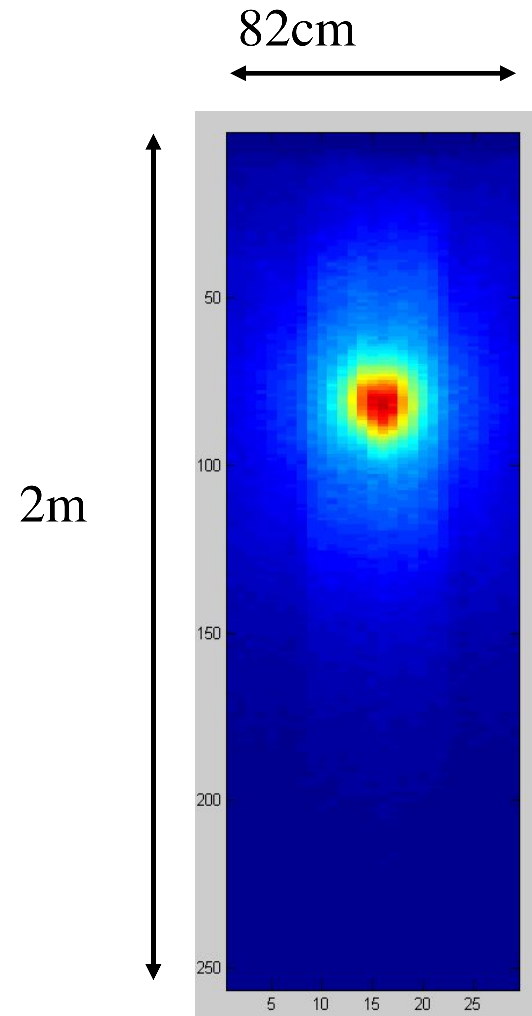

Image of Am-Be source
2 bars of BF3
HV = 3600V

Operation with BF3

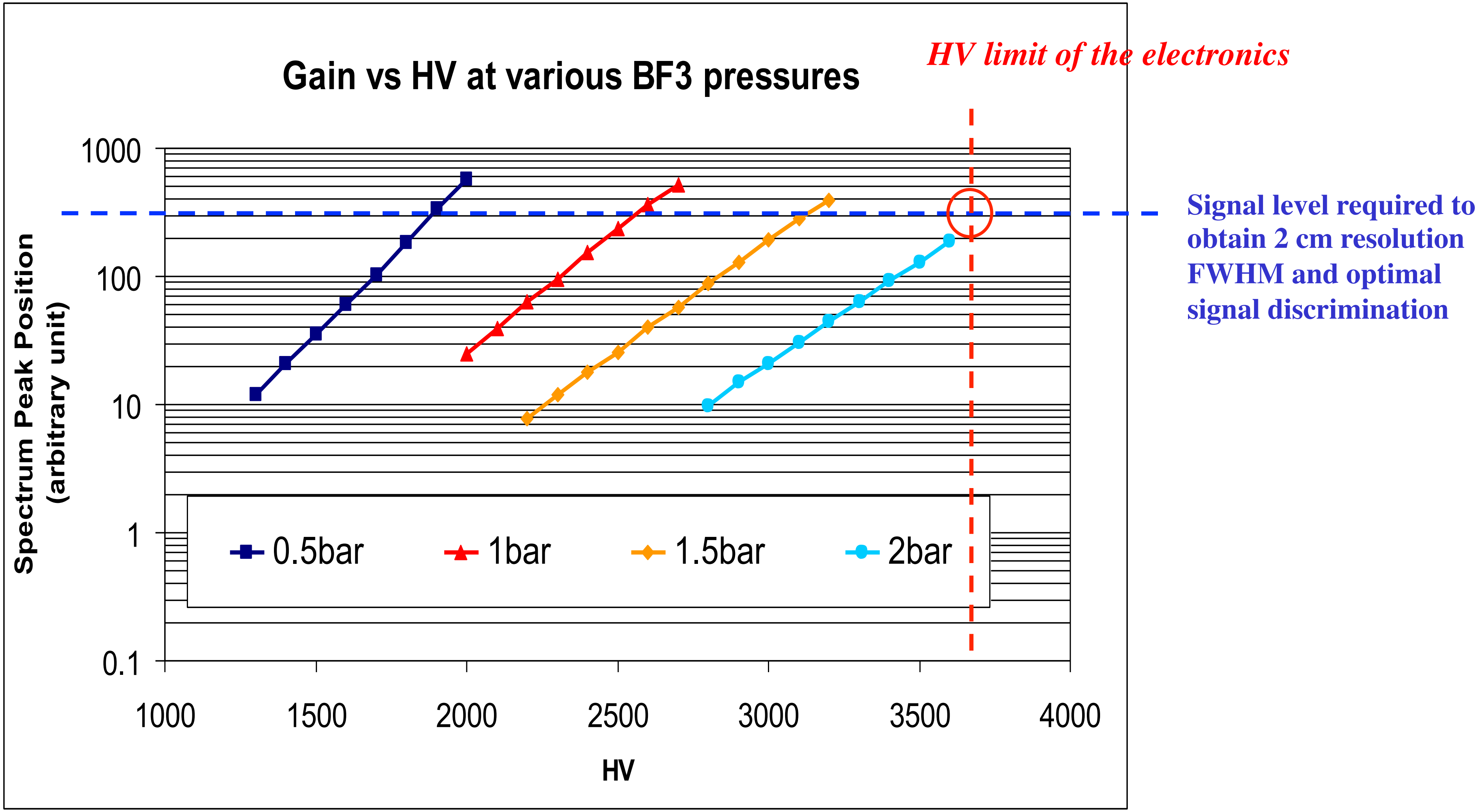

Operation with BF3

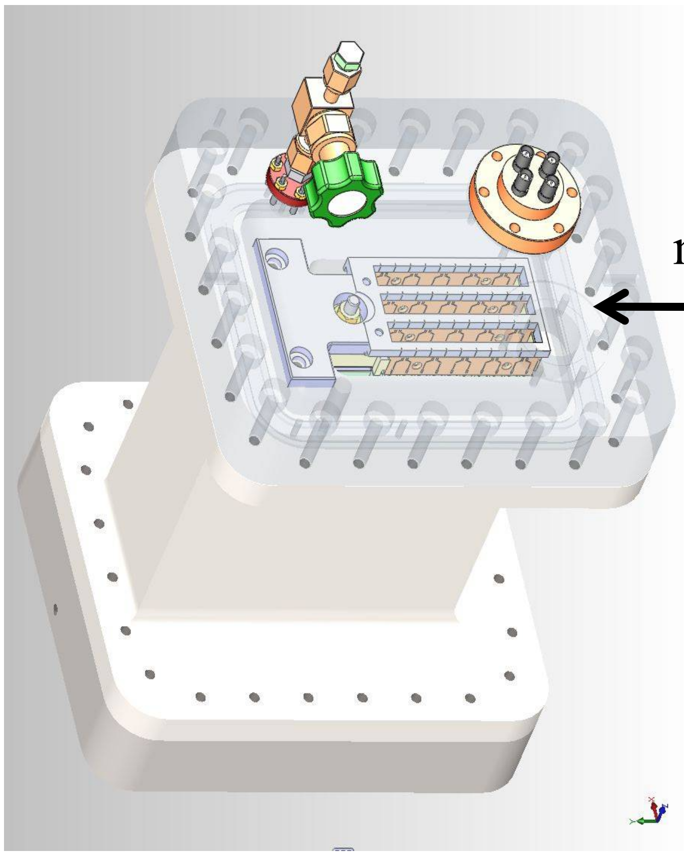

n

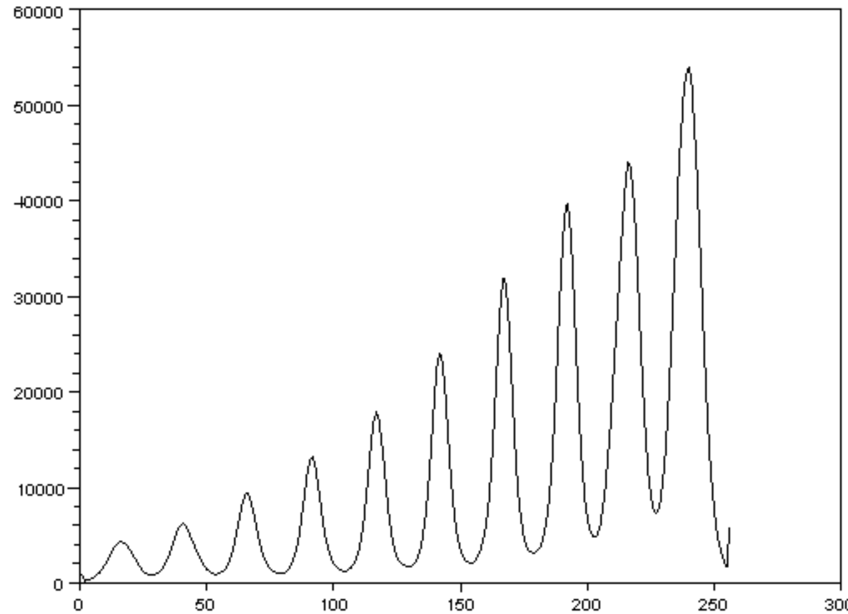

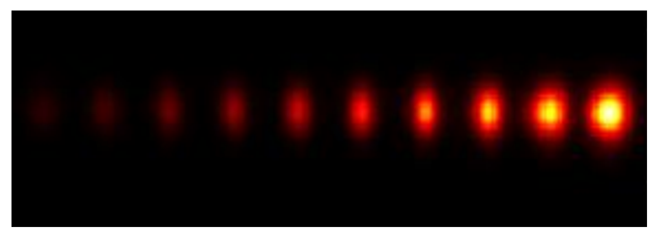

n

Measurement at BARC with a BF3 Multi-grid: 94% efficiency

Solid neutron convertor in gas detectors: B_4C thin films

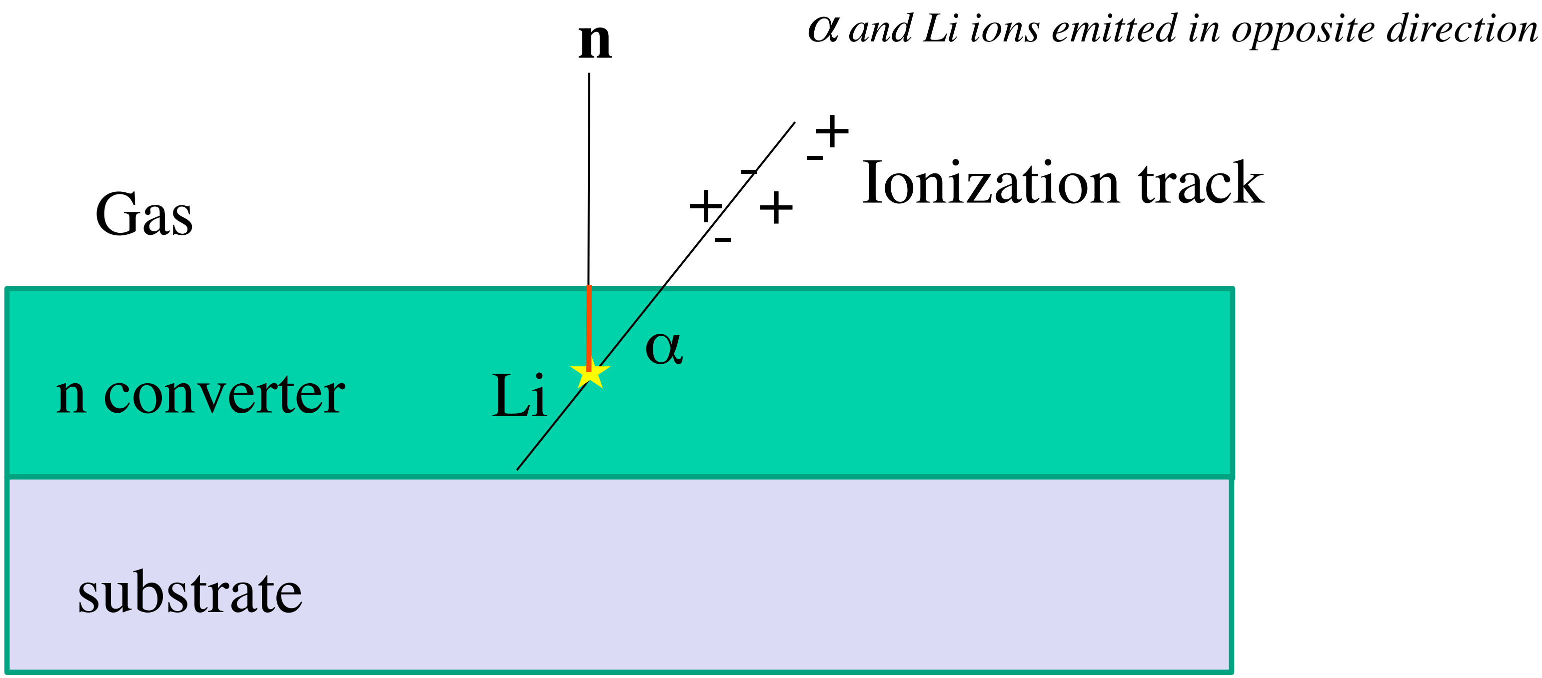

- n + ^{10}B → ^{7}Li* + ^{4}He → ^{7}Li + ^{4}He +2.31 MeV+ gamma (0.48 MeV) (93%)
  → ^{7}Li + ^{4}He +2.79 MeV (7%)

(σ_c = 3840 barns @1.8 Å)

Grazing angle (Multi-Blade)

eff X 5 at 10° → 23% (measured)

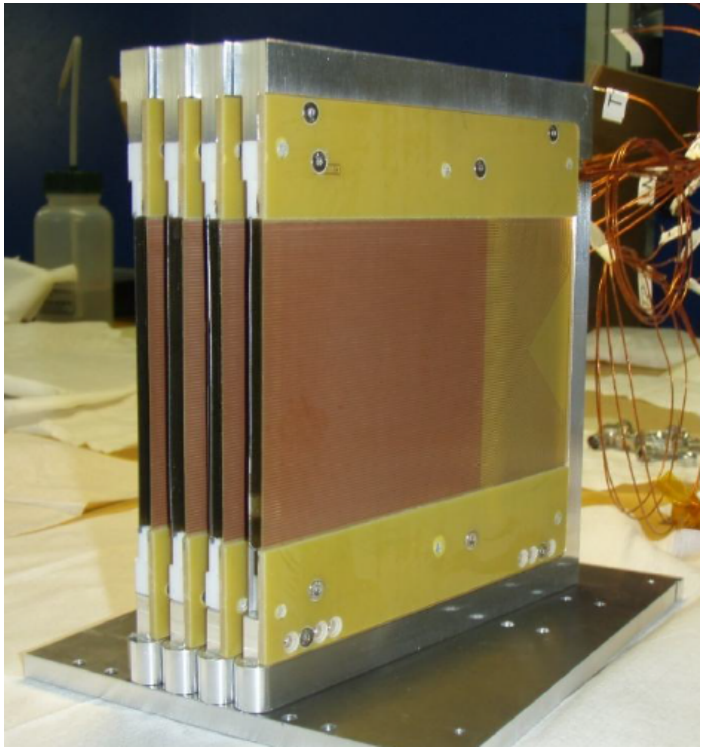

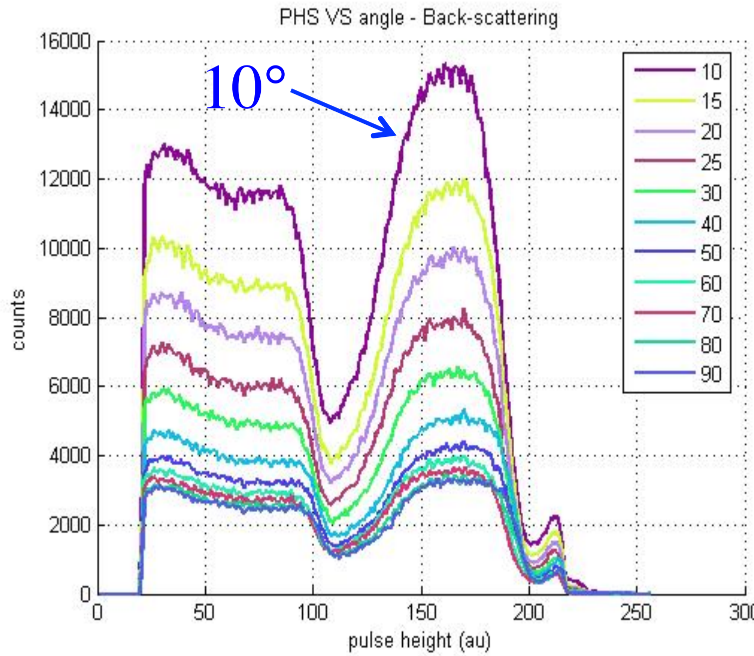

PH spectra for 2.5 Å neutrons and different angles

Principle: Neutrons are converted on a ^{10}B coated substrate oriented with a **small angle** to the incident neutrons
→ high efficiency + no parallax error + no dead zone

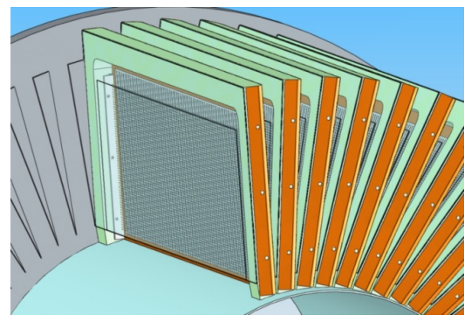

Simulation

Multiblade 10°
Radial geometry

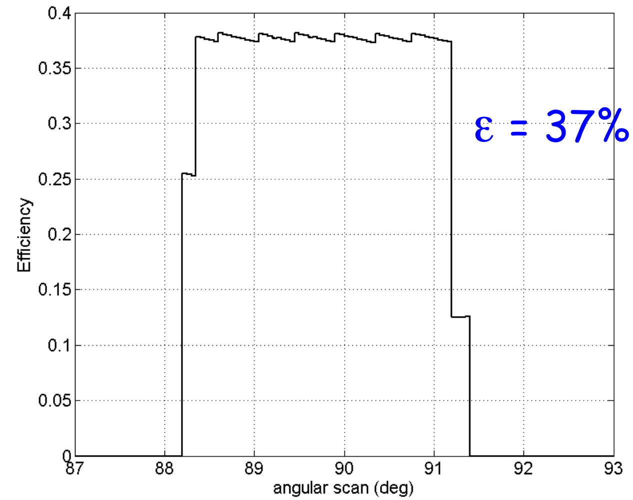

ε = 37%

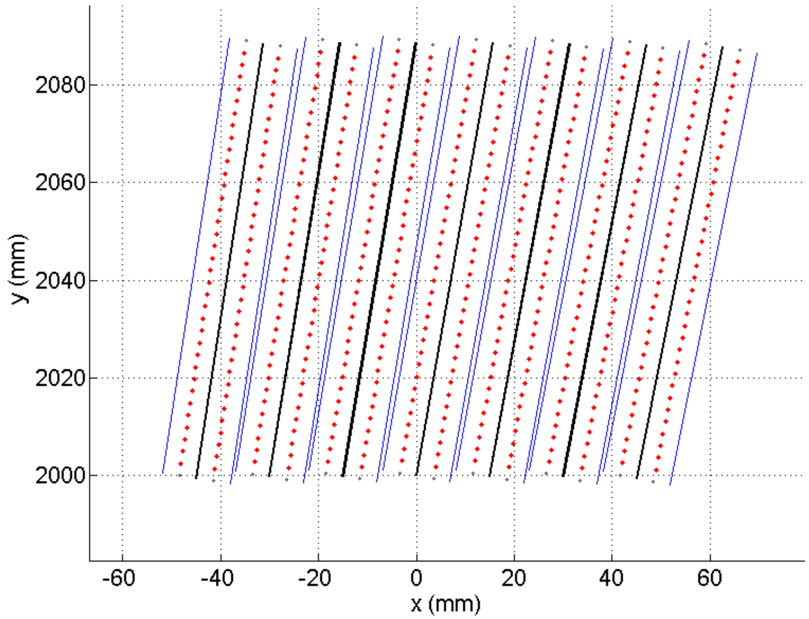

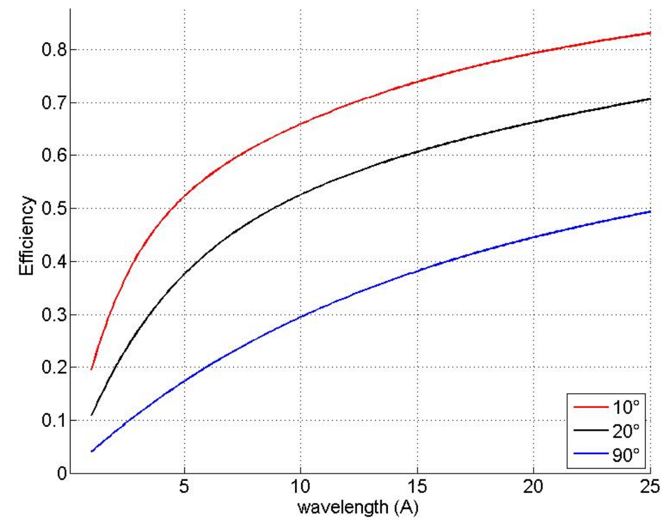

ε versus Wavelength

TPC readout mode

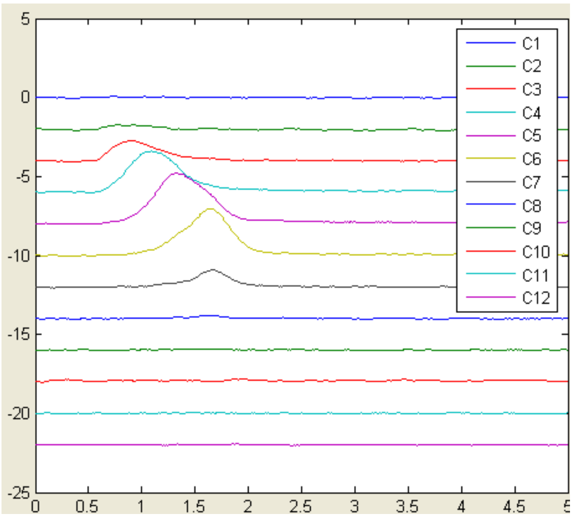

Signals measured on 10 wires in a 1D MWPC (anode pitch 2.5 mm) containing a ^{10}B coated foil and 1 bar of CF_4

The centre of gravity of the signals is measured for each time sample (every 10 ns).

The resulting curve gives the position of the ionization track projected onto the detection plan in function of the time.

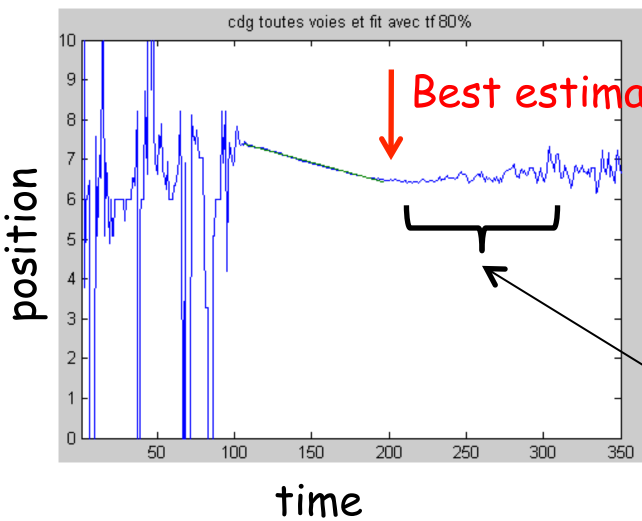

Best estimate of the n capture

The horizontal section corresponds to the induced signal after the last section of the ionization track has been collected on the anode frame.
This section is close from the neutron capture position

Normal angle (Multi-Grid)

17 Aluminium blades, 0.5 mm thick, 2 cm height, for each grid

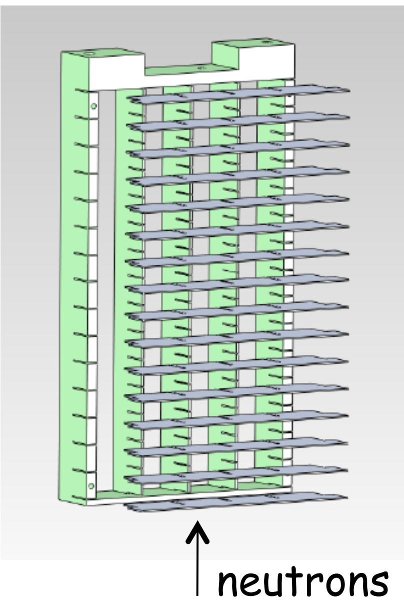

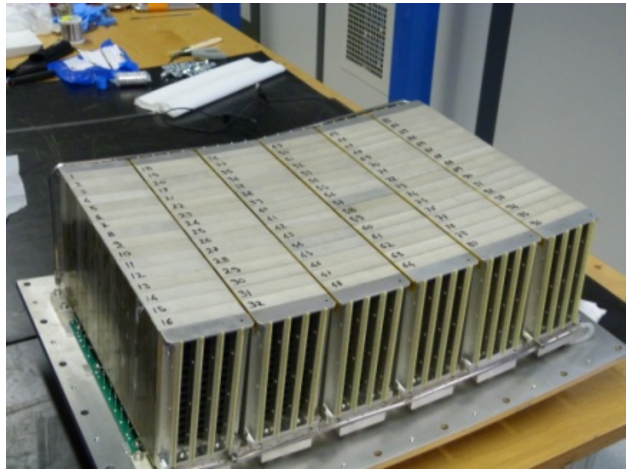

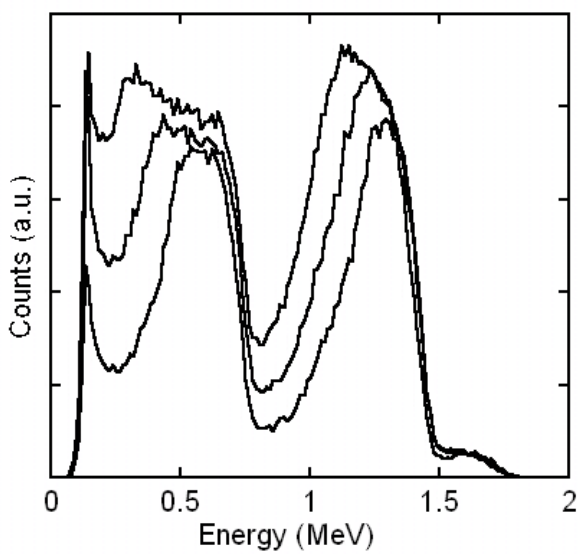

PH spectra for 2.5 Å neutrons and $^{10}B_4C$ film thickness of 445, 665, 895 μm

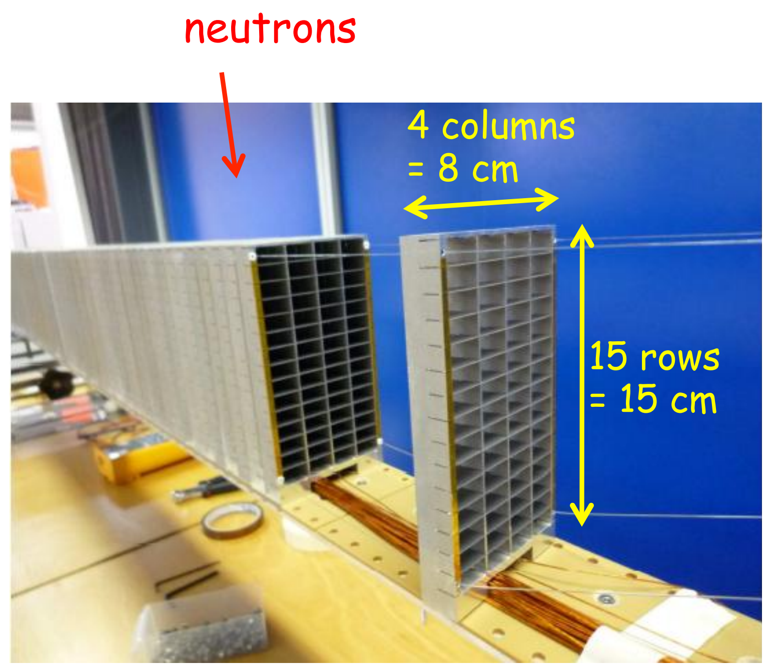

Stacking of 96 grids of 2 cm height electrically insulated from each other

Individual readout electronics (anodes and grids)

Multi layers optimisation by MC simulation

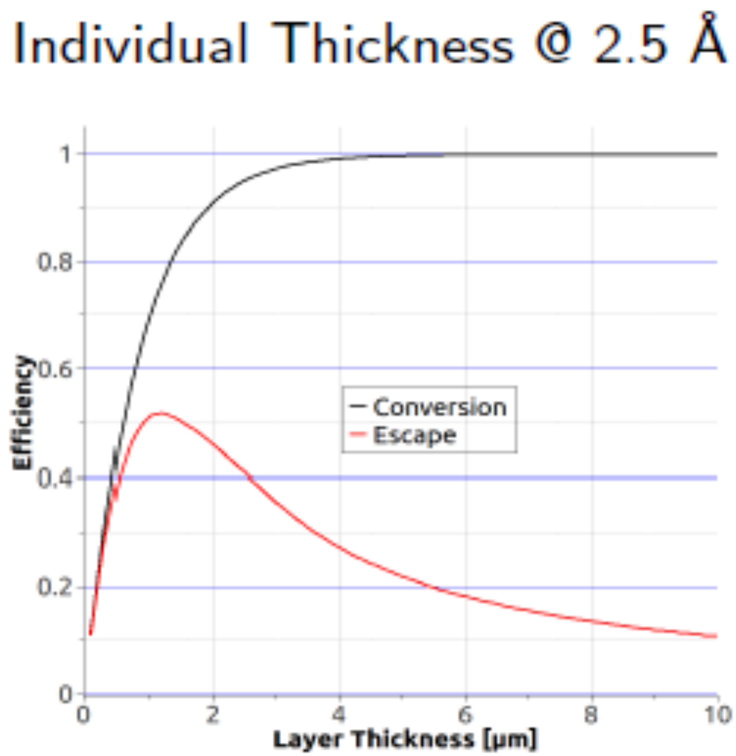

Detection efficiency vs thickness (30 layers)

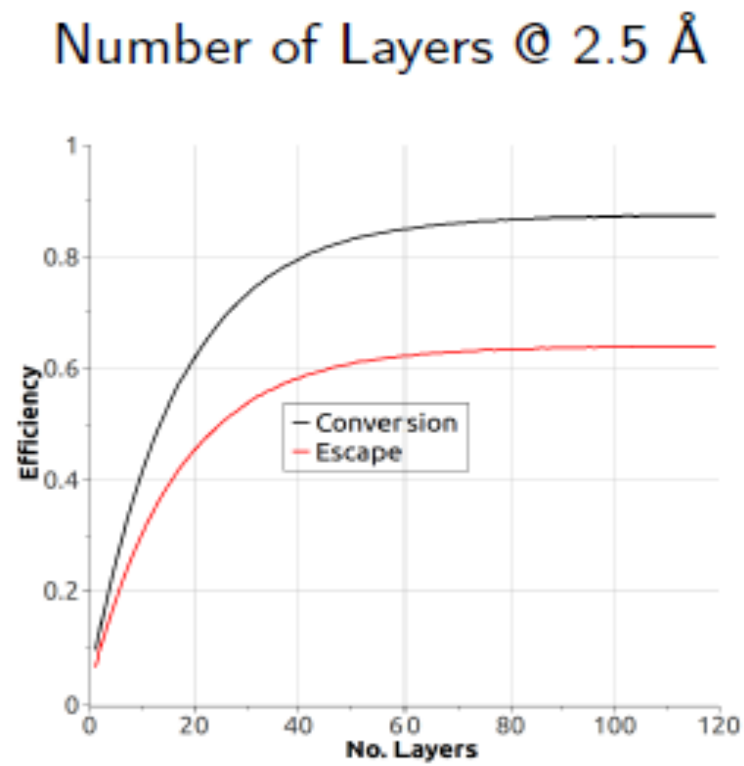

Detection efficiency vs number of layer (1 μm thick)

CRISP project (ILL, ESS, LU) Large Area detector study

- Mass production of ^{10}B films.
- Technical specification of the demonstrator compatible with operation in a vacuum TOF chamber

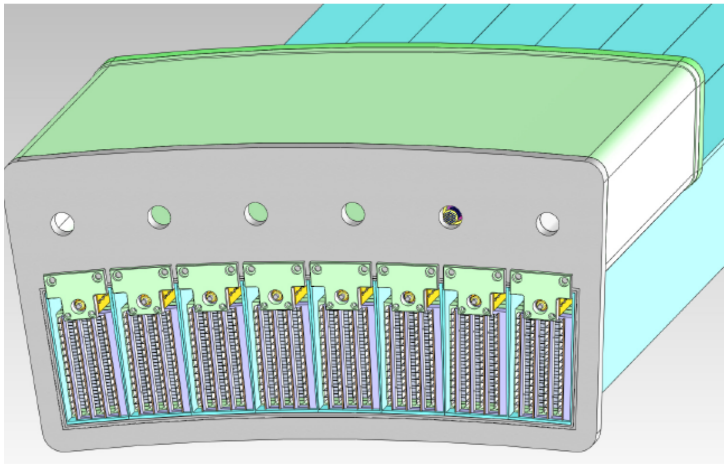

Detector vessel
compatible with vacuum

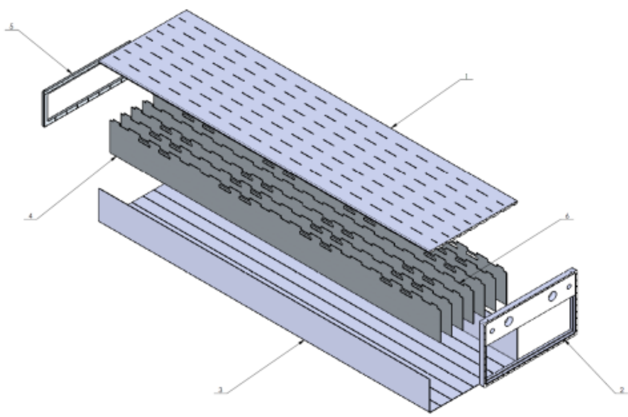

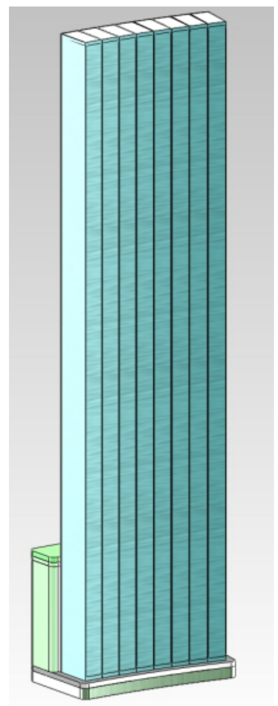

In circle: a module of IN5

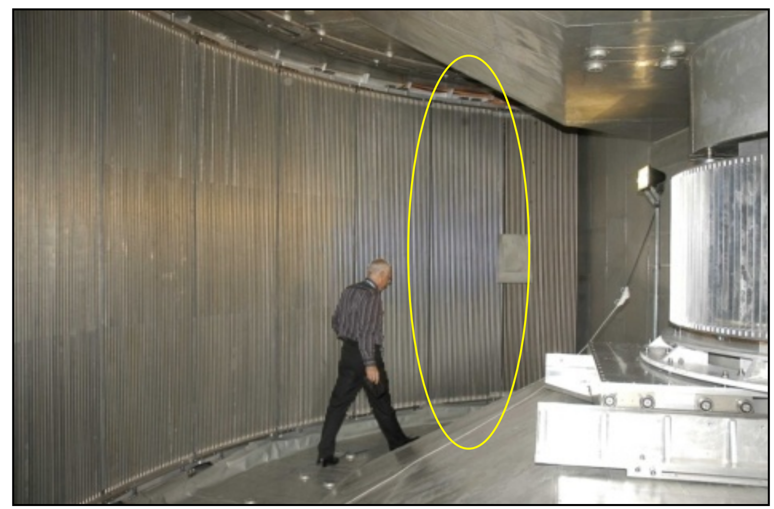

Goal: to demonstrate acceptable performances and mass production for large area detectors

Principle: Electronics

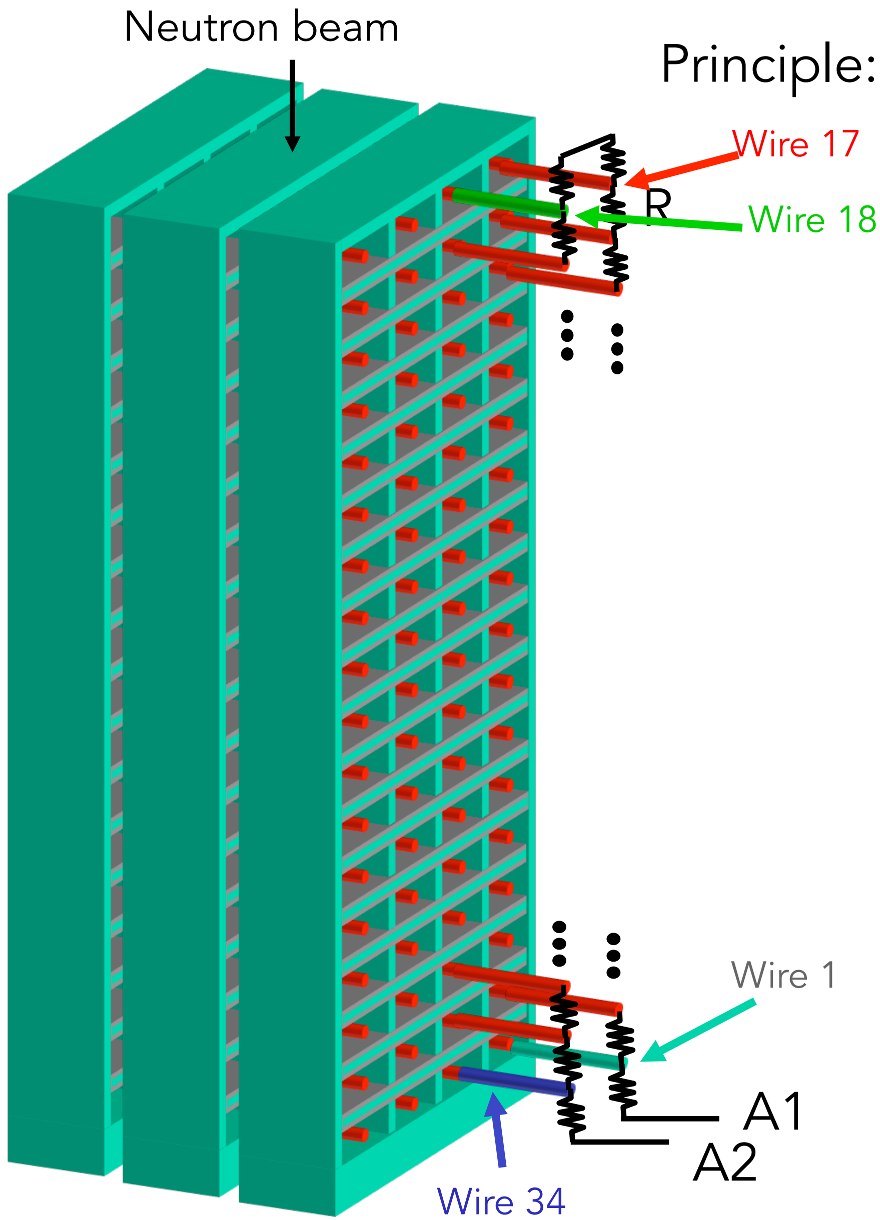

Charge division read out

17 x 4 = 68 wires

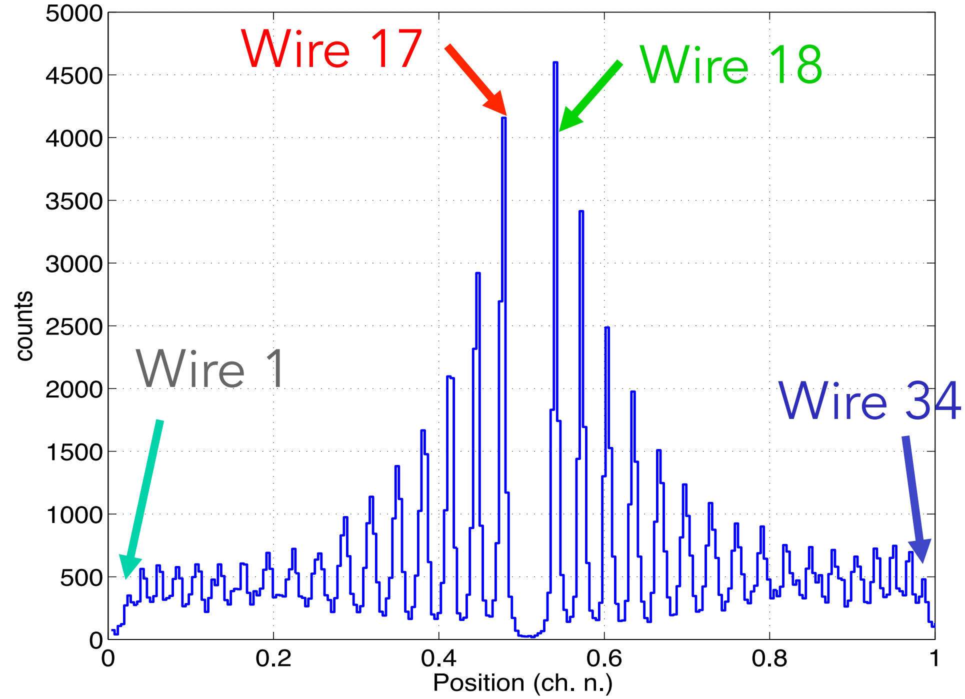

Gas studies

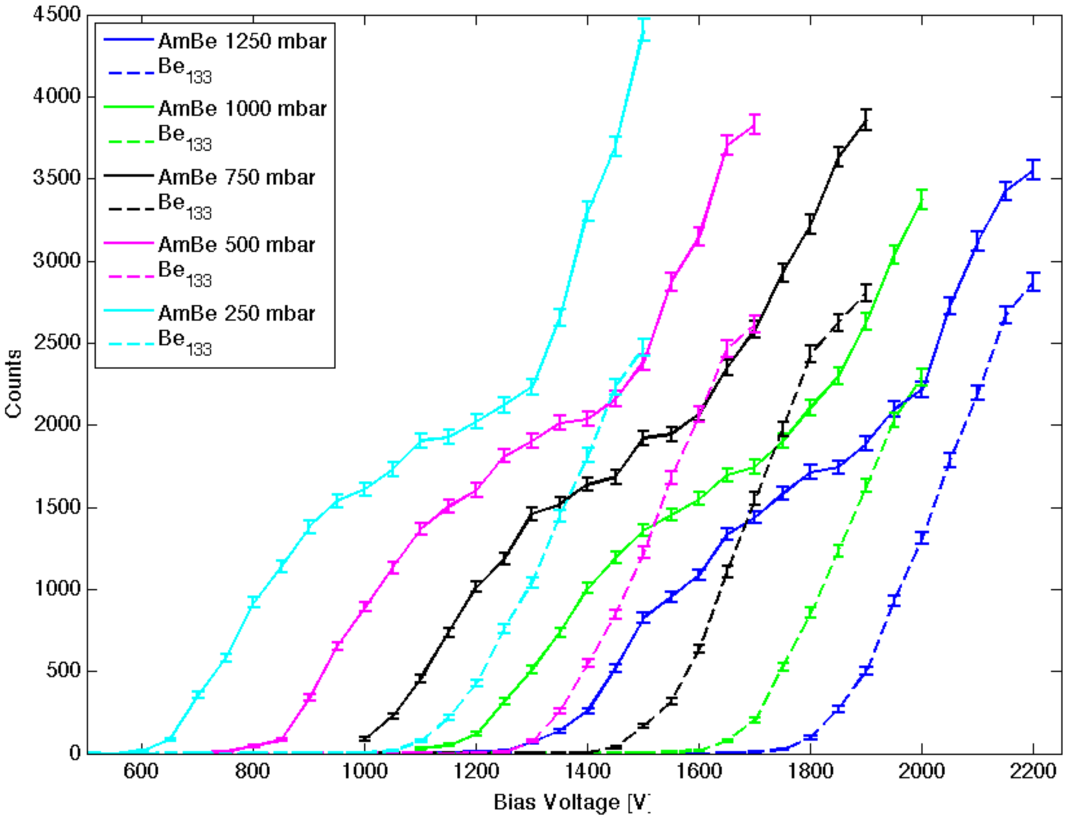

CF4 pressure from 0.25 to 1.25 bar

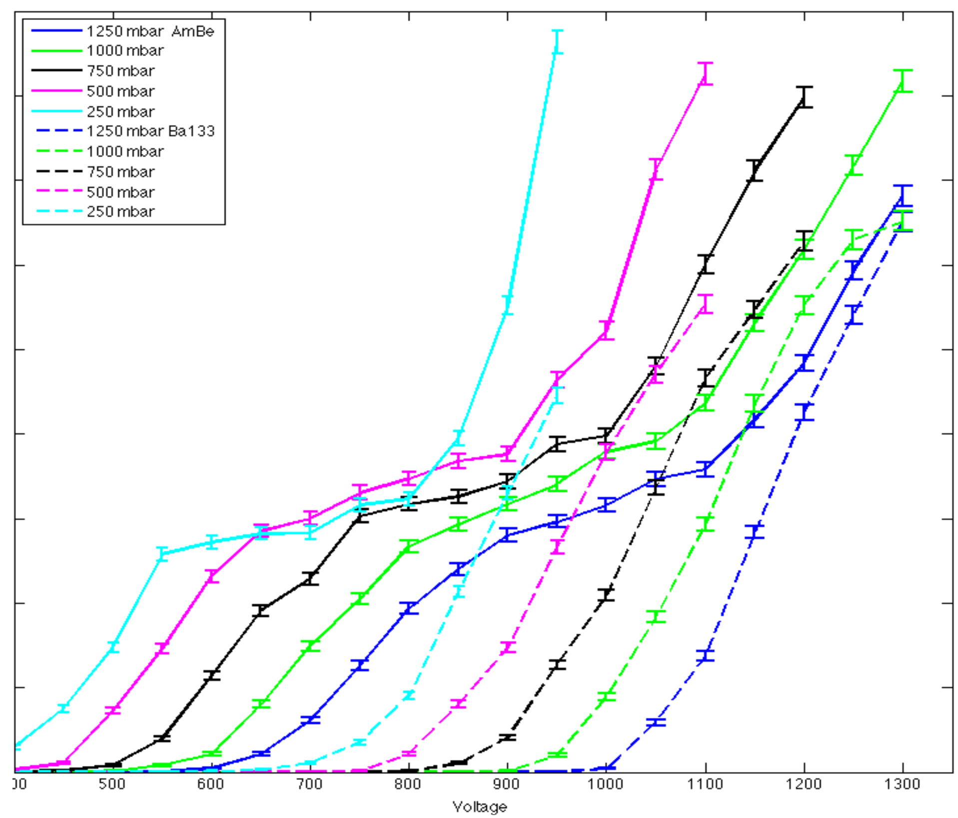

ArCO2 pressure from 0.25 to 1.25 bar

Operating voltage **~700 V with 0.25 bar of ArCO$_2$**

~1100 V with 0.25 bar of CF$_4$

Detection efficiency Measurement

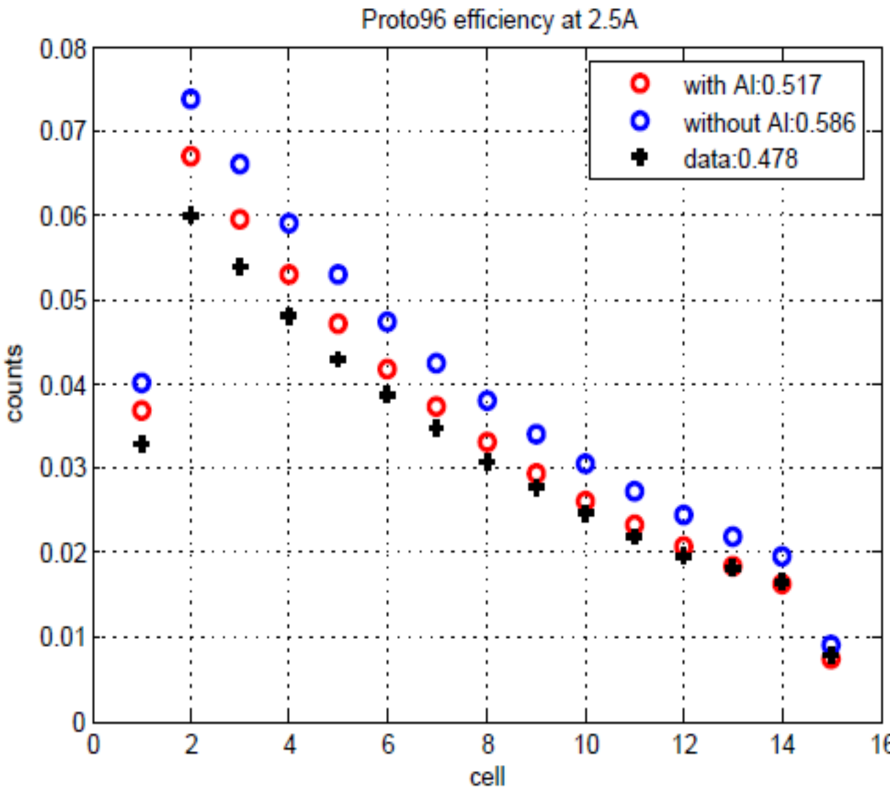

Gamma sensitivity

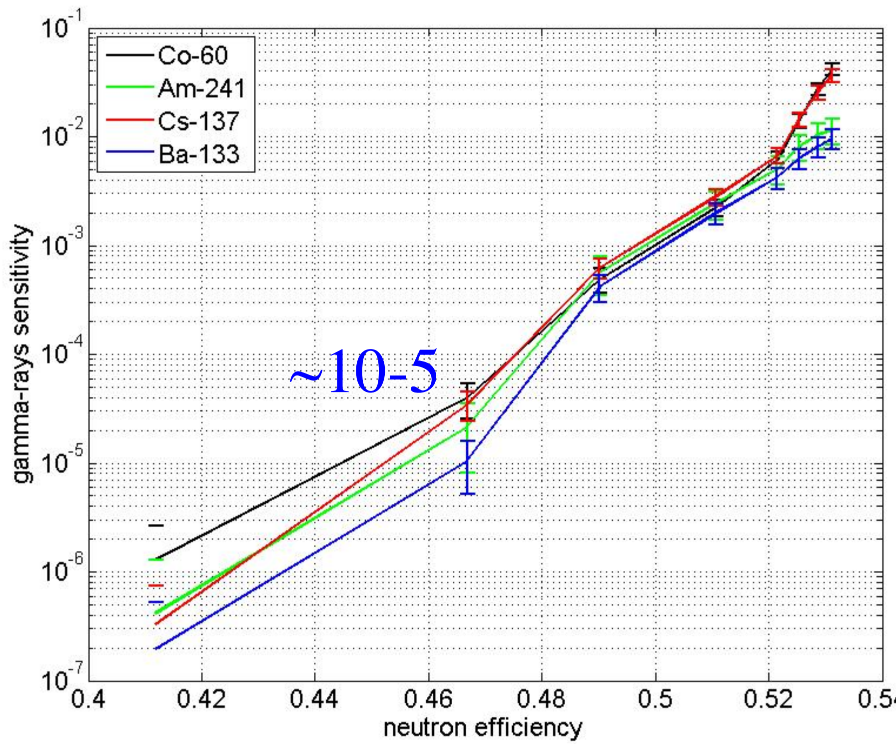

	2.5 [Å]	4.5 [Å]
MC Simulation	52.6	63.3
Measurement	46.8	–
IN5-PSD	∼ 73	∼ 80

Efficiency calculated and measured versus film thickness (2.5 A)

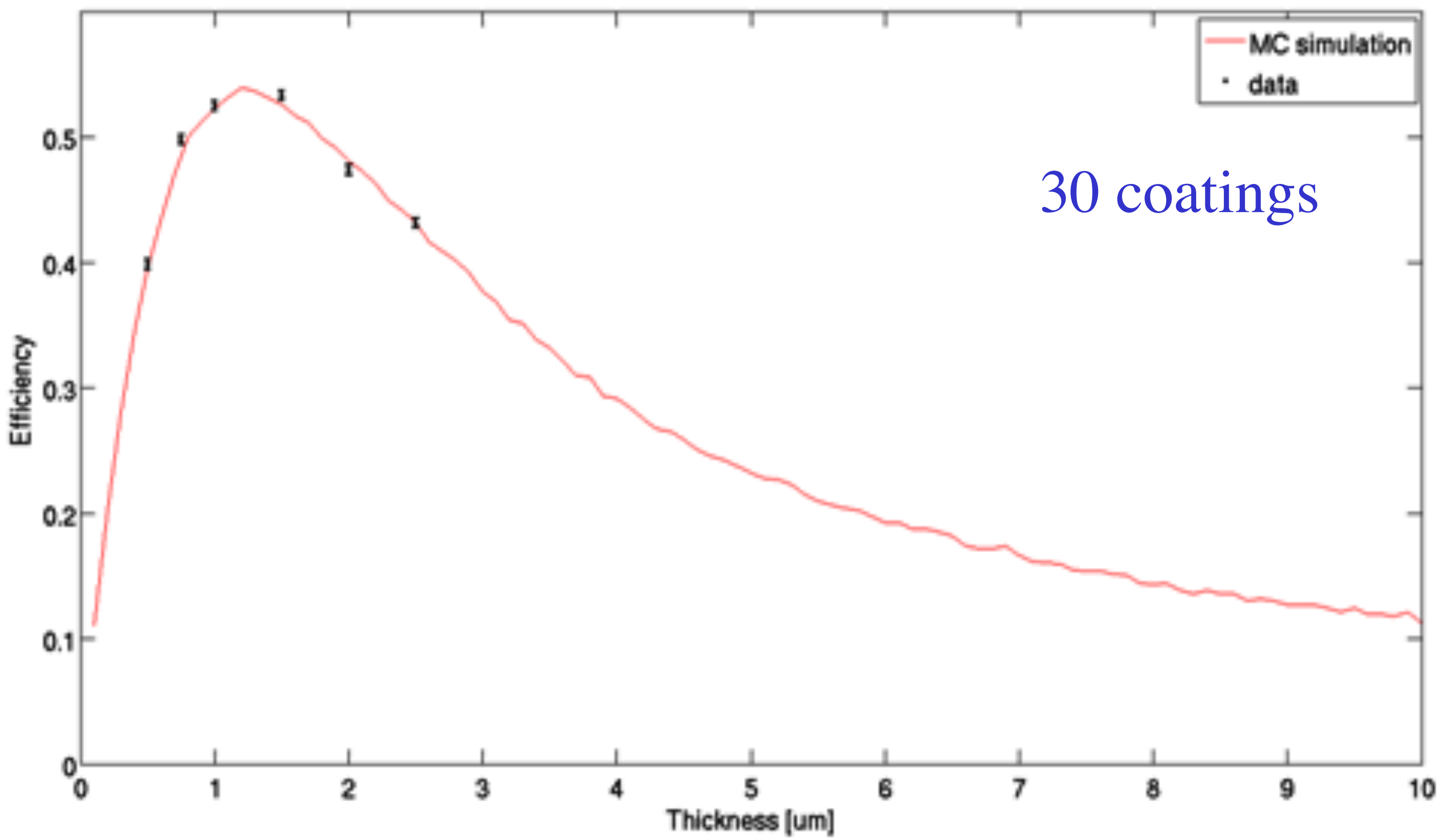

30 coatings

The IN6 prototype

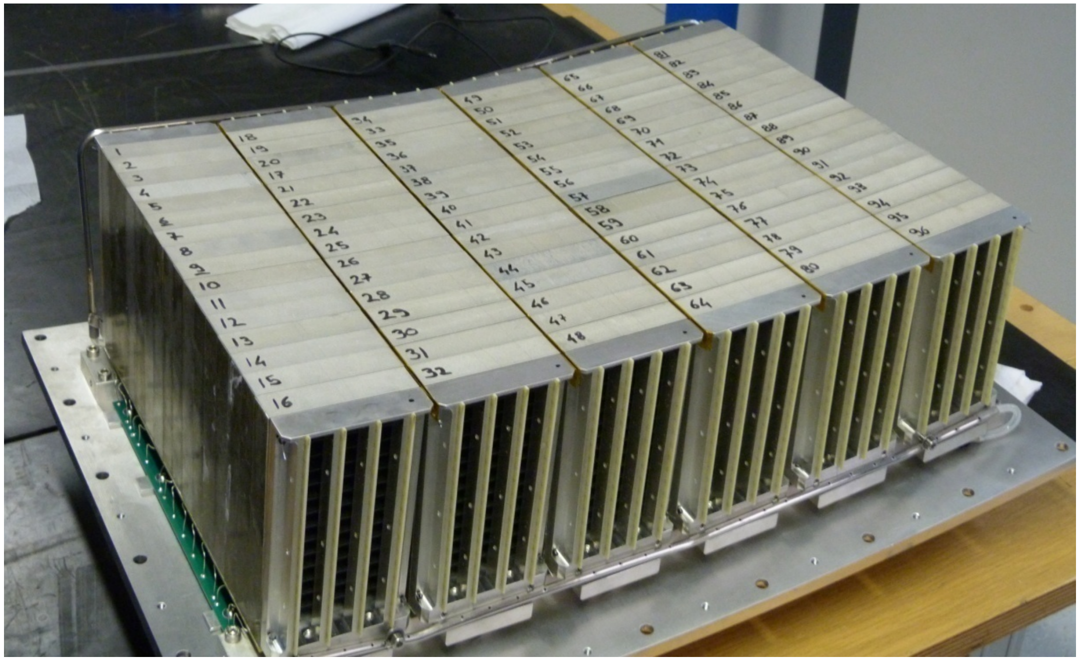

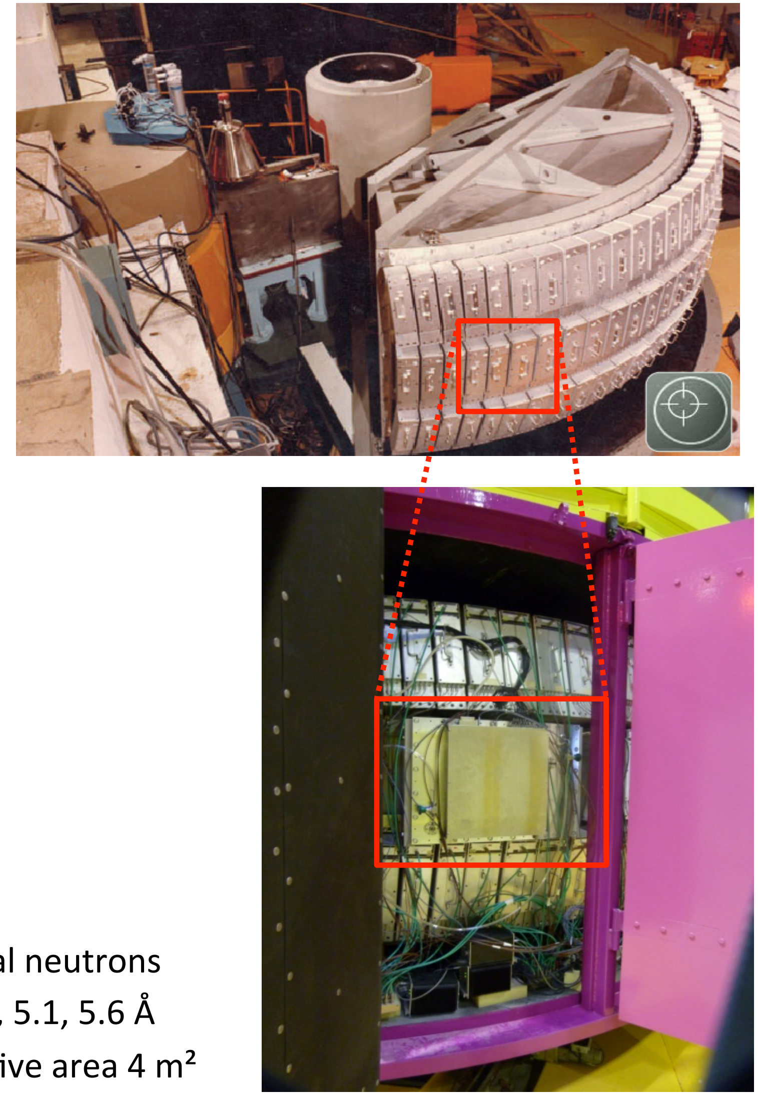

- ToF spectrometer in the range of thermal neutrons
- Available incident wavelengths : 4.1, 4.6, 5.1, 5.6 Å
- Detection system : 337 ^{3}He tubes (sensitive area 4 m²

Position measurement

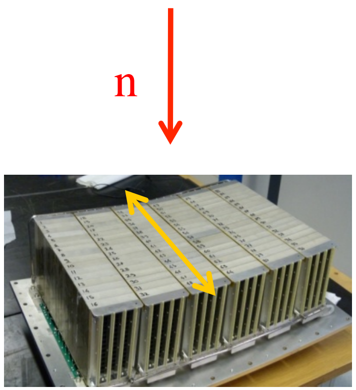

Scan along wires

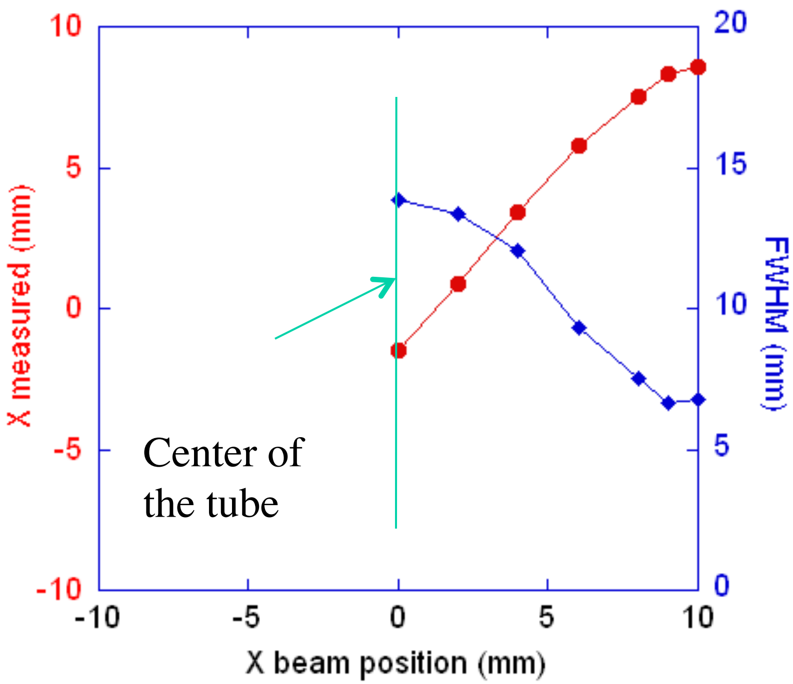

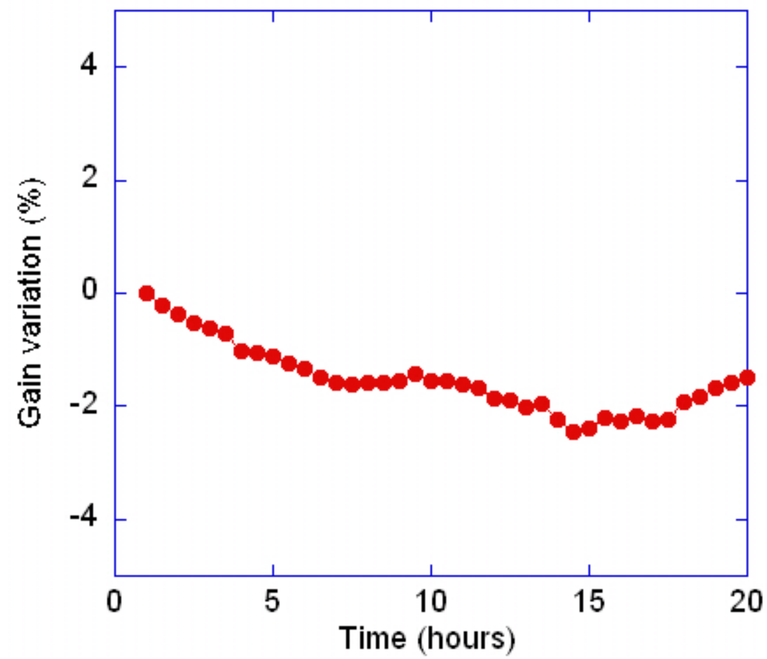

ADCs COG → Spatial resolution ~ 10 mm
Good local linearity

Gain variation with time

Next → TOT COG with FPGA

Scattering

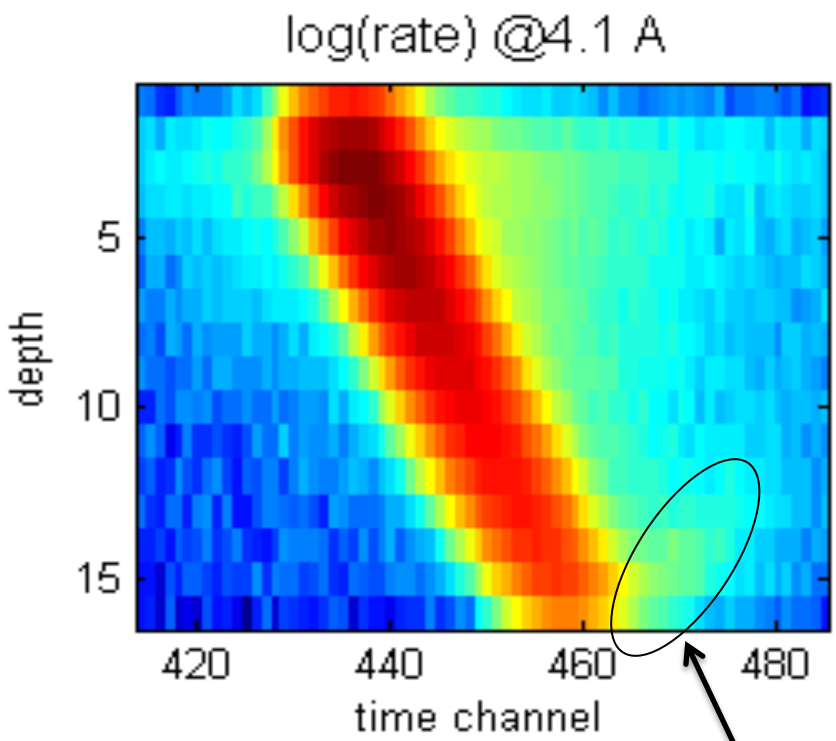

Scattering in Al

Background noise

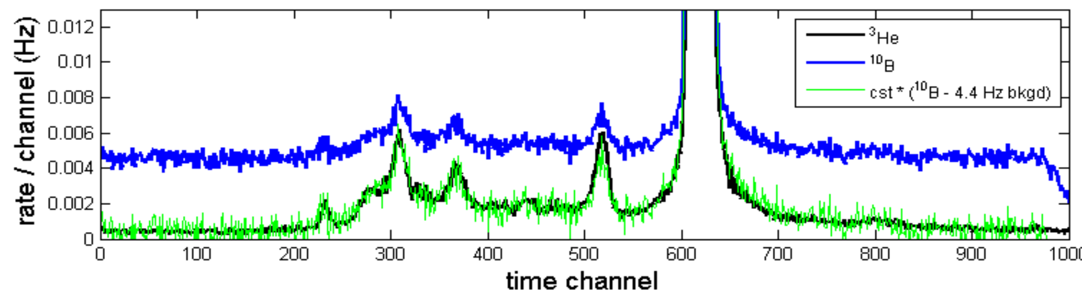

4.4 Hz flat background was observed (**no time structure**)

→ independent of the IN6 instrument / reactor

→ uniform throughout detector

Background noise suppression

1. Ni layer Electrolytic deposition
2. Ni layer Chemical deposition
3. Al pure

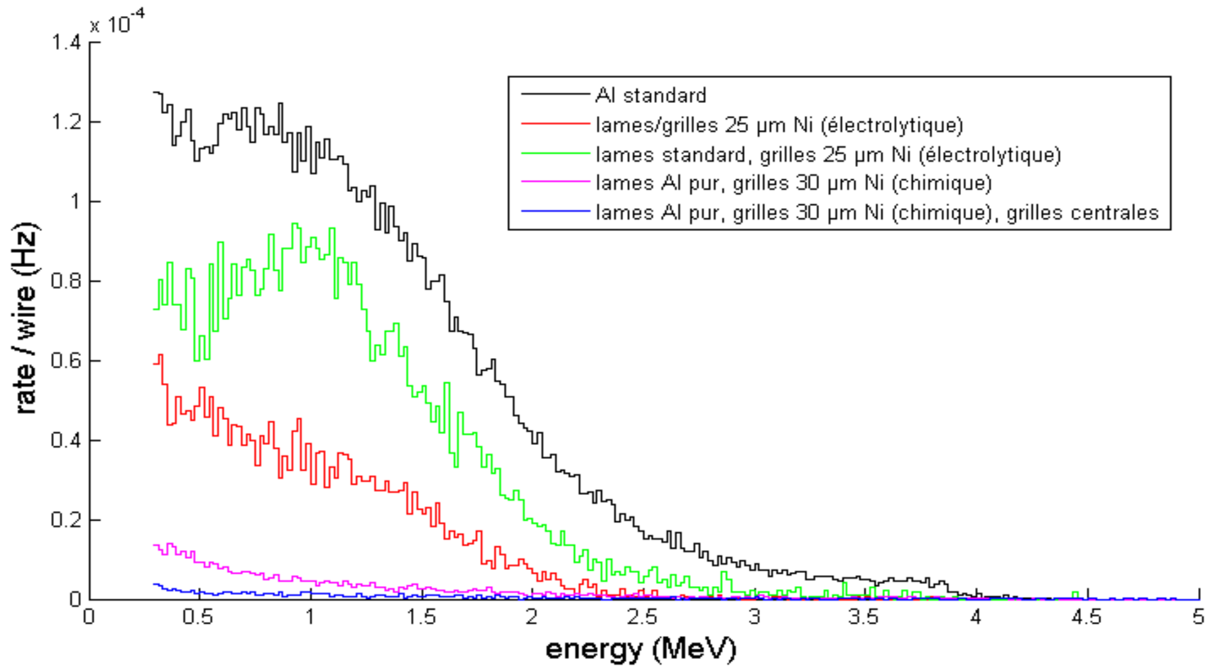

Gamma sensitivity

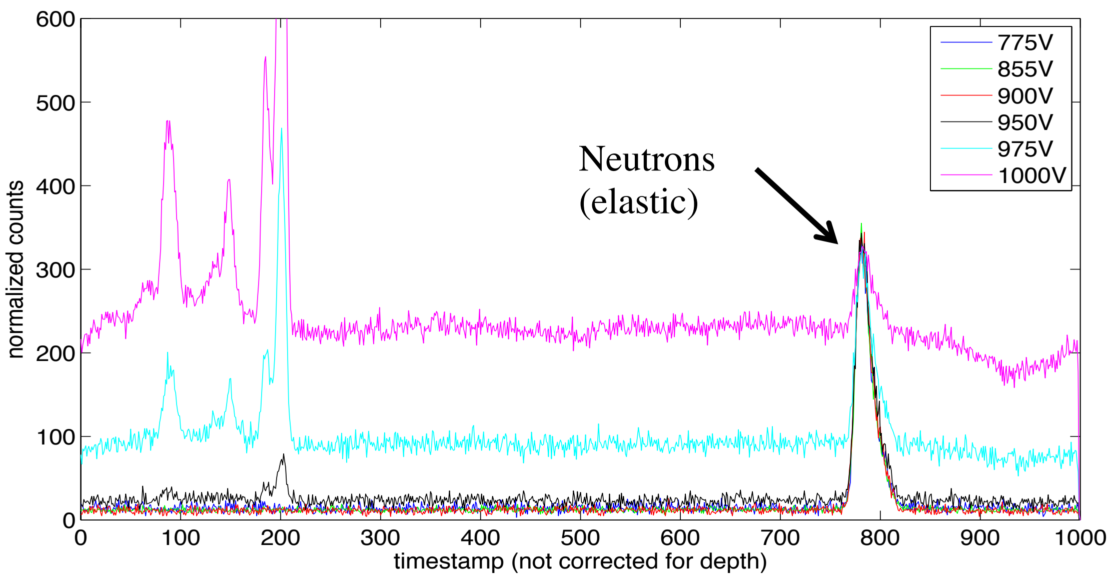

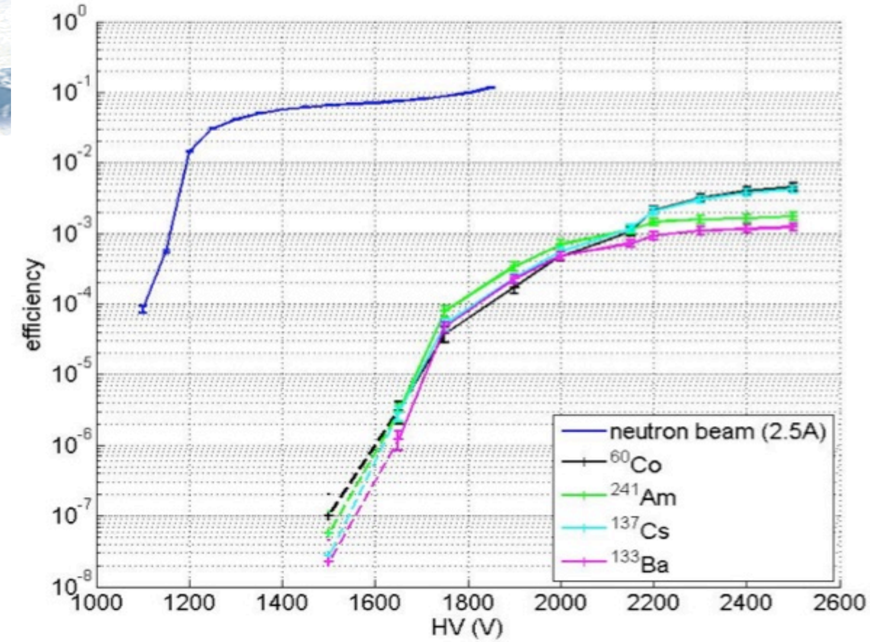

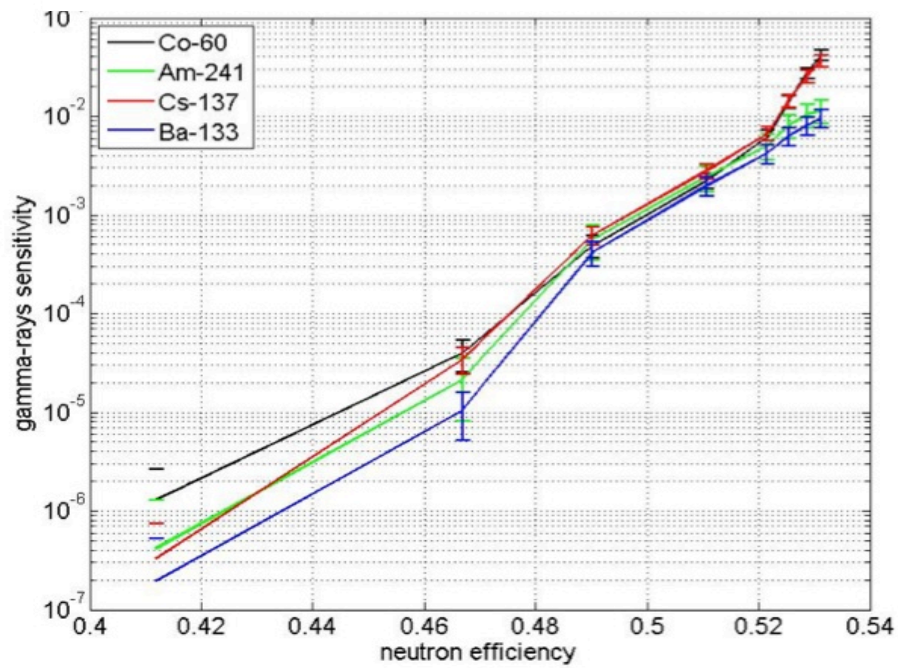

CRISP

The Cluster of Research Infrastructures for Synergies in Physics

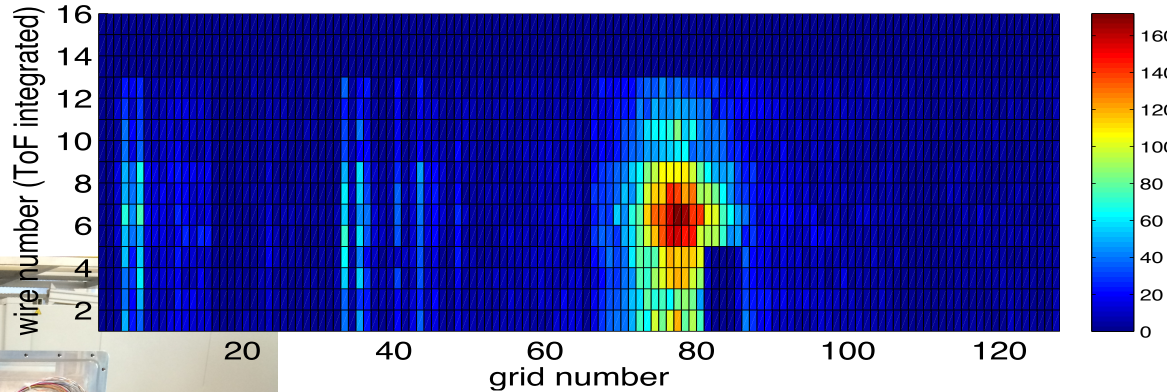

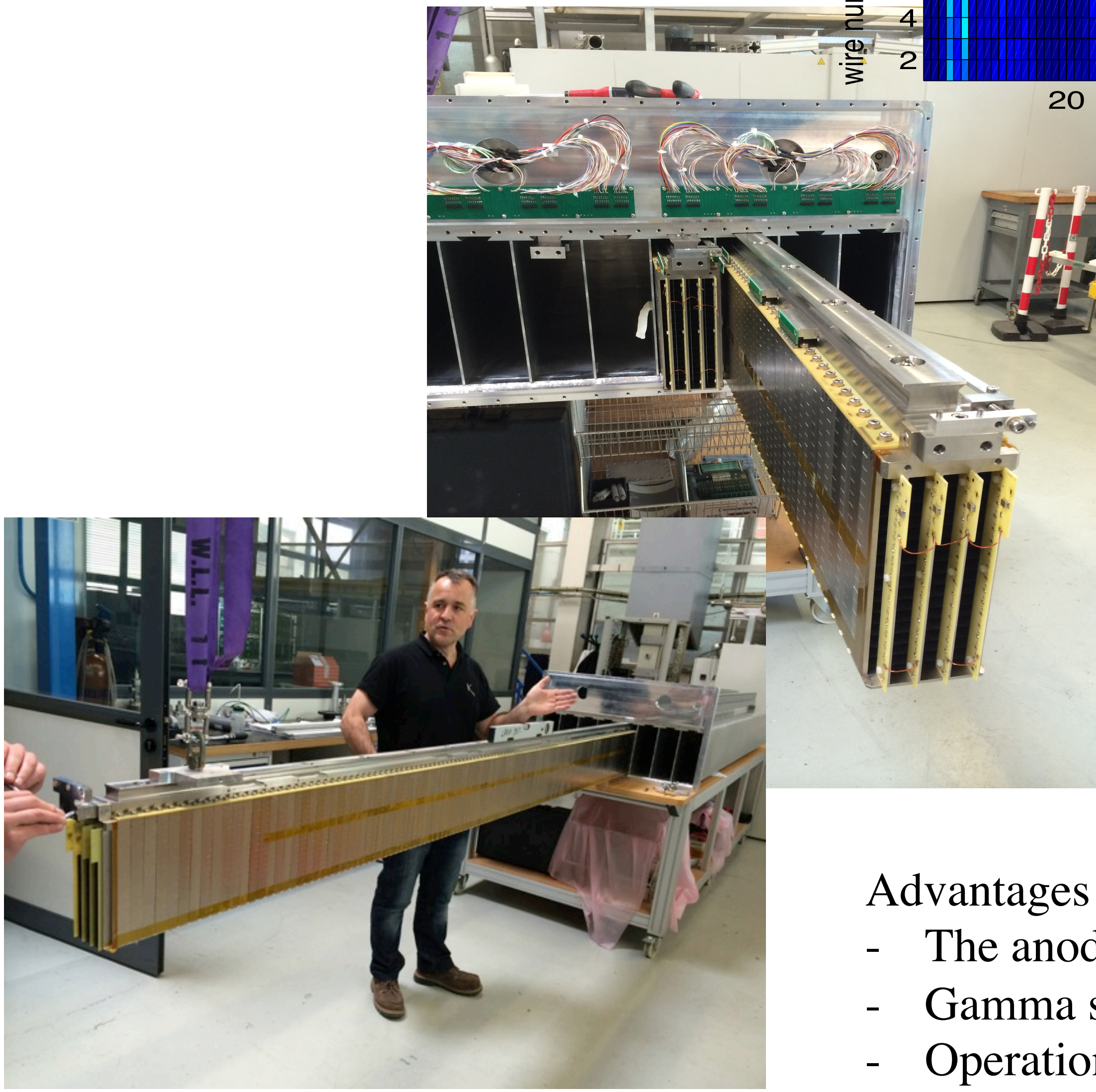

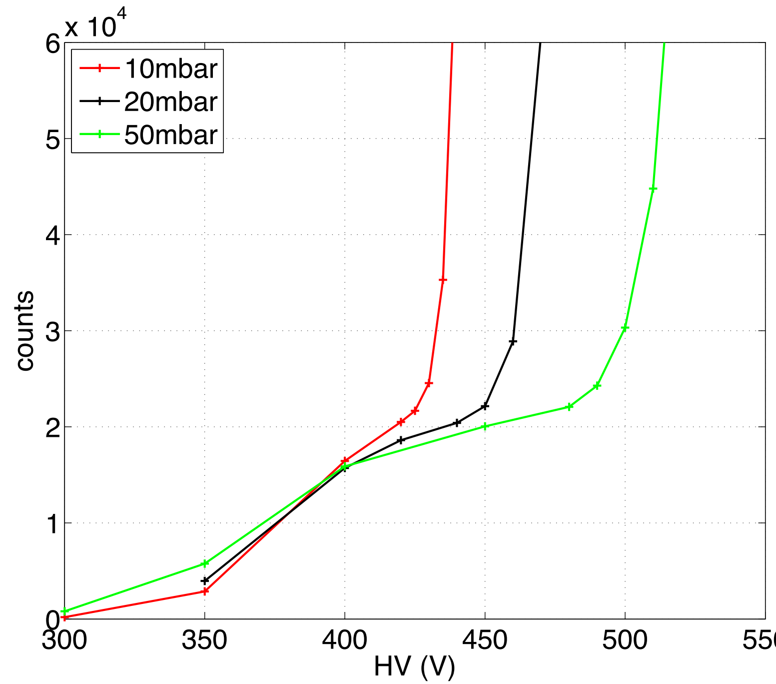

Advantages of the <u>low pressure</u> :

- The anode voltage is reduced by a factor of 2
- Gamma sensitivity is reduced
- Operation in vacuum is simpler → simpler vessel

CRISP
The Cluster of Research Infrastructures for Synergies in Physics

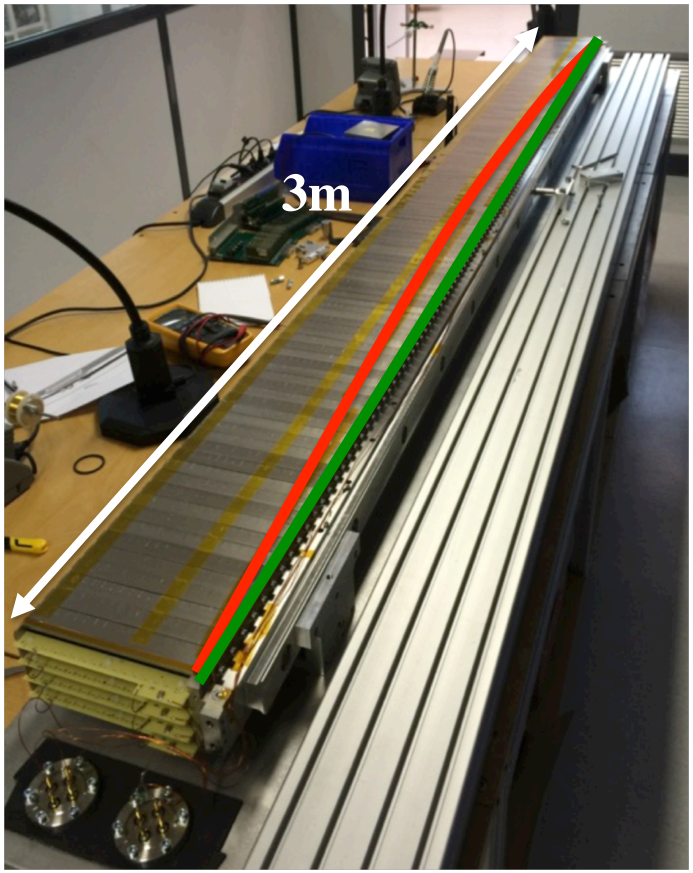

Miss-placement of the anode wire by 1 mm (more than expected) → only 5% increase of the detector counting

Counting stability versus time

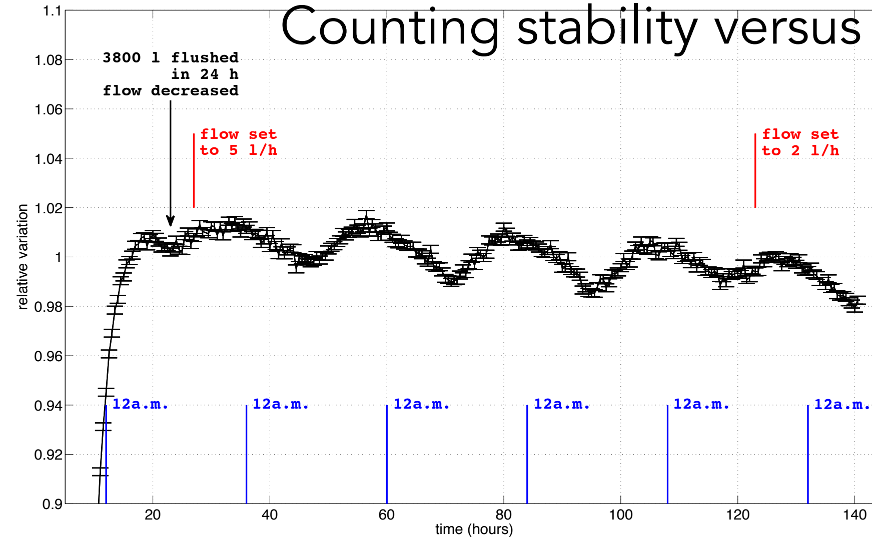

Rectangular tube

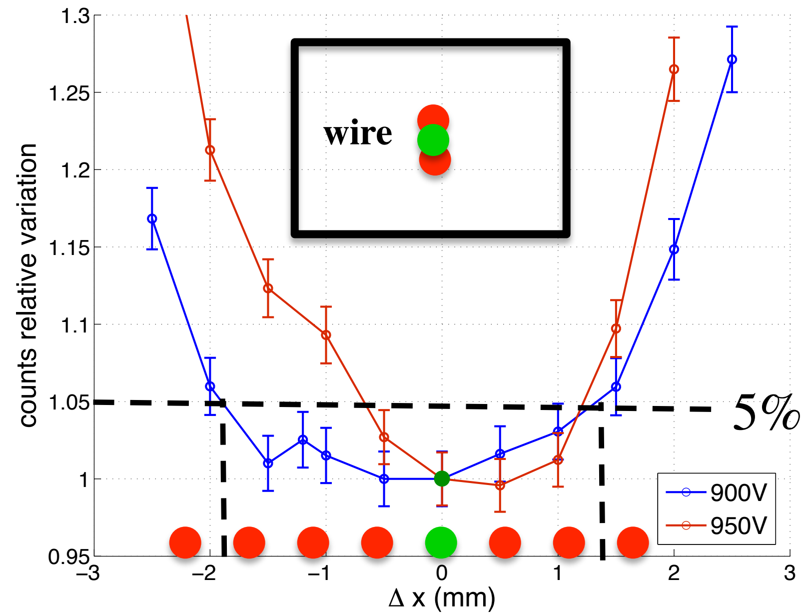

On-going development in BrightnESS

Started in Sept 2015

New design of the grids (32 x23) with more compact cells
Variable dimensions in X, but constant in Y and Z (no gain variation)

New design of the gas vessel for low pressure operation

Higher performance :
Reduced dead space
Reduced vessel weight
Thin entrance window

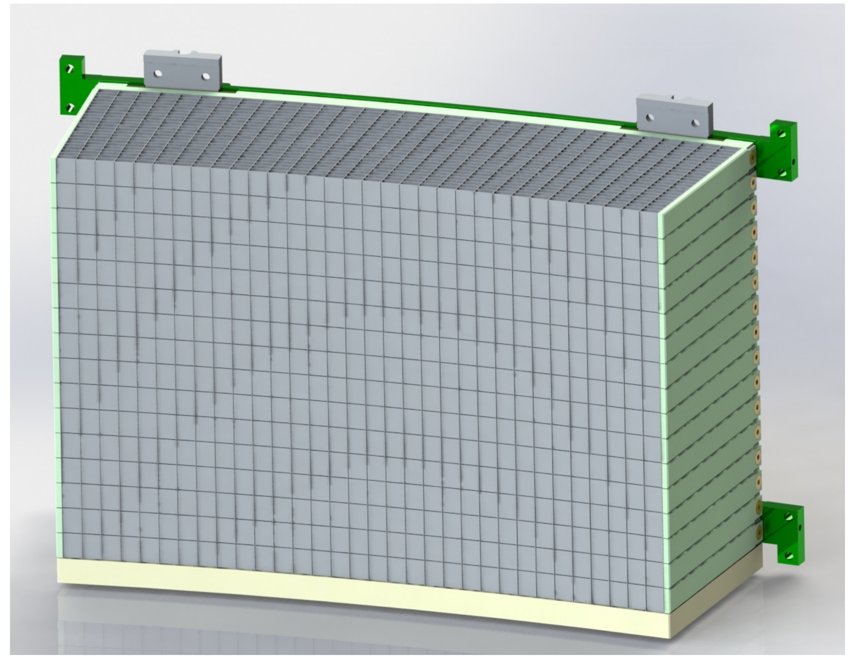

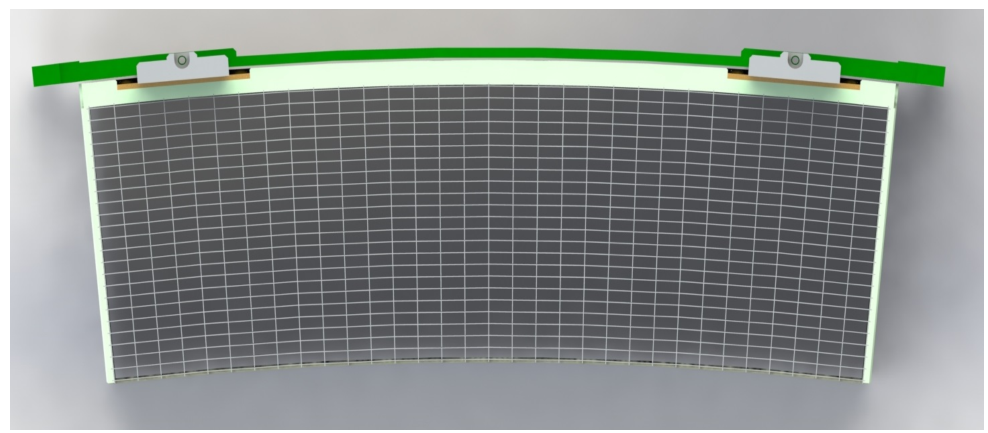

Large area 3He detector for IN4/PANTHER (In project)

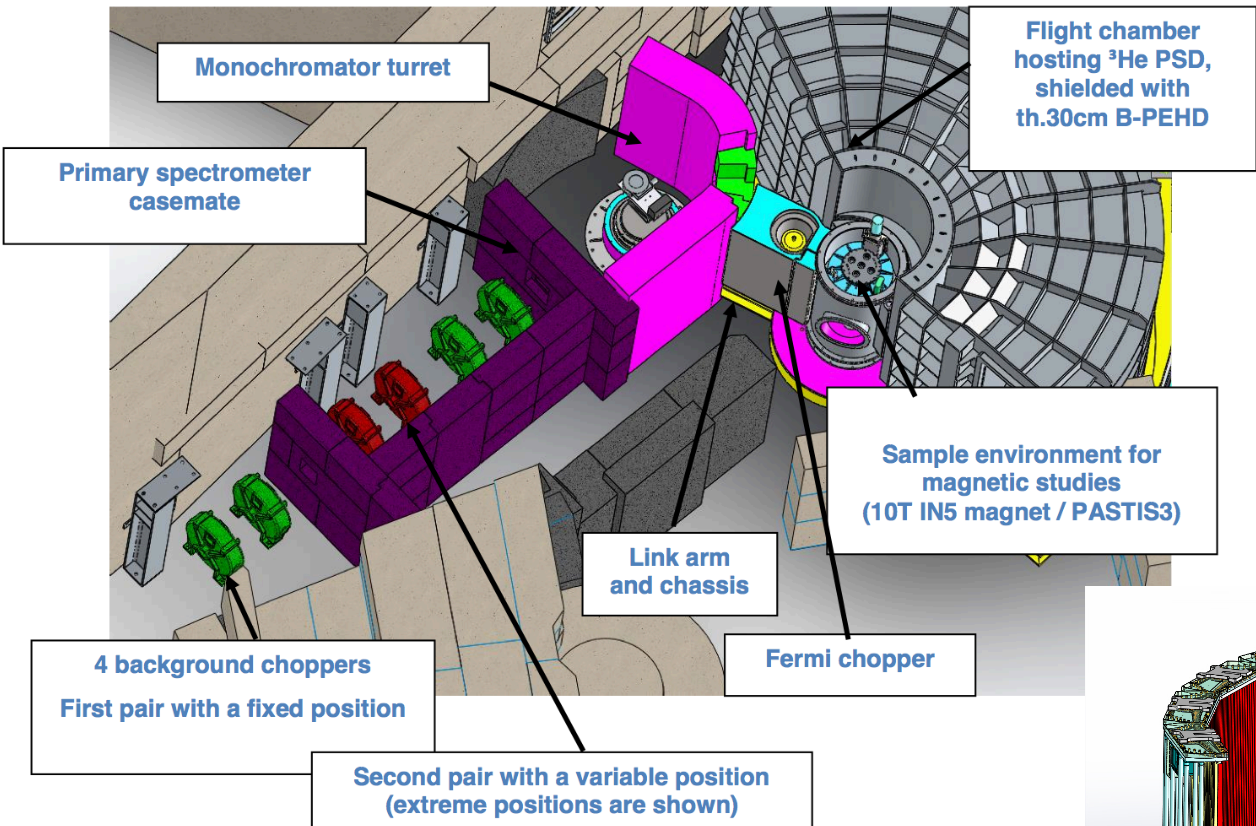

Fig. 1: Current Panther schematic design

similar to IN5

Tubes of 2 m long, 2 cm diam.

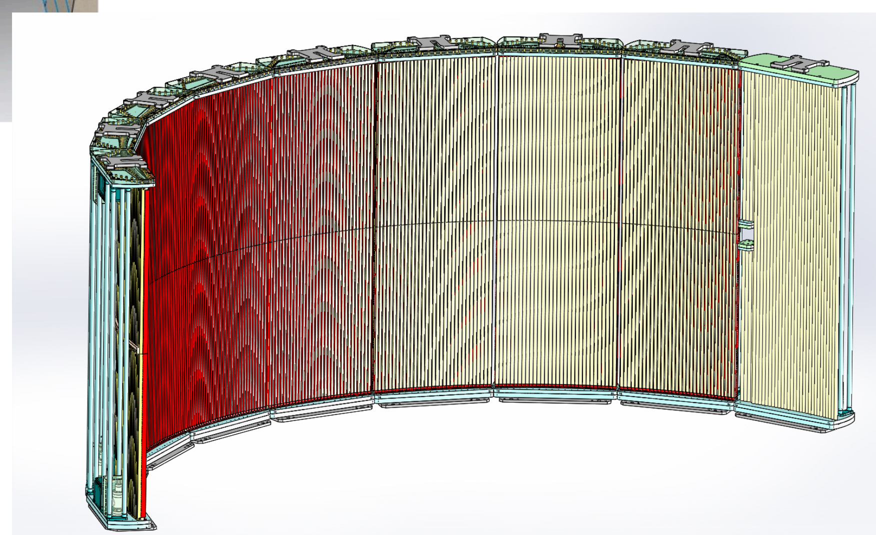

In project: EXED (HZB/berlin)

4 ^{3}He modules
2 with 32 tubes (now 31) of 2.38 m +
2 with 24 tubes of 2.0 m
Diam: 19 mm ext (0.4 mm wall)

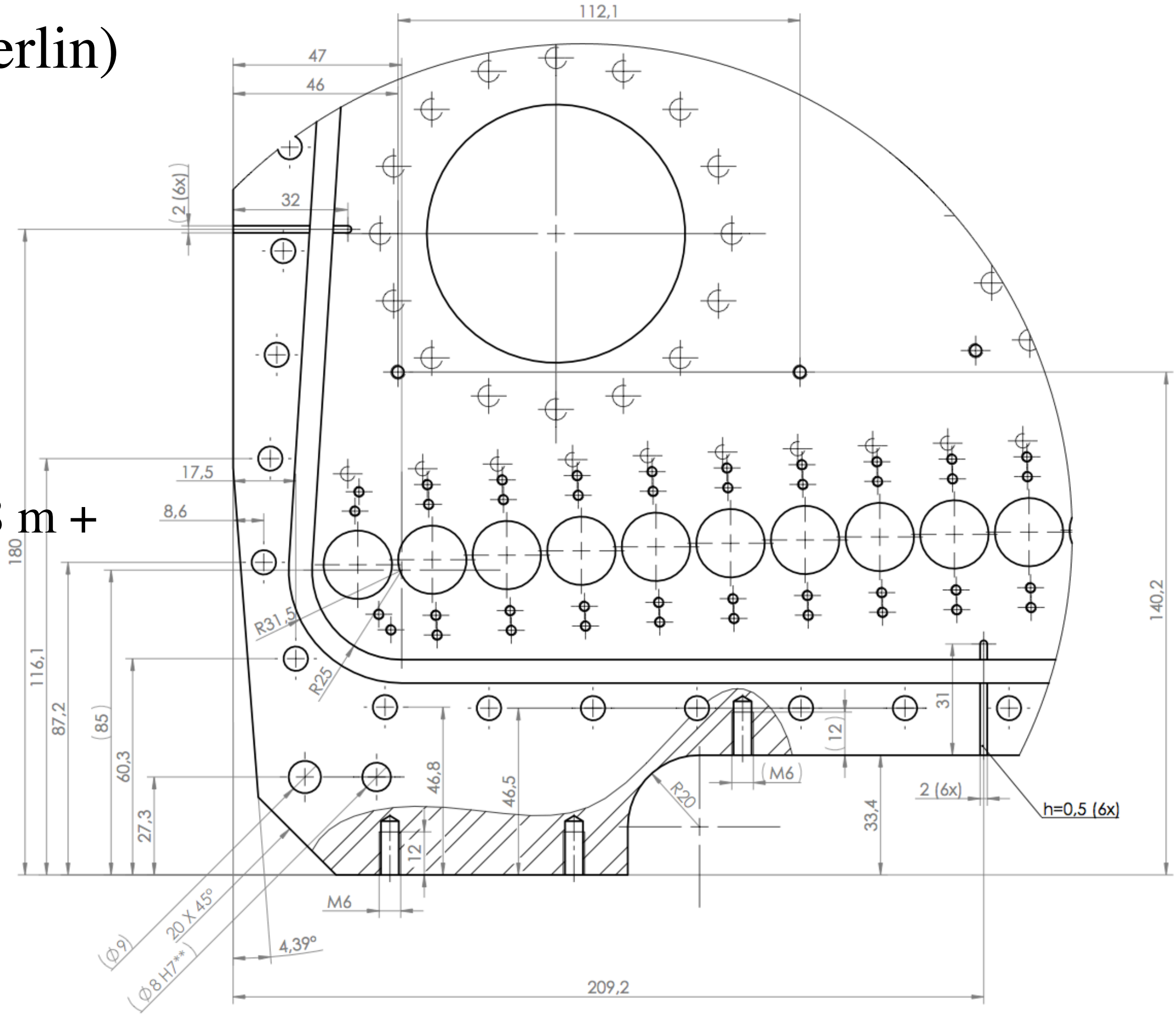

Z (1 : 1)

Guidelines for the development of a 2D curved MWPC for the future XtremeD instrument (in project)

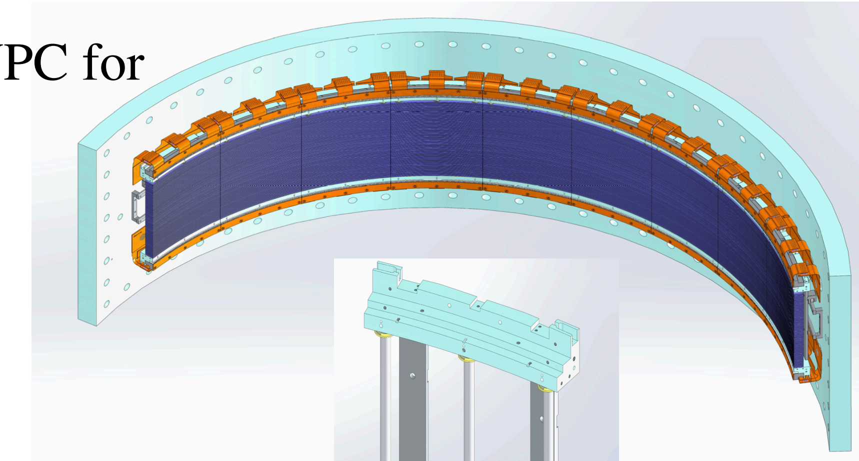

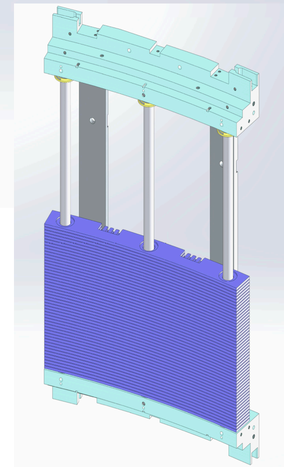

- Mechanical robustness; detector reliability; mounting simplicity
- Radiation hardness
  - Lower amplification gain operation
  - Use of Ar-CO2 instead of CF4
- Access for maintenance
  - no cathode wires on top of the anode wires
  - mounting/dismounting of modules in the detector vessel

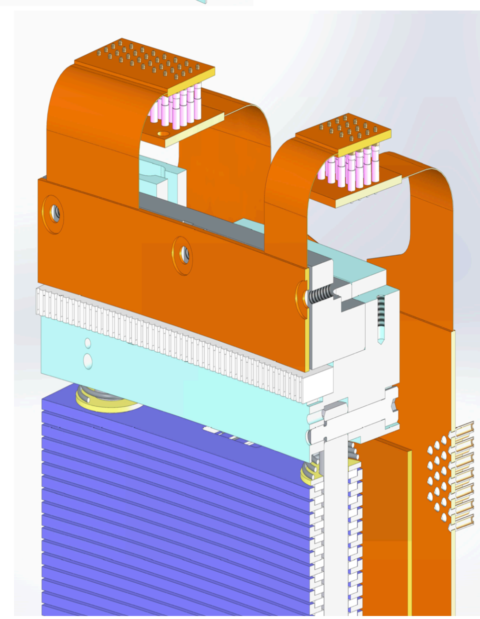

- Keep the detection gas clean : avoid organic materials and gas cleaning systems
- Minimise the volume of non-used ^{3}He
- Reduce risk by using « standard » components whenever possible:
  - D19 pressure vessel : Design + assembling tools
  - Wire soldering procedure
  - 32-pins feed throughs (used in most of the ILL PSD detectors)
  - 32-channels MILAND electronics boards (used in many ILL PSD detectors)
  - principle of the ceramic combs as used in the D16/MILAND detector
  - principle of the Kapton connectics as used in most of the ILL PSD detectors

XtremeD Prototype results

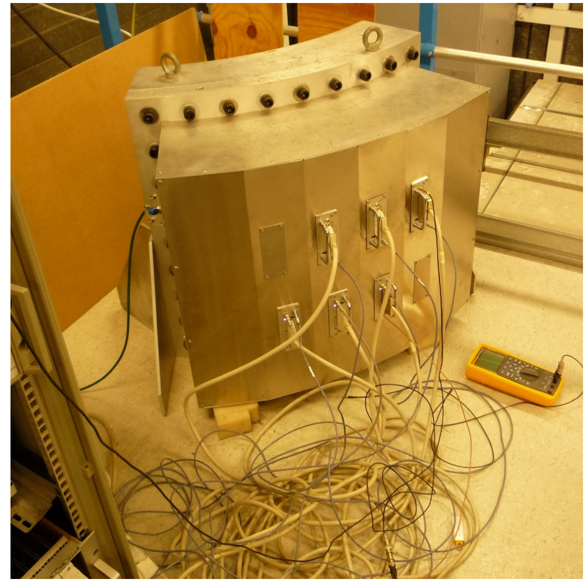

Anode wires:
3 M32MB cards 1us;20V/pC
32 channels per card ; Global threshold

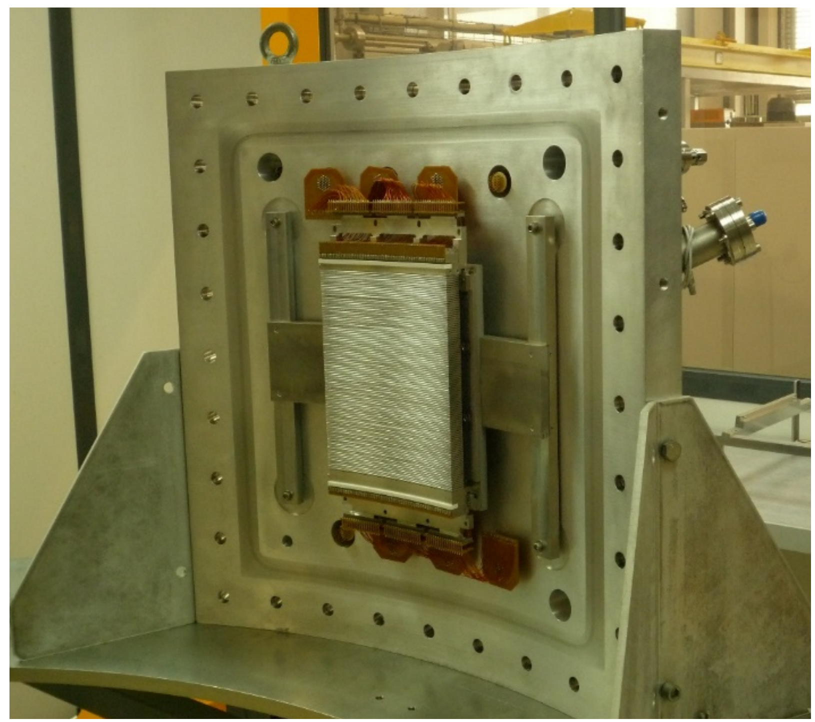

Cathode plates:
3 M32MB cards 1us;20V/pC
32 channels per card ; Global threshold

Hit cluster analysis and
XY coincidence in ILL MCCv2
Module
XY coinc. Window: 3.2 us

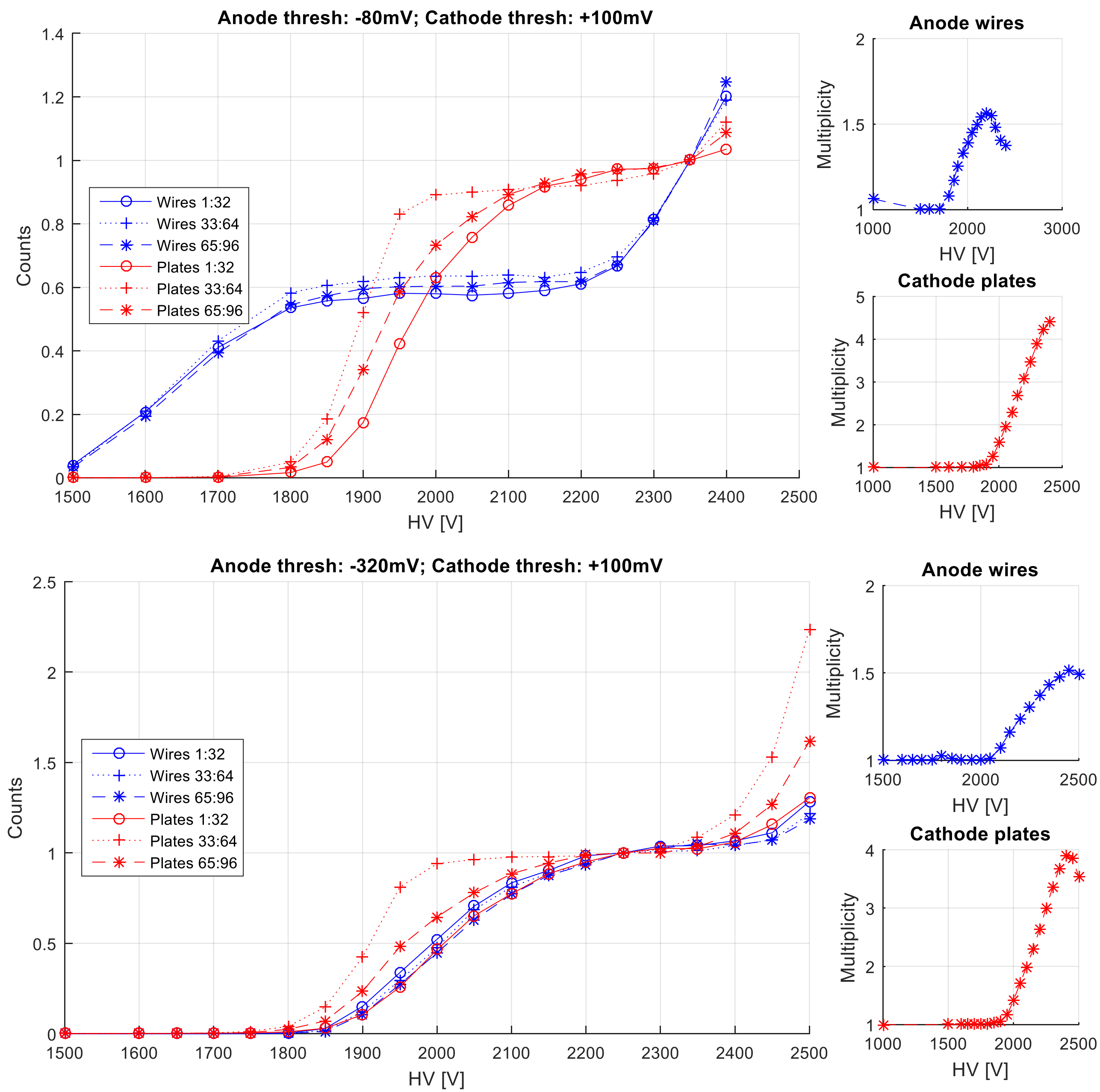

Anode thresh: -80mV; Cathode thresh: +100mV
Counts
HV [V]
Wires 1:32
Wires 33:64
Wires 65:96
Plates 1:32
Plates 33:64
Plates 65:96
Anode wires
Multiplicity
Cathode plates
Anode thresh: -320mV; Cathode thresh: +100mV

Counting curve with XY coincidence

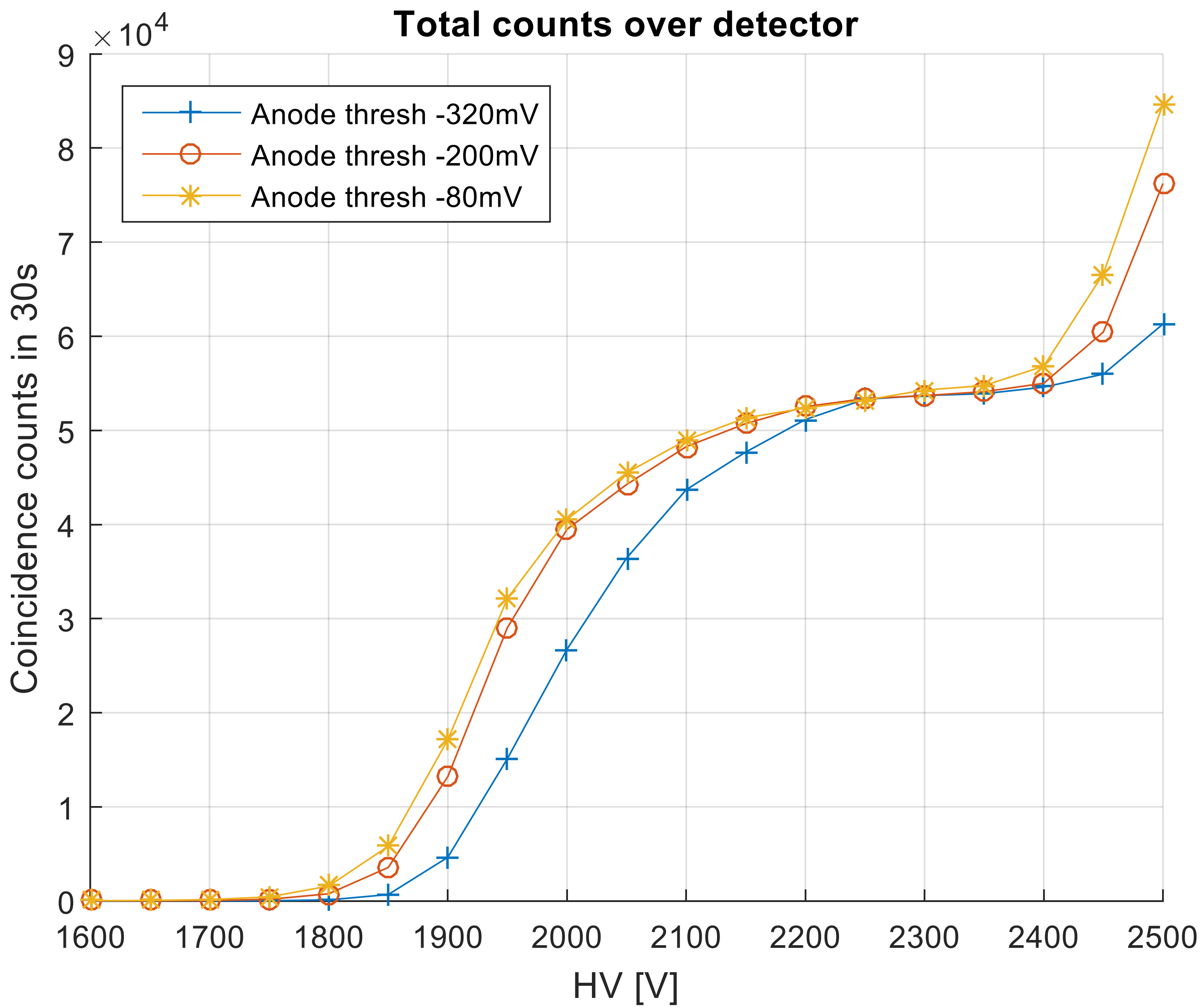

Anode/cathode time jitters

2300V ; Anode Thresh: -320mV ; Cathode Thresh: +100mV

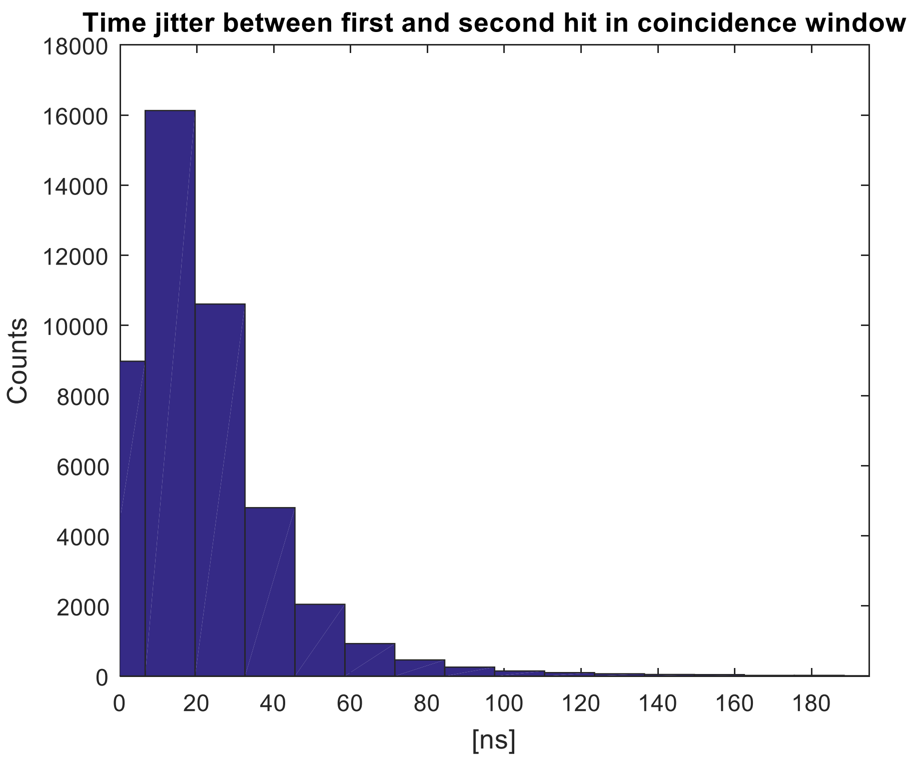

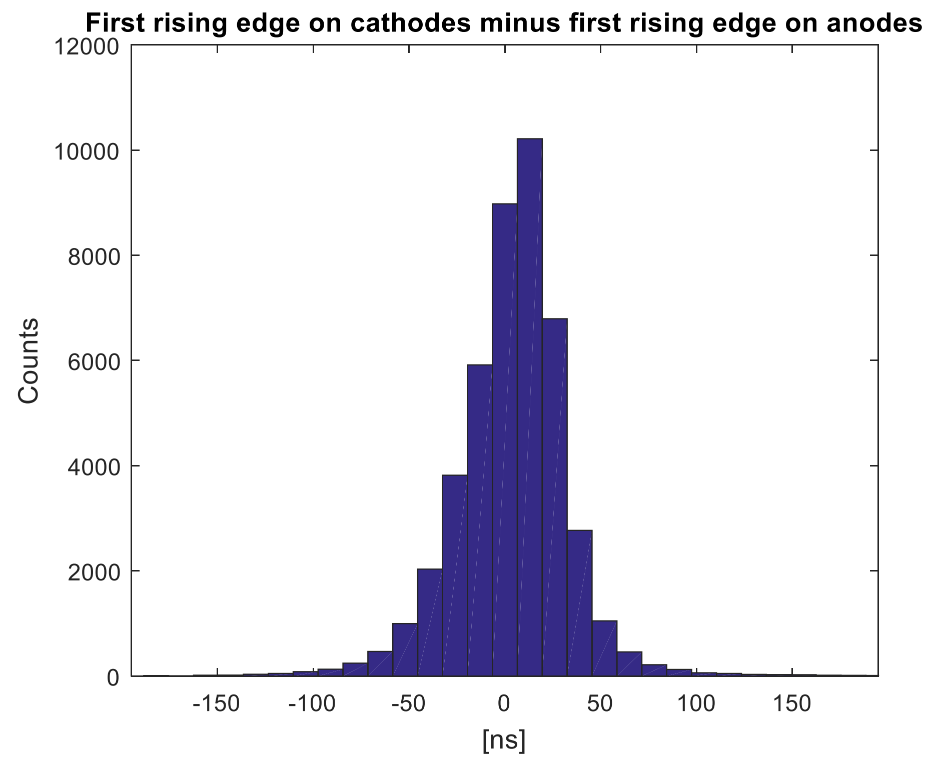

Flat-field corrected image (HV=2300V)

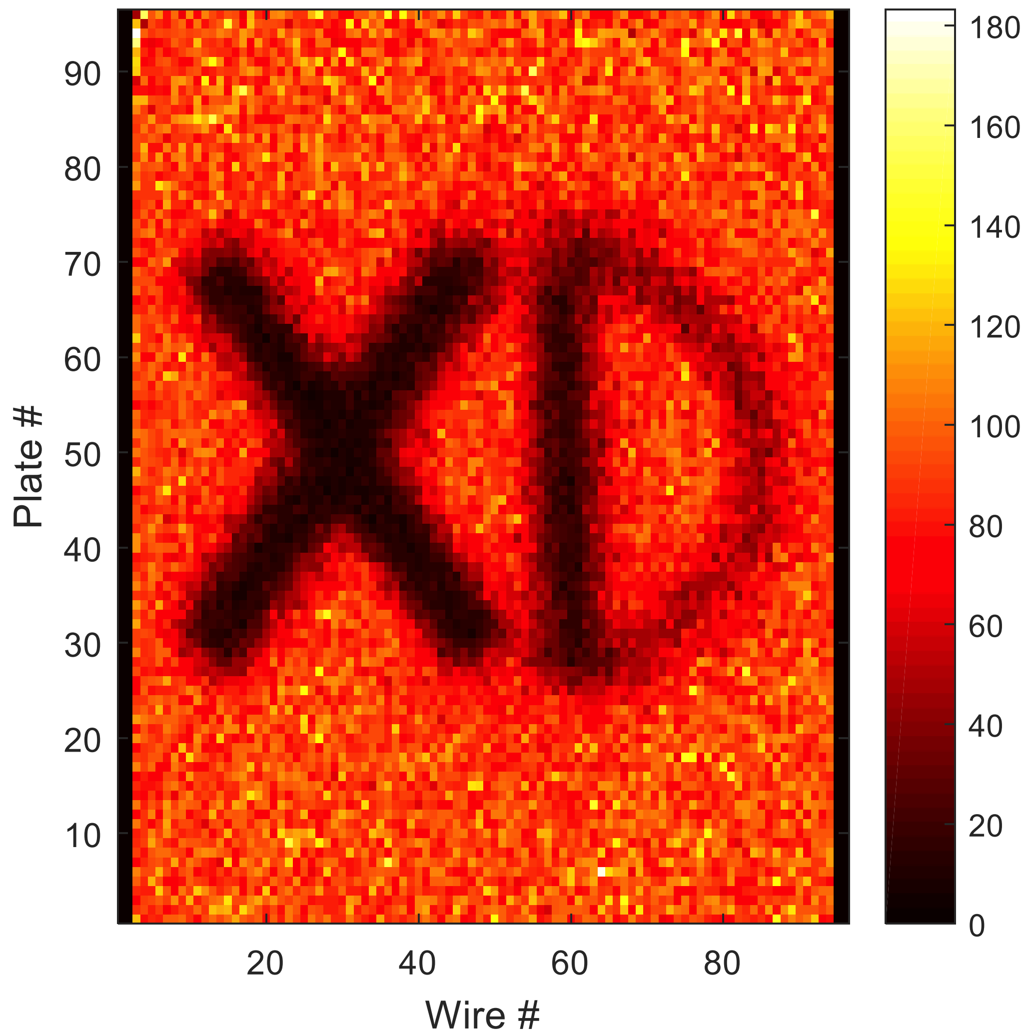

CONCLUSION

Gas detector development is still very active for neutron scattering science

Due to the 3He shortage, alternatives techniques are needed for large area detectors

For small detectors, 3He remain the best solution for many applications

More performing detectors are also needed for the future ESS and for current intense sources to benefit of the high flux delivered to the instruments.

Solutions based on thin convertor films are intensively developed

The broad range of instrumental conditions is a source of many interesting problems to solve for the detector … and for young scientists

NERID (in project): Neutron Eye Robot system for Inspection of fuel Debris

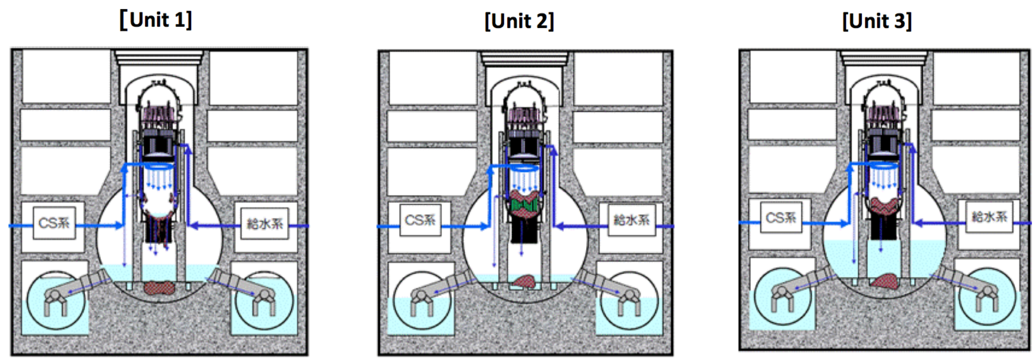

In late 2014, TEPCO began to investigate the removing of the melted fuel in 3 of the reactors at Fukushima. No one knows where the fuel debris is, and if they are in a solid state of cold shutdown. The fuel debris cannot be removed until we know where it is. This information is difficult to obtain because a PCV (Primary Containment Vessel) has only a few, narrow access routes by which it is possible to get inside. The technology needed to establish the location of the melted fuel rods remains to be developed. The purpose of NERID is to develop a functionality, implementable on an existing robot, to measure the distribution of fuel debris inside the PCV.

NERID (in project)

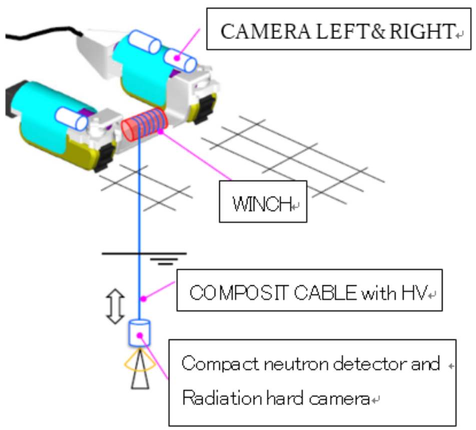

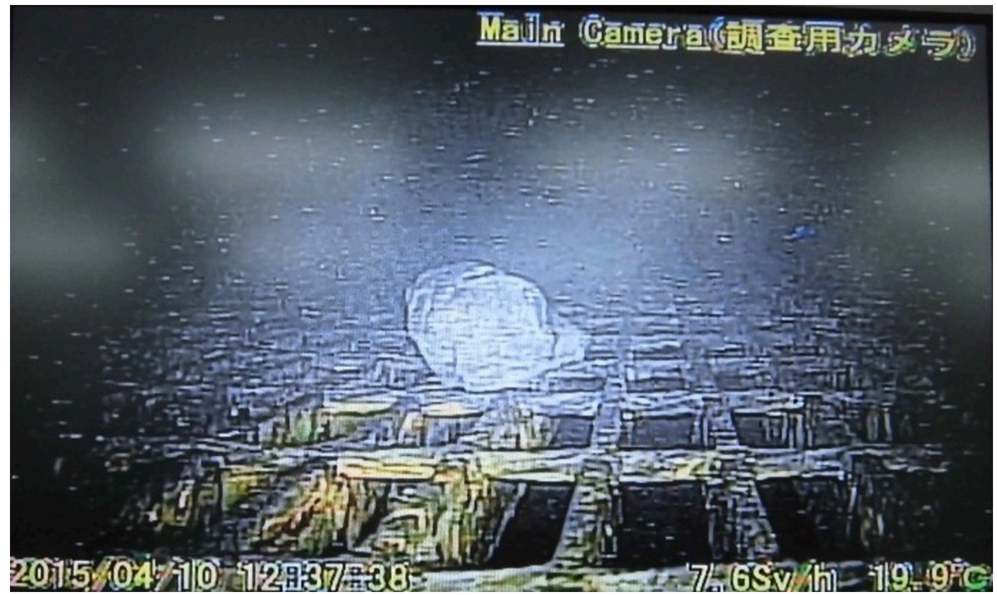

The "snake" robot developped by Hitashi and GE Nuclear

Photo of the grating floor inside the PCV obtained by a snake robot

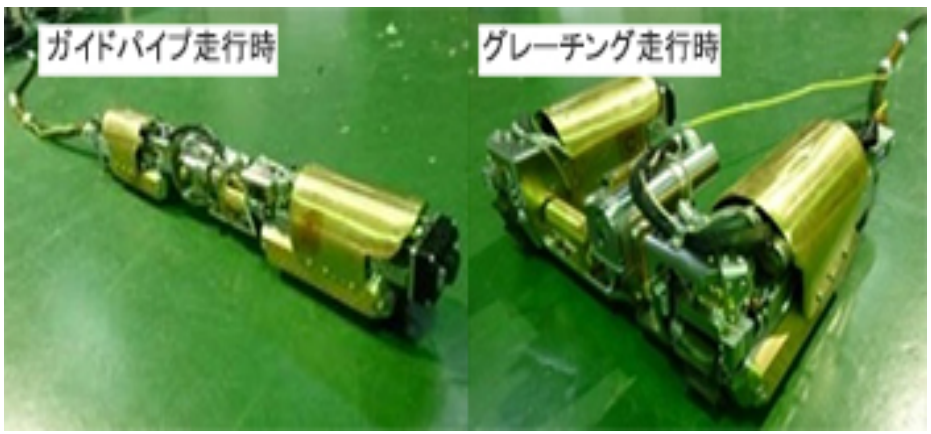

NERID (in project)

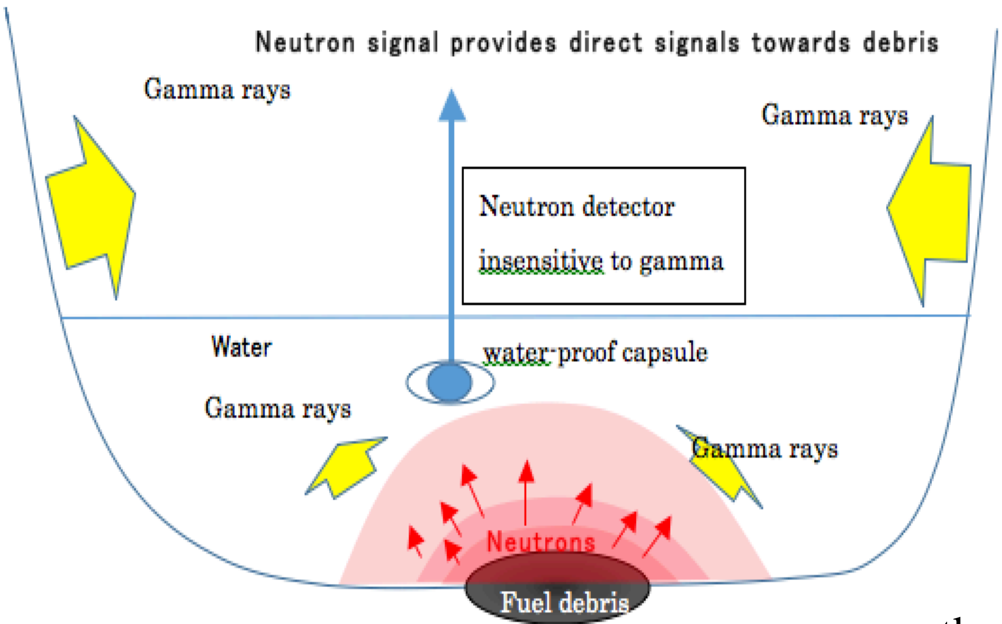

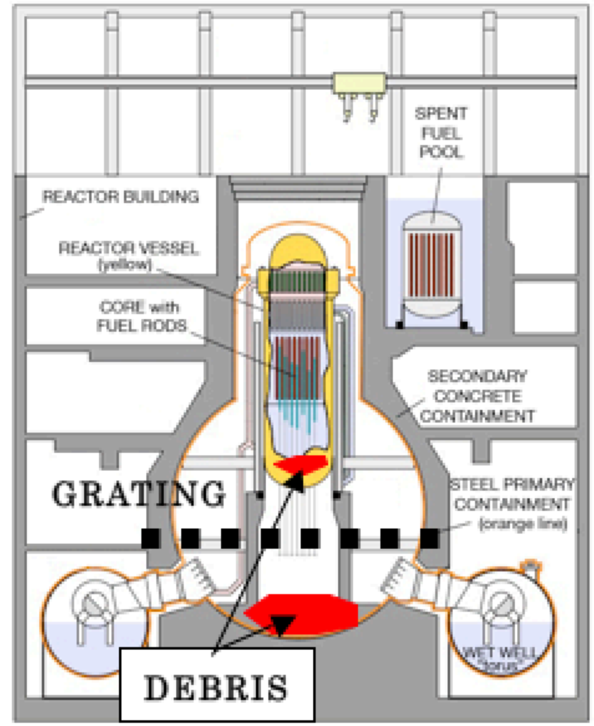

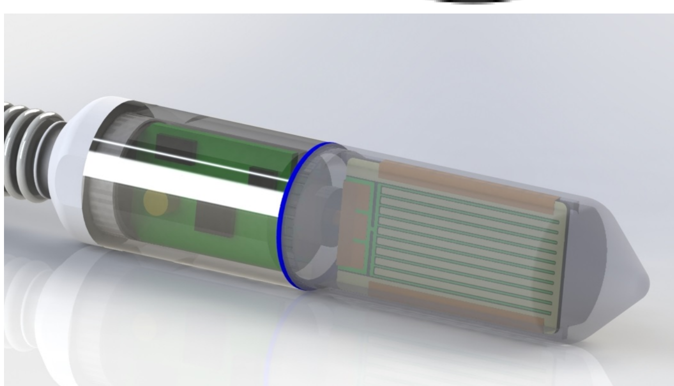

Principle of the MSGC capsule to be developed for NERID

the reactor building, showing the debris in Reactor Pressure Vessel, and in the Primary Containment Vessel. The shape-changing robot will be introduced in the PCV through a narrow pipe; it will then move on the grating floor to detect the presence of melted fuel underneath the grating floor. The compact radiation detector will be scrolled down via the apertures of the grating floor to measure neutrons and gammas near the basement.